DIPLOMARBEIT

The Decarbonization Potential of Space Heating Systems in Residential Buildings: A Vienna Case Study

unter der Leitung von

Univ.-Prof. Dipl.-Ing. Dr. techn. **Ardeshir Mahdavi**

Associate Prof. Dipl.-Ing. Dipl.-Ing. (FH) Dr. techn. **Matthias Wilhelm Schuß**

E 259-3 Abteilung für Bauphysik und Bauökologie

Institut für Architekturwissenschaften

eingereicht an der

Technischen Universität Wien

Fakultät für Architektur und Raumplanung

von

Mert Oktay

11838921

Wien, June 2021

KURZFASSUNG

Der Klimawandel aufgrund von Treibhausgasemissionen bedroht Leben, Lebensräume und Volkswirtschaften. Um diese Risiken zu mindern und den drohenden Gefahren des Klimawandels vorzubeugen, wurde 2015 das Klimaabkommen in Paris von fast allen Ländern der Welt unterzeichnet. Dieses Abkommen zielt darauf ab, die Emissionen von Treibhausgasen zu reduzieren, um die globale Erwärmung zu begrenzen. Um dieses Ziel zu erreichen, ist jedoch eine tiefgreifende Dekarbonisierung in allen Sektoren erforderlich. Dabei ist die Raumheizung besonders wichtig, da der Gebäudesektor nach wie vor einer der größten CO_2 Emissionsquellen ist. Daher wurde in dieser Masterarbeit eine Fallstudie für den vierten Wiener Gemeindebezirk, Österreich, durchgeführt, um das Dekarbonisierungpotenzial verschiedener Raumheizungssysteme im urbanen Maßstab aufzuzeigen. Zu diesem Zweck wurde die Bottom-up Methode der urbanen Gebäudeenergiemodellierung angewendet. Dafür wurden repräsentative Gebäude ermittelt und kalibriert. Anschließend wurden die Energiesimulationen mit alternativen Heizsystemen durchgeführt. Luftwärmepumpe, Erdwärmepumpe und Fernwärme wurden in Bezug auf bestehende Berichte und Forschungen als die am besten geeigneten und umweltfreundlichsten Alternativen zu den weit verbreiteten Erdgasheizungen angesehen. Bezüglich dieser Alternativen wurden drei Szenarien für den Vergleich des Potenzials zur aktuellen Situation erstellt. Danach wurden die simulierten Heizenergiewerte der einzelnen Standorte hochskaliert und monatlich in CO_2-äquivalente Emissionen berechnet, um das Potenzial auf städtischer Ebene zu erkunden. Die Ergebnisse zeigen, dass die Umstellung der Raumheizung, insbesondere auf Erdwärmepumpen, ein enormes Potenzial zur Reduzierung des Energieverbrauchs und zur Dekarbonisierung hat, während die Wirkung der Fernwärme unter Berücksichtigung der aktuellen Bedingungen begrenzt ist. Mit dem aktuellen Erzeugungsmix aus Strom und Wärme in Wien liegen die Dekarbonisierungspotenziale der Erdwärmepumpe (wo möglich), der Luftwärmepumpe und der Fernwärme bei 61%, 55% bzw. 22%. Vor dem Hintergrund dieser Erkenntnisse kann empfohlen werden, dass Wärmepumpensysteme eingesetzt werden, um die ehrgeizigen Dekarbonisierungsziele zu erreichen.

ABSTRACT

Climate change due to greenhouse gas emissions threatens lives, habitats, and economies. In order to mitigate these risks and prevent the impending danger of climate change, the Paris Agreement was signed by almost all countries in the world in 2015. That agreement aims to reduce emissions of greenhouse gasses to limit global warming. However, to accomplish that goal, deep decarbonization in all sectors is required. In this endeavor, space heating is particularly important, as the building sector is still one of the largest sources of CO_2 emissions. Hence, in this master thesis, a case study was conducted for the 4th district of Vienna, Austria, to indicate the decarbonization potential of different space heating systems on the urban scale. For this purpose, the bottom-up urban building energy modeling method was employed at the district scale. Initially, representative buildings were determined and calibrated. Then the energy simulations were performed with alternative heating systems. Air source heat pump, ground source heat pump, and district heating were considered the most appropriate and environmentally friendly alternatives to the heavily existing natural gas boiler systems regarding the reports and research. Concerning these alternatives, three scenarios were created for the comparison of the potential with the current situation. Afterward, these simulated individual site heating energy values were scaled up and converted monthly to CO_2 equivalent emissions to explore the potential at the urban level. The results show that the electrification of space heating, especially the ground source heat pump, has tremendous potential for site energy consumption reduction and decarbonization, whereas the effect of the district heating is actually limited. With the current generation source mix of electricity and district heating in Vienna, the decarbonization potentials of the ground-source heat pump (where possible), air-source heat pump, and district heating are 61%, 55%, and 22%, respectively. In light of these findings, it can be suggested that heat pump systems can be deployed to achieve the ambitious decarbonization targets.

Keywords

Building performance simulation, Climate change, Decarbonization, Heat pump, Space heating, Urban building energy modeling.

ACKNOWLEDGEMENTS

First and foremost, I would like to express my sincere gratitude to my supervisors, Univ.Prof. Dipl.-Ing. Dr.techn. Ardeshir Mahdavi and Associate Prof. Dipl.-Ing. Dipl.-Ing. (FH) Dr. techn. Matthias Wilhelm Schuß for their attention and guidance throughout this thesis.

I would also like to thank all the Building Physics and Building Ecology Department staff, whose contributions during my studies made this thesis possible.

In addition, I am deeply indebted to my family and friends for their love and support.

Beyond everything, I wish to dedicate this master thesis to my wife, Simge, who has committed herself to make this world greener and more livable for all living things.

CONTENTS

1 INTRODUCTION

1.1 Overview

Since the Paris agreement was adopted in 2015 to reduce the risks of climate change, 195 signatory countries have been formulating ambitious policies to achieve a climate-neutral world by 2050 (UNFCC 2015). European Commission's reports state that an 80% to 95% CO_2 emission reduction is required to fulfill this aim by 2050 compared to the 1990 CO_2 emission levels. For this purpose, in 2030, as the first milestone, a 40%, and in 2040 as the second milestone, a 60% CO_2 emission reduction is planned (Delbeke et al. 2015). In this endeavor, the decarbonization of the building stock has crucial importance because the building sector is responsible for 36% of overall energy consumption and 39% of related CO_2 emissions in the world (UNEP and IEA 2019). In detail, 16% of primary energy used in European Union (EU) countries is consumed in residential heating, and 70% of these primary energy sources are fossil-based (Bertelsen and Mathiesen 2020).

The majority of the European building stock is relatively old, 76,5% of them were constructed before 1980, and they need a thermal retrofit. However, with the current renovation rates, it will take decades to renovate the entire building stock. Additionally, achieving average energy efficiency levels with renovation in historical buildings constructed before 1945, which constitutes 26,4% of the whole stock, will cost extremely high (Troi 2011). Therefore, a vast and fast decarbonization potential lies in the retrofitting of space heating systems.

Various methods exist to fulfill this potential. However, in specific research and reports, heat pump technologies and district heating come to the forefront (Sheikh 2017, Treberspurg and Stadt Wien 2019, IRENA et al. 2020).

In this context, this master thesis aims to evaluate the decarbonization potential of these space heating systems in residential buildings. For this purpose:

Initially, the relevant sources were scanned, and the existing systems in Vienna and possible alternatives were determined. Next, the bottom-up approach of Urban Building Energy Modelling was adopted to calculate the decarbonization potential at an urban level. In accordance with this method, firstly, representative buildings were selected from previous studies for the analyses of the 4^{th} district of Vienna. Secondly, These samples were modeled in 3D and characterized according to the literature to prepare the models for computational simulations. Thirdly, a calibration process was performed by a trial-and-error approach. The heating energy consumption of the simulation models was calibrated. Afterward, these calibrated models of the samples were simulated individually with existing and predefined heating systems to obtain site energy consumption values of relevant fuels. Finally, these consumption values were converted monthly to CO_2 equivalent emissions with relevant fuel conversion factors and scaled up to the district level.

1.2 Motivation

In the long-term strategy (2019), Austria aims to create a carbon-free building sector by 2050. For this purpose, in the “Government Program, 2020–2024” announced by the Federal Chancellery of Austria (2020), it is planned that the coal and oil-based heating systems will be completely phased out by 2035. In addition, the gas heating system installations will be banned, and their network expansions will be stopped from 2025 (Republic of Austria 2020). That move for ambitious decarbonization will seemingly lead to a rapid transformation in the heating systems in the near future. Definitely, it is impossible to fulfill this goal by 2050 with only one perfect system investment. However, this endeavor can be sustained by implementing today’s promising systems to replace the current ones.

Therefore, it is assumed crucial to explore optimum systems with the lowest possible environmental loads as a first milestone in the way to the entire decarbonization. This study aims to calculate the decarbonization potential of the current possible alternative heating systems in Vienna conditions based on this target.

1.3 Background

1.3.1 Overview

In order to calculate the decarbonization potential of the space heating systems in the Vienna case, first of all, the current heating systems should be explained while determining the alternative systems.

Hence, in this chapter, the most widely used heating systems and their efficiencies were examined. Subsequently, the decarbonization technologies were investigated. As a result, electrification was identified as the most promising one. According to that conclusion, relevant low-carbon heating system technologies were explored as heat pumps.

Afterward, the suitable heat pump types for Vienna's climate were defined, and a general coefficient of performance range was defined for that heat pumps regarding their prevalence.

1.3.2 Most common space heating systems used in Vienna

Wood variations such as fuelwood, wood pellets, wood briquettes, and wood chips are the leading fuel type for space heating in Austrian households with a share of 37%. Natural gas is the second common space heating fuel with a 23% share, and then fuel oil and district heat follow them with 16% shares. However, if the values are analyzed specifically for Vienna, it can be easily observed in Figure 1 that natural gas dominated the energy carriers with a 55% share. District heating stands in second place with a 33% share, whereas heat generation for district heating in Vienna is supplied by mostly combined heat and power plants and waste incineration; that means district heating consumes fossil fuels as well (Ritter 2016). Unfortunately, the share of heat pumps, represented as ambient heat, has only a 4% prevalence in Austria and 0,3% prevalence in Vienna among all other fuel types (Statistik Austria 2020).

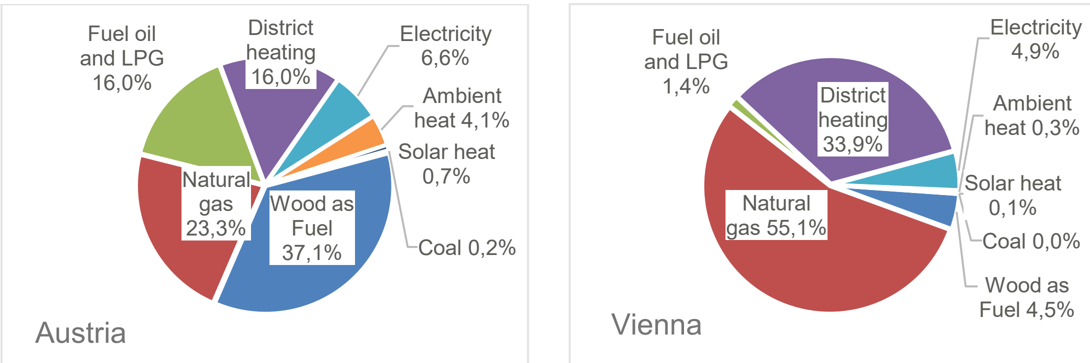

Figure 1 Share of fuel consumption for space heating

Regarding the installed space heating systems in Vienna, Table 1 shows that natural gas boilers constitute nearly half of all heating systems. Additionally, a further study by Bertelsen and Mathiesen (2020) about residential heat consumption states that the majority of those gas boilers are non-condensing types. Consequently, the less efficient, non-condensing type conventional system and combination natural gas boilers are the most prevalent systems in Vienna. The district heating system comes second. The number of dwellings heated by district heating is slightly less than the ones by gas boilers. Electric heating constitutes about 5% of all systems. This percentage fits well with the electric consumption rates for heating. This accordance means that most of those heaters are probably basic, direct electric convectors (instead of highly efficient HVAC units) used for single-zone heating or used as supporting heating systems for a brief time. The gas convectors are also used for single-zone heating and are in fourth place (Statistik Austria 2020).

Table 1 Space heating by fuel and heating system in Vienna, 2020 (Source: Statistik Austria)

Fuel	Dwellings	Heating system				
		Stove	**Gas furnace**	**Electric heating**	**Central heating**	**District heating**
Fuelwood, wood chips, pellets, wood briquettes	14.226	6.369	-	-	7.857	-
Coal, coke, brown coal briquettes	-	-	-	-	-	-
Fuel oil, LPG	10.175	-	-	-	10.175	-
Electricity	45.898	-	-	45.898	-	-
Natural gas	442.287	-	37.254	-	405.033	-
Solar heat and ambient heat	8.435	-	-	-	8.435	-
District heat	390.491	-	-	-	-	390.491
Total	**911.512**	**6.369**	**37.254**	**45.898**	**431.500**	**390.491**

Briefly, the gas boilers are installed in 45% of all dwellings and consume 55% of all heating energy. Meanwhile, the district heating system supplies heat to 43% of all dwellings, consuming only 34% of the final heating energy. These statistics also support the simple fact that the efficiency of the district heating is higher than the efficiency of the natural gas boiler systems.

In conclusion, non-condensing natural gas boilers together with district heating comprise the vast majority of all space heating systems in Vienna. Therefore, these systems will be shortly explained in the following sections.

1.3.2.1. Non-condensing gas boilers

ASHRAE's HVAC systems and equipment handbook (2020 p.32.1) define a boiler as "*a cast-iron, carbon or stainless steel, aluminum, or copper pressure vessel heat exchanger designed to burn fossil fuels or use electric current and transfer the released heat to water in water boilers or to water and steam in steam boilers.*" In addition to that definition, simply, if the burning fuel in the boiler is natural gas, then it is called a natural gas boiler (NGB). There are multiple classifications, but especially the gas boilers can be grouped into three types. First, the combination boiler is a central, compact unit that can instantly generate a limited amount of heating water and domestic hot water to supply single dwellings such as apartments or single-family houses. There is no domestic hot water storage tank, water pump, long pipings, etc., in these boilers. Second, the system boiler is a central boiler that generates heating water and stores domestic hot water in a tank to supply buildings or multifamily houses. Third, the conventional boiler is a central traditional boiler that generates heating water and stores domestic hot water in a tank. Coldwater storage is also used to feed the system water and domestic hot water tank. In the last decades, their popularity has been decreasing because of the combination boilers. However, they can still be found in old buildings and multifamily houses (Worcester-Bosch n.d.). In addition, each boiler system can be installed multiply as a cascade to increase the heat power load or provide chancing heat demands.

Condensing boilers can benefit from the exhaust heat of the hot flue gases, whereas the non-condensing ones do not extract the latent heat from the flue gasses. Condensing boilers cool down the flue gases with additional heat exchangers till the water vapor in them condenses to profit from this latent heat. These boilers increase efficiency by reducing heat losses. Therefore, the condensing boilers are more efficient and environmentally friendly than the non-condensing ones. If the efficiencies are compared, condensing boilers are generally more than 90% efficient, while the non-condensing boilers' are between 50% to 80% regarding their age and model (Viessmann n.d.).

1.3.2.2. District heating

District heating is a term for distributing the generated heat from a central plant to its surrounding area or a district with insulated pipes. That generated heat is obtained from different sources such as heating plants, cogeneration plants, waste heat from industry, geothermal energy, central solar heating, heat pumps, and seldomly conversion from surplus electrical power (Woods and Overgaard 2015, Potente Prieto 2019).

In Vienna, the district heating system, Fernwärme Wien, is run by Wien Energie Group and distributed with 1192 km of pipeline from eleven plant locations. Although district heating has a significant contribution in reducing CO_2 emissions in Vienna, the total installed district heating capacity comprises 44.7% cogeneration plants and 44.6% peak-load district heating plants, which simply means this thermal energy is generated mainly from fossil fuels (Potente Prieto 2019).

Combined heat and power plants or shortly cogeneration plants deploy the waste heat while generating electricity or mechanical power. Utilizing instead of releasing the waste heat makes this system more efficient than other plant types. However, they are generally fueled by natural gas and oil because electricity generation requires high-quality primary energy sources. Peak-load district heating plants are simply boilers that are operated to support heat generation and meet the demand at peak loads. They can be fired with fossil fuels, biofuels, waste, etc. In addition to these plants, 7% of the total installed capacity belongs to the municipal waste incineration plants. In which the garbage is incinerated by boilers equipped with special flue gas treatment systems to generate heat (Potente Prieto 2019).

1.3.3 Alternative space heating technologies for decarbonization

Besides improving system efficiencies, International Energy Agency (2020) identifies five transition strategies to achieve decarbonization in heating and cooling systems: renewables-based electrification, renewable gases, sustainable use of biomass, direct use of solar thermal heat, direct use of geothermal heat. Sheikh (2017) with his study that explores decarbonization potential, considered that the following technologies could switch a building stock to emission-free in an efficient way;

- Solar thermal heating
- Pipeline gas decarbonization via using biogas, synthetic methane, or hydrogen instead of natural gas
- Electrification via switching fossil-fueled furnaces and boilers to heat pumps powered by electricity from renewable energy sources or low carbon electricity

1.3.3.1. Solar thermal heating

Currently, instead of supplying the whole demand, solar thermal heating (STH) uses auxiliary heaters or is used as auxiliary space heating and supports the primary heating system to reduce the total fuel demand (Chwieduk 2016). A solar thermal collector transfers the heat energy from solar radiation to a heating fluid that is pumped through it. Additionally, a heat exchanger is employed if the heating fluid is not water. Thus, this hot water can be directly used or stored in a solar storage tank. The water is heated more with a heater if it is not hot enough for domestic hot water (DHW) or space heating (Hudon 2013).

A solar collector installation can provide 20% to 60% of the total energy for a dwelling's DHW and space heating needs in Austria. Nevertheless, this solar fraction can be improved with a proper collector and seasonal storage size up to 50% to 70% (Weiss 2004). However, this time, surplus heat would occur at certain times that may cause overheating. Despite that risk, in a scenario that all buildings are equipped with STH with the possible maximum solar fraction, the space heating and DHW related emissions can be 70% reduced. However, it is impossible due to orientation and space availability.

Another issue is photovoltaic (PV) panels. They are also implemented in the exact locations such as terraces, roofs, and gardens with STH collectors. Although the STH has better efficiency than PV (40-60% vs. 15-20%) (Lupu et al. 2018), the need for heat has been declining in recent years thanks to the insulations and renovation strategies. Furthermore, PV can deliver electric energy, which can be converted into heat energy and is more valuable than heat since it can be used in multiple ways. The efficiency of the PV panels increases while their cost decreases every day. Also, a combined PV and thermal collector (PVT) can feed a solar-assisted heat pump for space heating as a better solution. PVT can generate electricity and thermal energy simultaneously. Thus, a heat pump can use both the heated fluid and the electricity generated by the PVT for maximum efficiency (Sheikh 2017; Hudon 2014).

In conclusion, the STH would significantly affect CO_2 emissions. However, it seems it is far from eliminating the whole residential heating emissions itself. In the best case, one-third of the heating-related CO_2 emissions remain. Consequently, implementing STH systems could lock the remaining emissions and may hinder the total decarbonization efforts. (Sheikh 2017)

1.3.3.2. Pipeline gas decarbonization

Ideally, the logic behind the pipeline decarbonization is to keep natural gas or oil-carrying networks but replacing these conventional fossil fuels with low-carbon or carbon-neutral alternatives. In practice, usually, a minor adjustment and investment for heating systems and pipelines are enough for this transition. Therefore, ease of transition makes this option an economical and quick solution that attracts consumers and policymakers. Additionally, since natural gas is the major fuel in Vienna, it has an extensive transmission network so that central planning can enable a mass transition and a considerable decarbonization opportunity.

For now, three main alternative fuels are considered to be pumped through the pipelines; biogas and biomethane, Hydrogen via methane, and power-to-gas: Synthetic natural gas via power to gas (Stern 2019).

a. Biogas and biomethane

Biogas is a product of the decomposition of organic matter with the help of anaerobic bacteria. These bacteria digest organic compounds such as municipal waste, animal waste, energy crops, wood, and agricultural residues. As an output of this bacterial digestion, a gas consisted of 60% methane and 40% CO_2 is released besides residual materials. This output biogas was then cleaned and filtered from CO_2 to obtain methane since the natural gas is also mainly methane. Therefore, processed biogas can be called renewable natural gas or biomethane (Islam et al. 2019, EIA 2021)

In terms of environmental impacts, although the biomass releases CO_2 emissions when it burns, it is assumed as carbon-neutral since the forest and agricultural-based residues consume CO_2 and emit O_2 when they grow. Thus, biogas sourced by energy crops, wood, and agriculture can also be considered carbon neutral. Furthermore, biomass combustion with an installed carbon capture and storage (CCS) system may result in a negative net emission. However, combustion in distributed boilers makes CCS impossible. On the other hand, utilizing these biodegradable wastes and burning these gasses will help to decrease the dependency on fossil fuels and positively affect the environment, while the use of these organic materials instead of composting may negatively impact (Sheikh 2017).

Unfortunately, in a scenario where all organic waste can be used for biogas production, the output can only meet 20% of the current natural gas and other fossil fuel demand (Ghosh et al. 2020). At the Vienna scale, the overall natural gas consumption is approximately 17,3 million GJ which roughly equals 465 million m^3, while the current biogas production is only 1,5 million m^3 (Stadt Wien 2021). Hence biogas cannot be a replacement for natural gas or other energy sources but shall be viewed as a backup source.

As a result, instead of residential heating, biogas can be a better option for other purposes such as electricity generation, industrial process heat production, and vehicles (Sheikh 2017).

b. Hydrogen

The most promising way to total decarbonization is using hydrogen as fuel in fuel cells, combustion engines, and boilers. Although hydrogen causes brittleness in metals, it can be pumped into the current pipelines with some alterations. At the heating system level, the conversion of conventional boilers with hydrogen boilers is necessary. In a no-adjustment scenario, a small fraction of hydrogen mixing with natural gas can be inserted directly into the pipeline to fuel the end-use appliances. (Erin Blanton et al. 2021).

Nowadays, most of the hydrogen is produced by the steam methane reforming process, which is an endothermic chemical reaction of methane with steam to generate hydrogen and carbon monoxide. Afterward, the product carbon monoxide is reacted with steam again to generate more hydrogen in the water-gas shift reaction. These processes are powered by fossil fuels and thus release CO_2. As a result, produced hydrogen is called “grey hydrogen.” Otherwise, if low-carbon fuels or a CCS system are involving to eliminate output CO_2, then called “blue hydrogen.” (Energy.gov n.d., Yu et al. 2021)

Also, hydrogen can be produced via electrolyzing water with electricity. If this electricity used in water electrolysis is excess or renewable-sourced, then produced hydrogen is called “green hydrogen” and can lead to deep decarbonization (Yu et al. 2021)

c. Synthetic natural gas

In this context, producing a gaseous fuel from electrical power is known as the power to gas (P2G) process. Besides electrolyzation, another P2G application for decarbonization is the methanation process. Carbon monoxide and dioxide can be converted into methane and water with hydrogen as a reagent in that reaction. The product methane is called substitute or synthetic natural gas (SNG). SNG is an identical replacement for natural gas and requires no adjustment in the pipelines and heating systems (Erin Blanton et al. 2021).

The most significant advantage of P2G is the storage capability of seasonal, intermittent energy. Meanwhile, the main drawback of P2G is efficiency. The efficiency of SNG production and acquisition of hydrogen by methane reforming is very low compare to other options. For every one-unit electricity input, a P2G process can deliver only 0,45 units of heat. The hydrogen production with electrolysis has relatively high efficiency. However, this green hydrogen production is strictly limited with renewable energy production and electrolyzer capacity (Sheikh 2017).

As a result of gas decarbonization, hydrogen technologies such as fuel cells and hydrogen burners/boilers are currently immature and uncommon. Nevertheless, they are developing fast, and with the improvements, these technologies will proliferate in the near future. Presently, using hydrogen in vehicles or electricity generation with fuel cells is more effective than directly using it in residential heating. For now, using the electricity generated by fuel cells to power the heat pumps has a much higher total system efficiency than burning those gasses in boilers for heating.

Briefly, decarbonized gas will definitely play a part in the future energy system. The storage possibility of excess energy is a tremendous advantage for these gasses.

Unfortunately, in terms of production, they cannot be produced enough to meet even a tiny fraction of the natural gas demand at the moment (Sheikh 2017).

1.3.3.3. Electrification

Electrification of the space heating means replacing the existing heating systems that cause direct emissions, such as fossil fuel furnaces, boilers, etc., with electric resistance or heat pump systems (Sheikh 2017). Although resistance heaters are inefficient, they are very cheap. Thus, using them in individual room heating for a brief time is more suitable. On the contrary, heat pump systems are highly efficient. Regarding their seasonal efficiency, Air-to-Air/Air-to-Water heat pumps and ground-source heat pumps are the two most efficient heating systems among the modern heating systems (Martinopoulos et al. 2018). In an overall assessment, they are one of the most suitable systems for the end-users. They can simultaneously provide cost-effectiveness and good environmental performance (Georges et al. 2012).

Among alternatives, electrification has almost no strict limitations. Resources for electricity generation are theoretically unlimited and continuous. Additionally, there is a massive production that possibly enables total electrification without building additional infrastructure. Europewide, if all fossil-fueled heating systems are shifted into the heat pumps systems, they would constitute 26% of the total electricity demand. Currently, average power generation in EU countries can supply the firm power for electrification up to 32% (Kavvadias et al. 2019).

Unfortunately, the general problem of electrification is that renewable electricity production is still not enough for total decarbonization, although it has been growing incredibly fast. In the current state, 78% of the electricity generated in Austria is sourced from renewables (IEA 2020a). The Austrian Long Term Strategy 2050 plan (2019) states that until 2030, 100% of electricity demand will be covered by renewables. Concerning the increment in demand by 2050, the achievement of this goal shall be secured. As a result of these facts and efforts mentioned above, electrification seems like the best opportunity for total decarbonization in the short term for Austria.

1.3.3.4. Conclusion

To sum up, electrification appears to be the most suitable way to decarbonize Austria's space heating in the near future. As Table 2 illustrates, theoretically, if electricity is clean enough, electrification can realize 100% decarbonization in space heating. In that regard, it has superiority over the other options.

Currently, all other options except electrification are short on production to be able to meet the heating demand by themselves. Due to decreasing PV panels costs, instead of using solar thermal collectors (STC) directly, implementing PV panels to generate electricity to assist electrification sounds better. Current and possible future biogas resources are far from supplying the demand, and they cannot contribute to decarbonization properly without CCS systems. On the P2G side, the SNG has the same emission releasing problem as biogas, and the SNG production is inefficient. Hydrogen is rising as the next promising option. It is one of the most promising alternatives in decarbonization for the future. Along with seasonal storage availability, device technologies are advancing, and their efficiency is increasing. However, presently these systems are not ripe for operation and are uncommon in service for space heating.

Table 2 Comparison of decarbonization options (Source: Sheikh 2017)

Option	Potential reduction
Solar thermal	70%
Biogas	20%
Synthetic methane	2%
Electrification	100%

1.3.4 Suitable heating systems for Vienna

Austria lies in central Europe between 46°N-49°N latitudes and 9°E-17°E longitudes. Mountains cover 62% of the country. Therefore, the continental climate is mainly seen with warm, wet summers and cold, dry winters. In northern and southern parts have a humid continental climate with Dfb Köppen climate classification. A dominant alpine climate influences the region with different Köppen groups Dfc, EF, and ET in the Alps region. However, the north-central, central, southern, and western parts, where Vienna lies, have an oceanic climate with Cfb Köppen (Weather-Atlas n.d., Kottek et al. 2006).

The Cfb climate class refers to (C) temperate climate with (f) no dry seasons and (b) warm summers. It is a warm temperate humid climate with the warmest month lower than 22° C over average and four or more months 10° C average (Arnfield 2020).

The HVAC system selection is based on multiple criteria according to ASHRAE (2020), including thermal comfort, local climate, building conditions, capacity, efficiency, investment, and operation cost. These criteria come to the forefront in selection. There are also various HVAC system classifications available. However, in this study, considering the criteria mentioned above, especially due to climatic conditions and residential building stock properties/conditions, it is assumed best to assess the HVAC system consistency according to working fluid classification in zoned air conditioning. While these systems can be divided into four, they can be examined in two major classes for heating: all air systems and all water systems (McDowall 2007).

1.3.4.1. All-air system

The heating fluid is air in the all-air system, and thermal energy is distributed through the building by that heated air via air ducts. Air can be conditioned in the air handling units (AHU), furnaces, split air conditioners (A/C), packaged terminal (PTAC) units, air to air heat pumps to supply heat into multiple zones or single zones (Seyam 2018).

The main advantages of this system are: it enables air ventilation inside for hygienic purposes, responds quickly to the heating demand, provides cooling and heating simultaneously in dual duct system types, and utilizes waste heat. The disadvantages are that it requires ample, separate space for implementing central units, large air ducts for heat distribution, and as the duct length increases, the system efficiency drops. (Gheji et al. 2016). As a result, in climates where the average temperatures are relatively low, the required air and the duct size would be too much to supply the high loads because the air's specific heat capacity and density are low. Therefore, installing this system in existing buildings in Vienna is difficult because of the old building stock situation and climate conditions.

1.3.4.2. All-water system

In the all-water system, the heating fluid is water, and the thermal energy is distributed through the building by heated water in the water pipes. Water can be conditioned in various boilers, solar thermal panels, district heating plants, and heat pumps to supply heat into multiple zones. The hot water heats the zones with different terminal units such as fan coil, convector, and radiator.

This system's main advantages are that it requires less system space and small pipe dimensions for the same load of an all-air system, costs less, and can provide cooling and heating simultaneously. Last but not least it can be easily installed in the old buildings with a bit of change. On the other hand, the disadvantages are: it lacks humidity control and mechanical ventilation (Gheji et al. 2016).

Evidently, all-water systems are more efficient and cost-effective in moderate climates. The heat can be generated in smaller units and transferred easily in small-sized pipes by water than air in big-sized ducts. That trait also gives the availability of easy implementation on old buildings and existing system shifting. Together this combination makes the all-water heating systems more suitable for Vienna and Austria conditions.

Finally, in the search for suitable heating systems for Vienna, in addition to the previous HVAC definitions, the heat pump systems are unrivaled in system technology. A recent academic study by Dermentzis et al. (2021) shows that heat pump is preferable to district heating, and district heating is preferable to NGB in Austria. According to the study, besides efficiency advantages, heat pump causes 75% less CO_2 emissions than NGB, and the district heating can achieve only 52%. Another significant finding is that implementing a heat pump at the building level saves 23% more primary energy than integrating heat pumps at the district level. The study reveals that individual ground-source (ground-coupled) heat pumps and then individual air-source heat pumps are the two most effective systems for both emissions and primary energy savings.

According to the “Technical report on the amendment to the building regulations for Vienna - 2018 (§2b energy room plans)-Economic comparison of different heating and hot water systems” published by the City of Vienna, ground-source heat pumps and air-source heat pumps are considered economically reasonable compared to other competitors due to their low operating costs. Moreover, these systems show significantly better performance than others in terms of greenhouse gas emissions. (Treberspurg and Stadt Wien 2019). Finally, administratively, as a policymaker, the City of Vienna encourages and enforces implementing HP systems and district heating with renewable sources (Stadt Wien 2020).

1.3.5 Heat pumps

Heat pumps (HP) are devices that can move heat from one medium to another by using electrical energy. Their efficiency comes basically from their ability to move heat from the source to the sink instead of generating heat by burning fuel. Since the HP cycle is reversible, it can be used for heating and cooling so that the heat can be moved from the outdoor to indoors during the heating season, from indoor to outdoor during the cooling season (Hailu 2021).

The efficiency of an HP depends on the temperature difference of the mediums and supplementary heat rate. Therefore, according to the weather and climate, an HP’s efficiency can differ in heating or cooling operations seasonally. As a result, there are various assessment terms to grade HP efficiency concerning their heating, cooling, seasonal and annual performance. They are mainly Coefficient of Performance (COP), Primary Energy Ratio (PER), Energy Efficiency Ratio (EER), Heating Season

Performance Factor (HSPF), Seasonal Energy Efficiency Ratio (SEER). Among them, COP is the most common method to compare HP systems heating efficiency and expressed as similar to basic efficiency formula in equation 1 (Dincer and Rosen 2015);

$$COP = \frac{Product\ Heat\ Output}{Electrical\ Energy\ Input} \tag{1}$$

HPs can be classified as shown in Table 3 regarding heat sources and sub-classified regarding heat source/sink relations.

Table 3 Heat pump classification (Source: Dincer and Rosen 2015)

Source	**Source/Sink**
Water Source	Water to water Water to air
Air Source	Air to air Air to water
Ground / Geothermal Source	Ground to water Ground to air
Solar Source	

In this study, the heat sink is thought of as water. That means, regarding the HP type, heat is transferred from air, ground, or groundwater to the water in the heat exchanger unit. The main reason for this limitation is the climate conditions and current residential building stock of Austria. As mentioned in chapter 1.3.2 Most common space heating systems used in Vienna, the average temperatures are low in the winter, so transferring generated heat via water is more feasible than air. When this reality combined with the fact that this system is cheaper and hot water boilers (with radiator/fan coil) dominate the Viennese building stock with district heating (water as heating fluid in radiator/fan coil terminal), water systems were considered the optimum solution. Hence this study searches for the most appropriate way to transform the systems for decarbonization, considering the retrofitting of existing systems with minimal intervention, it was deemed to evaluate two types of heat pumps that run water as a heating fluid in the further simulations. Thus, it will be possible to transform the current heating systems without changing the distribution lines and a few changes in their terminal systems.

1.3.5.1. Ground source heat pump

Ground/Brine to water heat pump or ground-source heat pump (GSHP) draws heat energy from the soil, groundwater, or both. The main idea is to benefit from the temperature below a particular depth underground, which is relatively constant over a year and typically between 5-10°C. Thus, heat can easily be absorbed in winter and ejected in summer. For heating, heat is transferred from the soil to the heating/working fluid (usually glycol solution) that flows through the buried pipes (Hundy et al. 2016). Those collector pipes for heat exchange from the soil can be installed horizontally and vertically under the ground (Vaillant 2020), as shown in Figures 2 a) and b).

The most significant advantage of this system is that owing to the constant underground temperature, it has a very high and stable COP for heating and cooling operations in different seasons, unlike air-source heat pumps. However, some critical handicaps make the application difficult. Firstly, this system requires a large area for heat transfer. Depending on the heating loads, 100-200 m deep drills and adequate space between multiple boreholes may be necessary for vertical systems. In horizontal systems, approximately double the size of the heated area is sought to meet the loads. That generally means a large amount of land. In a dense city, this empty area and free depth necessities highly restrict the usage of this system. Secondly, due to efficiency issues, it is not suitable for high-temperature radiators above 60°C. Thirdly, leakage of the working fluid would be very problematic. Finally, concerning loads, piping and drilling tend to be expensive for both vertical and horizontal applications. These disadvantages cause GSHPs less common than air-source heat pumps (Dincer and Rosen 2015, NRCAN 2004).

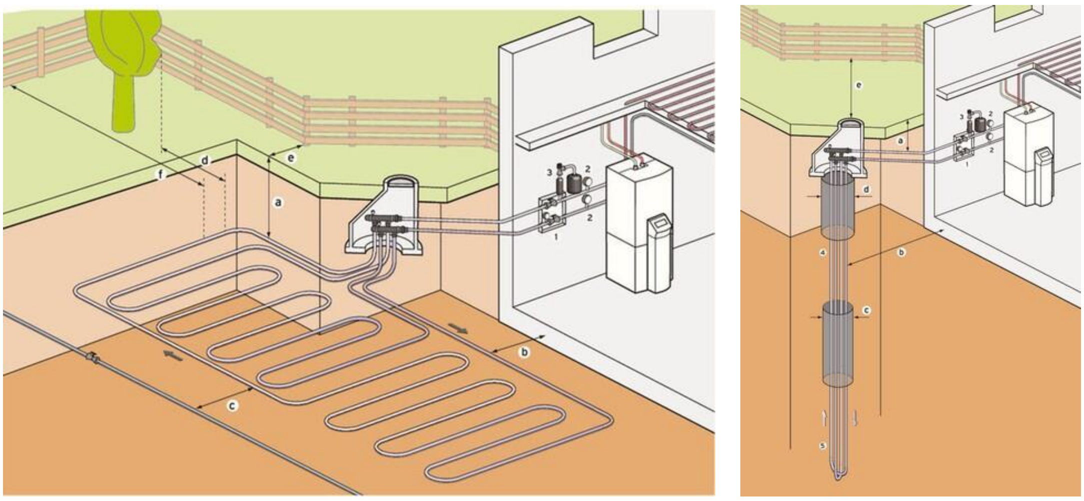

Figure 2 a) Horizontally and b) vertically installed GSHP collectors (source: www.vaillant.info)

1.3.5.2. Air source heat pump

The air-to-water type air-source heat pump (ASHP) draws the heat energy from the outdoor air. After the energy is drained from the air, that cooled air is discharged to the surrounding environment. Air-to-water HPs can still be operated in climates where the temperature drops to -20°C (Vaillant 2020). However, in cold and humid climates, frost may occur in outdoor units. Additionally, their efficiency drops drastically as the temperature difference increases between indoor and outdoor. Air-to-water HPs are used less frequently than air-to-air HPs; to be specific, air-to-air HPs are the most widely installed type of heat pump worldwide (Dincer and Rosen 2015, IEA 2020).

The air-to-water HP transfers ambient outdoor air heat to the water that flows in piping and terminal units. The same high-temperature supply problem as ground-to-water heat pump exists in this system as well, and thus it is unsuitable for supplying radiators above 60°C (NRCAN 2004).

Although their efficiency is slightly lower than GSHPs, the application of an ASHP is cheap, easy, and requires a little space. As shown in Figure 3, unlike GSHP, it does not require drilling or large spaces to install. Therefore, they fit better for the retrofitting regarding land properties, existing system installation, and easy capacity expansion availability. Those conveniences make it highly preferred in the market (NRCAN 2004).

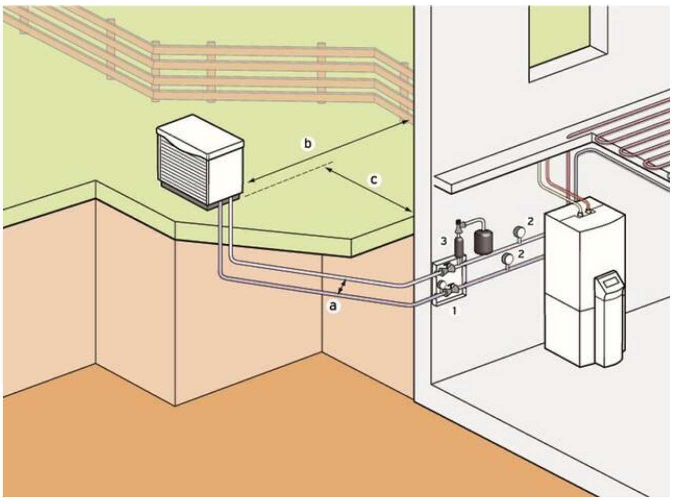

Figure 3 ASHP installation (source: www.vaillant.info)

1.3.5.3. Coefficient of performance

The average COP values for GSHP and ASHP are calculated from the data of the registered brands and their models to Energy Star. Energy Star is an agency backed by the Department of Energy of the U.S. Government to boost and certify the products according to their energy efficiency. Even though it is a U.S.-based agency, it has an enormous database about the COP values of the evaluated products worldwide.

Figure 4 and Figure 5 present the COP values of the Energy Star registered GSHPs and ASHPs in the market. According to those figures, the maximum range of COP goes 5.5 in GSHP while it goes 4.0 in ASHP systems. Most GSHP systems have a COP value between 3.9 and 4.5 (mean 4.3), whereas almost all ASHP systems have a COP value between 3.0 and 3.4 (mean 3.2).

Although these values are manufacturer data, the COP of an HP depends on the supply and heat source temperature. Especially for an ASHP, the instability of the outside air temperature affects the system COP. Therefore, in the characterization chapter, the COP values for these systems were considered within the range of these findings.

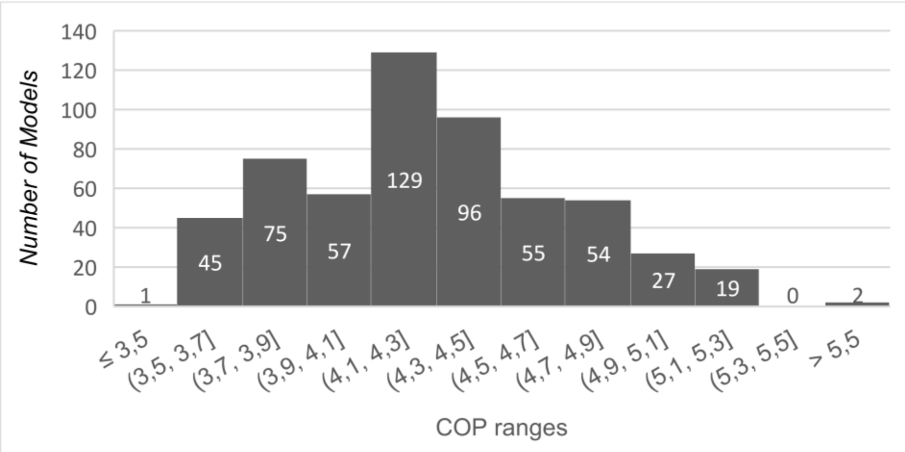

Figure 4 COP values of GSHPs in the market

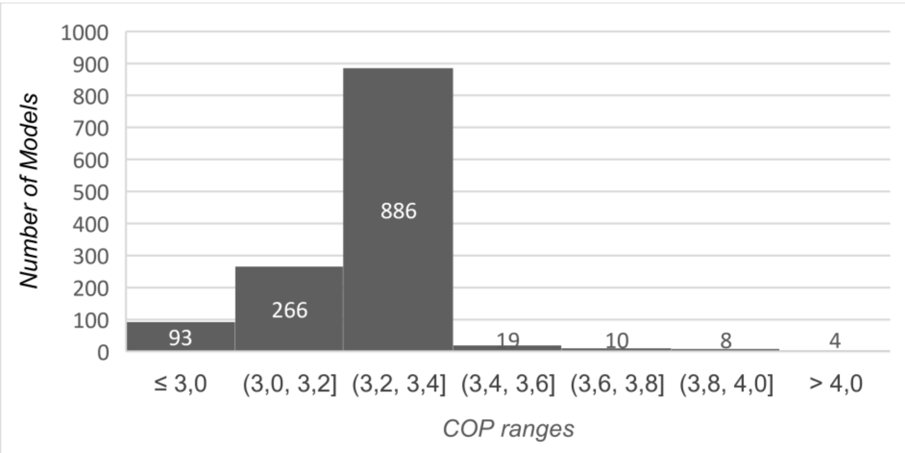

Figure 5 COP values of ASHPs in the market

2 METHOD

2.1 Overview

In order to assess the CO_2 reduction potential at the district scale in Vienna, the bottom-up approach of Urban Building Energy Modelling (see 2.2.1 Urban building energy modeling) was employed and performed in the following steps.

In the first step, five representative residential buildings classified within the 4th district were adopted from Ghiassi (2017). Afterward, geometric properties of those buildings were modeled 3-D with zones by Rhinoceros 3D version 7 (McNeel and others 2020) software.

In the second step, samples were characterized regarding to the available literature. The determined non-geometric properties pertaining to each sample building were assigned via Ladybug Tools v.1.2 (LT LCC 2021) add-on and Openstudio 3.2 (NREL 2021) software to run EnergyPlus energy simulation. Additionally, occupant-related parameters were set from standards and statistics to fulfill the energy simulation input parameters.

In the third step, manual calibrations were conducted by adjusting envelope properties to match the literature data's energy consumption values and increase result accuracy.

In the fourth step, the simulations were performed with current and predefined alternative heating systems to simulate the monthly energy and fuel demand. Subsequently, those demand values were converted into CO_2 emission rates by monthly CO_2 emission conversion factors.

Finally, these emission values were scaled up to the district scale to reach the total emission values, and consequently, the results were interpreted.

2.2 Case Study

2.2.1 Urban building energy modeling

Urban Building Energy Modelling (UBEM) enables the energy-based prediction and simulation of buildings at large scales. Its main purpose is to model the building stock to analyze, optimize and improve the energy systems (Ali et al. 2021). Swan and Ugursal (2009) categorized UBEM methods into two major approaches: top-down and bottom-up. Although sub-categories vary regarding studies, these approaches are generally classified into sub-categories, as in Figure 6.

The top-down approach uses any kind of statistical data and variables related to the energy consumption of the buildings and occupants to determine the energy requirements and effects of consumption at the target scale. Thus, it does not rely on individual building details or information. However, while it requires fewer input data to model, it is unsuitable for future energy predictions since inputs are based on past data. Additionally, it sometimes gives just cumulative data as results that lack spatial or temporal detail precision. Conversely, in the bottom-up approach, the energy consumption of individual sample buildings reflecting similar group properties are calculated and aggregated to find upscaled consumptions of that target scale (Ferrando et al. 2020, Ali et al. 2021).

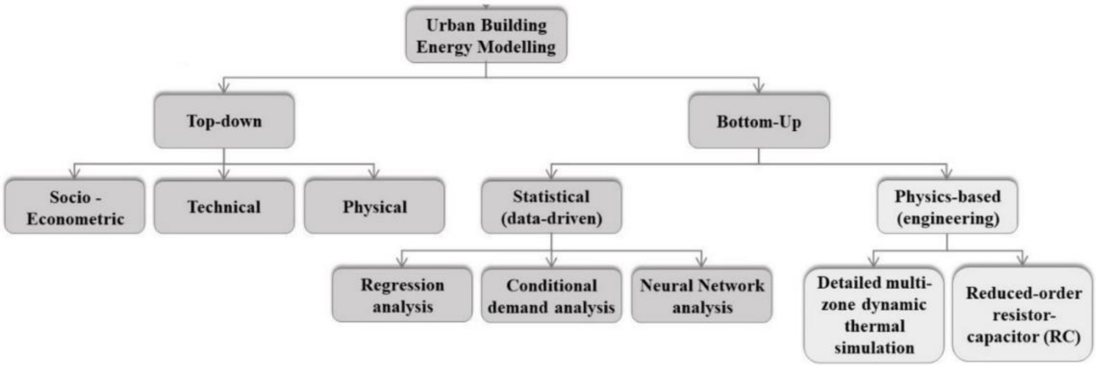

Figure 6 UBEM approaches (source: Ferrando et al. 2020)

Ang et al. (2020) define four main UBEM applications, including stock-level carbon reduction strategies. Briefly, they state that among similar types, age, categories, or archetypes, the effect of the energy-saving upgrades on the buildings should be calculated/simulated to assess the benefits of those upgrades at urban scale. Thus, energy saving from upgrades, such as enhanced lighting, weatherization, or HVAC systems, can be compared between themselves and the current state. Afterward, the total CO_2 emission reduction and energy savings potential can be assessed using these simulation results and the applied model. Table 4 presents some selected studies about stock-level carbon reduction strategies and energy policies specifically simulated using Rhinoceros 3D and EnergyPlus and modeled by a bottom-up physics-based approach of UBEM.

Table 4 Selected studies on stock-level carbon reduction strategies (source: Ang et al. 2020)

City/Region	Number of buildings	Target Use/Application	Calibration Level	Accuracy or Uncertainty
Boston (USA)	83,541	Energy policy, district level interventions	None/Not found	An error of averaged modeled EUI ranged between 5% and 20%
Kuwait	336	Support urban energy efficiency strategies	Archetype	Maximum error of 15% in 10th and 90th percentile for best performing model (Bayesian calibrated)
Cambridge (USA)	2,662	Assess retrofit strategies and energy supply options	Archetype	16.5% of buildings unexplained when calibrating to monthly data vs. < 1% when using annual

The physics-based/engineering approach has strengths in evaluating new technology implementations without any previous consumption data. In this approach, by simulating the energy consumption of sample buildings of the residential stock, the total consumption of that stock can be extrapolated. In the case that the building stock can be classified regarding size, age, type like geometrical properties, the archetypes can be created to represent each major class in the stock. These archetype descriptions are used in modeling to obtain energy consumption estimations. Then individual estimations are multiplied by the number of houses that fit the description of each archetype to provide stock level "scaled-up" results (Swan and Ugursal 2009).

Reinhart and Cerezo Davila (2016) discussed the bottom-up approach and pointed that the archetype approach is widely used to evaluate the impact of new technologies and policies in bottom-up models. Swan and Ugursal (2009 p.1833) pointed in their research, *"Bottom-up engineering techniques are used to explicitly calculate the energy consumption of end-uses based on detailed descriptions of a representative set of houses, and these techniques have the capability of determining the impact of new technologies."*

Hence this study assesses the CO_2 reduction potential through heating system retrofit, the physics-based bottom-up approach (PBBU) has been adopted as the research method due to previous conclusions.

Cerezo Davila, Reinhart, and Bemis (2016) identify an efficient PBBU-UBEM workflow in the following steps, "Model characterization, Model generation, Model simulation, and Analysis." In a further study, Cerezo et al. (2017) has applied the following workflow "Archetype classification, Archetype characterization, Occupant related parameters, and Archetype calibration in UBEM" for model characterization and generation.

2.2.2 Representative building determination

Owing to the upscaling process, the urban scale results rely entirely on the selected buildings' representation ability within the stock. Therefore, this stage is essential to ensure the results' correctness.

The representative building definition and selection among a stock requires another expertise. Therefore, instead of developing adequate representatives for Vienna's building stock, existing sources were investigated to obtain them (Please see 2.2.3 Representative building selection). In this section, the representative buildings were selected and adopted from Ghiassi's (2017) dissertation "An Hourglass Approach to Urban Energy Computing."

Then, these buildings were analyzed regarding their current heating systems and alternative heating system availabilities. At last, they were modeled geometrically with Rhinoceros 3D version 7 (McNeel and others 2020) in accordance with their blueprints.

2.2.3 Representative building selection

To employ a representative model for a UBEM upscaling process, Swan and Ugursal (2009) identified three definitions: distributions, archetypes, and samples.

Distributions: The models are created according to the distribution of appliance ownership. The model demand is the product of this distribution and the related common energy rating of those appliances. Consequently, the total consumption of the stock is estimated via aggregating model demand (Swan and Ugursal 2009).

Archetypes: The models are defined based on the classification of the housing stock regarding its age, size, purpose, etc. The representative buildings generally define each major class in the stock. Features belong to those major classes are assigned as input for energy simulations. The total consumption of the stock is estimated by multiplying the energy consumption of each modeled archetype with the number of houses represented by them (Swan and Ugursal 2009).

Samples: The samples are selected among the existing houses in the stock so that actual features such as building dimensions, usage, system type, operation scenario are used in energy simulation as well. Further, actual data can be used to calibrate the simulations and results. The total consumption of the stock is estimated by applying appropriate weightings to the individual results. This method can provide a high accuracy on results. However, the need for an extensive database of representative buildings to determine samples and intensive feature information for simulation limits its application (Swan and Ugursal 2009).

According to the definitions, modeling with samples has an apparent strength in accuracy over other methods. Therefore, besides reports and research, the data from the Austrian Statistical Institute, Stadt Wien, Entranze project, and Tabula project were considered to find a suitable representative model for this study. Consequently, concerning the method and aim of this study, it was decided that Ghiassi's (2017) dissertation work offers the most comprehensive and detailed information about representative buildings for a case study in Vienna.

In her work, Ghiassi (2017) selected an area in the center of Vienna where comprises the first, fourth, and sixth districts and covers approximately 1.3 square kilometers of land (see Figure 32 in Appendix). This area includes 744 buildings with different features and reflects Vienna's predominant historical building stock very well. In the downscaling process, multivariate cluster analyses were performed concerning various indicators such as geometry, solar gains, thermal quality, operational parameters to classify the building stock in the selected area. Finally, the best-performing clustering scenario resulted in seven clusters that share similar descriptive indicators. That means seven major building classes can represent the stock accurately enough. Among them, except clusters four and six, all remaining five clusters are residentials.

Since this study researches the potential in residential stock, five of these seven sample buildings were accepted as representative buildings, all of which lie in Vienna's fourth district.

2.2.4 Sample building analyses

The selected buildings were analyzed regarding their age, area, and location to comprehend how to provide the missing features about the models, such as their envelope types and current heating systems, and determine alternative heating systems' availability.

The buildings' age distribution is as follows: Two of the five buildings were constructed before 1900, one was constructed before 1945, one was constructed between 1945-1960, and one was constructed after 1993. This age categorization is essential in chapter 2.2.6 Sample characterization to assign and limit U-values according to reference values in ÖIB-6 guidelines.

In Vienna, 90% of the heating systems are NGBs and district heating; also, Fernwärme Wien is the sole district heating supplier. Therefore, to detect the current heating system, an address-based web search about district availability "ist Fernwärme bei mir verfügbar?" was conducted on Wien Energie's webpage (Wien Energie 2021). Regarding the search results, when a connection is found, the heating system was assumed to be district heating; otherwise, the system was assumed to be an NGB. As a result of these searches, it was concluded that only the first sample building in the Mühlgasse 7,1040 seems to have a connection to district heating.

Possible heating systems availability was performed visually by checking the yards and roofs of the buildings. Visual inspection shows that all sample buildings have an ASHP implementation availability owing to roof and yard spaces. In contrast, only three of them have a suitable space for any GSHP probe installation. Additionally, the walls and windows of the buildings are suitable for split unit installations, though it is not recommended. Table 5 shows the heating system availabilities in the sample buildings.

Nevertheless, only one building among the samples connects district heating; the City of Vienna aims to decarbonize the district heating and supports the expansion and utilization of this system besides HPs (Stadt Wien et al. 2019). Therefore, district heating was assumed as another system with decarbonization potential.

Table 5 Heating system availabilities of the sample buildings

Possible Systems	**Sample 1** (Cluster 1)	**Sample 2** (Cluster 2)	**Sample 3** (Cluster 3)	**Sample 4** (Cluster 5)	**Sample 5** (Cluster 7)
DH	✓	✓	✓	✓	✓
ASHP	✓	✓	✓	✓	✓
GSHP	✓	✓	×	×	✓

a. Sample building 1 for Cluster 1

The first sample building was constructed in 1914 and facing North-West direction. District heating is connected as a heating system. According to Figure 7, the building has an available yard for a GSHP with a vertical probe. Further, the roof and the yard are suitable for ASHP systems.

Figure 7 First sample building's aerial views (source: Google Earth)

b. Sample building 2 for Cluster 2

The second sample building was constructed in 1953 and facing North-West direction. Central/combi boiler is employed as a heating system. According to Figure 8, the building has an available yard for a GSHP with a vertical probe. Further, the roof and the yard are suitable for ASHP systems

Figure 8 Second sample building's aerial view (source: Google Earth)

c. Sample building 3 for Cluster 3

The third sample building was constructed in 1846 and facing South-East direction. Central/combi boiler is employed as a heating system. According to Figure 9, the building does not have an available yard for a GSHP. However, the roof is suitable for ASHP systems.

Figure 9 Third sample building's aerial view (source: Google Earth)

d. Sample building 4 for Cluster 5

The fourth sample building was constructed in 1872 and facing South-West direction. Central/combi boiler is employed as a heating system. According to Figure 10, the building does not have an available yard for a GSHP. However, the roof is suitable for ASHP systems.

Figure 10 Fourth sample building's aerial view (source: Google Earth)

e. Sample building 5 for Cluster 7

The fifth sample building was constructed in 2000 and facing North-West direction. Central/combi boiler is employed as a heating system. According to Figure 11, the building has an available yard for a GSHP with a vertical probe. Further, the roof and the yard are suitable for ASHP systems.

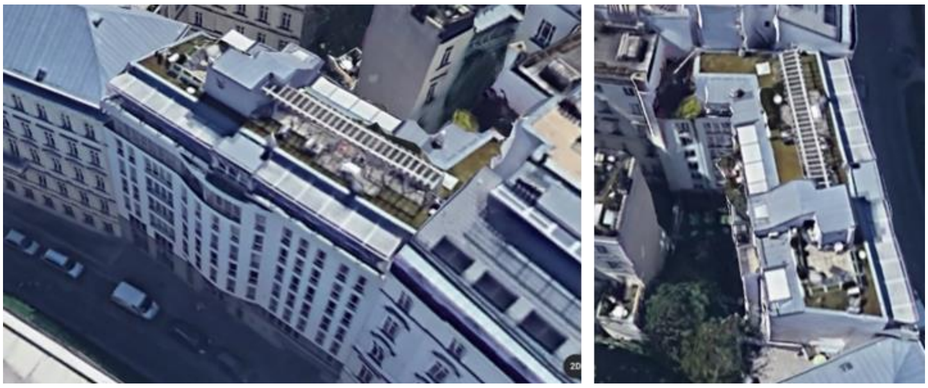

Figure 11 Fifth sample building's aerial view (source: Google Earth)

2.2.5 Sample building modeling

Five samples were 3D modeled according to their registered blueprints (MA-37 Baupolizei, Stadt Wien) by Rhinocherous 7 software. In this section, only the geometric properties had been assigned to the CAD, then the non-geometric features and occupant factors were assigned (with Grasshopper toolkit of Rhinocherous 7 software) to the simulation model in the succeeding chapters.

Instead of generating shoebox models, the buildings were modeled highly detailed. Inner walls were defined in order to create a realistic thermal mass. Additionally, each room, stair, roof, and basement correspond to a zone, thanks to inner wall definitions. Thus, the proper model-layer definition in this stage eased the thermal zone definition and occupant-related parameter assignment to the zones in the simulation phase. Windows and doors were modeled as in the blueprints to employ the original windows-wall ratios in the simulation.

Figure 12 illustrates the CAD model of the first sample building (Please see Appendix for the sample buildings' 3D model illustrations). In that model, red spaces represent conditioned zones while the blue ones represent unconditioned. Thus, ÖNORM definitions and the "Mid-rise apartment: Apartment" schedule were assigned to red spaces where contain rooms, and the "Mid-rise apartment: Corridor" schedule for blue spaces where includes the roof, basement, and stairs. Except for balconies and indoor apertures, all details were modeled as blueprints while the surrounding geometries were inputted as shoebox geometries.

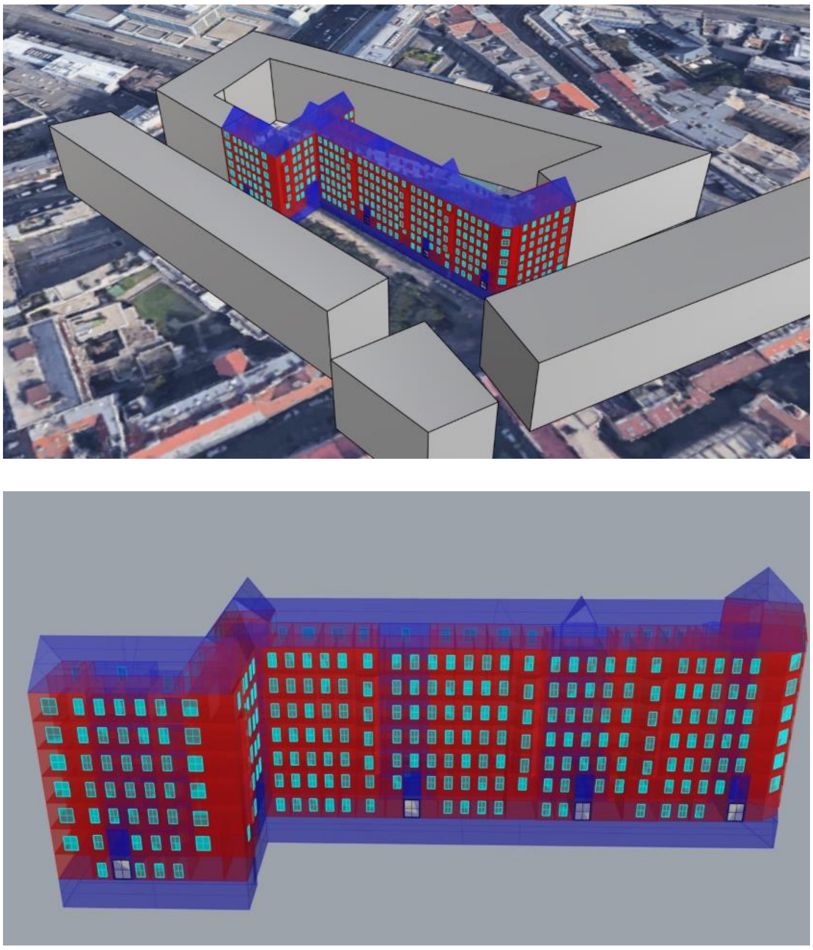

Figure 12 CAD model of the first sample building

2.2.6 Sample characterization

Building characterization refers to allocating relevant energy simulation parameters to the model, including non-geometric and occupant-related factors. Namely, these parameters are building envelope details, HVAC system properties, internal loads, relevant schedules of occupants, lighting, and equipment that enable heat transfer and energy demand calculations (Cerezo et al. 2017).

Although the representatives are existing buildings sampled from the target stock, unfortunately, there is no information other than their geometries. Therefore, to fill the missing input parameters for simulations, the existing methods were examined. As a result, two methods, including deterministic and probabilistic, can be applied to determine these parameters. In a deterministic way, a single value or class is assigned for each parameter, while in a probabilistic way, multiple values or classes are assigned to simulation calculations (Mohammadiziazi et al. 2021).

In this regard, the deterministic way is widely applied in characterization via allocation of actual building characteristics or average data from the literature (Cerezo et al. 2017). Since there is no non-geometric information about actual buildings, to achieve the parameter determination, the required data were searched and extracted from the relevant literature such as building surveys, codes, standards, statistics, reports, research. Next, determined values from the literature were assigned to every building in the corresponding age group.

Table 6 illustrates the literature that the missing parameters were obtained to run the energy simulations. Construction details were taken from the "Handbook for Thermal Retrofit of Buildings" (Schöberl et al. 2012). The envelope properties were controlled according to the reference U-values stated in guidelines of the Austrian Institute of Construction Engineering (ÖIB 2019). Occupancy schedules were taken from Openstudio (NREL 2021) templates using ASHRAE 90.1 (2013) and IECC (2015), and ÖNORM B 8110-5 (2019). Meanwhile, people per area statistic was obtained from the City of Vienna (Stadt Wien 2011). Lightning and electrical equipment related heat gain and their relevant schedules were taken from Austrian Standards "Thermal insulation in building construction - Part 5: Model of climate and user profiles" ÖNORM B 8110-5 (2019). Ventilation and heating setpoint values and schedules were also assigned according to ÖNORM B 8110-5 (2019). The weather data of Vienna (Schwechat) was downloaded from the Energyplus weather data library.

Table 6 Literature list used for building characterization parameters assignment

	Non-geometric parameter	**Resources/References**
Construction	Envelope Details	WKO, ÖIB 6
Occupancy	People per Area	Statistics from the City of Vienna
	Occupancy Schedule Activity Schedule	OpenStudio, ÖNORM B 8110-5
Lightning	Watts per Area Schedule	ÖNORM B 8110-5
Appliances	Watts per Area Schedule	ÖNORM B 8110-5
Infiltration	ACH Schedule	OpenStudio
Ventilation	ACH Schedule	ÖNORM B 8110-5
Heating Setpoint	Setpoint Temperature Schedule	ÖNORM B 8110-5
	Weather Data	EnergyPlus

The Handbook for Thermal Retrofit of Buildings (Schöberl et al. 2012), published by the Austrian Chamber of Commerce (WKO), describes building components for three construction groups: historical buildings, historical buildings with preserved facades, and new buildings constructed after 2000. In this study, the second and the fifth sample buildings' construction sets were characterized as new buildings while the rest were historical buildings as in the handbook. The properties such as thermal conductivity, density, and specific heat capacity of the layer materials of the building components were filled from the web-based database called MASEA (Masea 2014). After the components and their properties were assigned, the resultant U-values were controlled if they were in range with the default values stated in the OIB-6 guideline. This guideline defines default U-values for specific eras. Openstudio's template schedules were used in the occupancy schedule. Two schedule programs were used "2013: Midrise Apartment: Apartment" for all rooms, namely conditioned zones, and "2013: Midrise Apartment: Corridor" for all basement, stairs, and roof, namely unconditioned zones. Austrian Standart B 8110-5 recommends usage profile values, including thermostat temperatures, air change rates, and heat gains, for the heating energy use calculations. According to the standard, the residential heating setpoint temperature should be 22°C for 24 hours and 365 days in heating calculations. The ventilation is only for hygienic purposes, and the air change rate is 0.38 1/h. The internal heat gains are defined as 4.0625 W/m^2, and 0.64% of this value corresponds to appliances. The standard defines these loads as constant and continuous as well. Last but not least, infiltration was also assigned from Openstudio templates between three definitions. The fifth sample was defined as "tight building," meanwhile all others were defined as "leaky building." These values are summarized in Table 7.

Table 7 Acquired reference values of characterization parameters

Parameter	Unit	Period	Value
Basement Floor U -value			1.25
Top Floor U-value			0.75
Outer Wall U-value		Before 1900	1.55
Roof U-value			1.30
Windows U-value			2.50
Basement Floor U -value			1.20
Top Floor U-value			1.20
Outer Wall U-value		Between 1900 to 1945	1.50
Roof U-value			1.00
Windows U-value	W/m^2K		2.50
Basement Floor U -value			1.10
Top Floor U-value			1.35
Outer Wall U-value		Between 1945 to 1960	1.30
Roof U-value			1.30
Windows U-value			2.50
Basement Floor U -value			0.40
Top Floor U-value			0.20
Outer Wall U-value		After 1993	0.50
Roof U-value			0.20
Windows U-value			1.90
Occupant density	$1/m^2$	All periods	0.026
Appliance and Lighting Heat Gain Rate	W/m^2	All periods	2.60
Infiltration Rate	$(m^3/s)/m^2$	Before 1993	0.0006
		After 1993	0.0001
Ventilation Rate	ACH	All periods	0.38
Heating Setpoint	°C	All periods	22 (constant)
Heating Schedule			24 h / 365 d

These determined parameters were paired with the predefined 3D models via the Grasshopper toolkit of Rhinoceros 3D version 7 (McNeel and others 2020). The components of “Ladybug Tools,” an add-on for Grasshopper, were used to assign parameters to generate energy models of each sample building. Briefly, Ladybug Tools v.1.2 (LT LCC 2021) connects the geometries and parameters in Grasshopper and transfers this data into an IDF (input data files) format to run the EnergyPlus (2021) simulation via Openstudio (NREL 2021).

2.2.7 Calibration of the characterized models

In their research, Ferrando et al. (2020) state that simplification for modeling, such as downscaling and characterization, causes uncertainties in the BEM and UBEM results. Therefore, calibration and validation are required to avoid uncertainties and improve the results. Cerezo et al. (2017) conclude that calibration can reduce errors on EUI distribution 14-35% against typical models and express in their work that calibration for UBEM can be applied at any level from building to target stock as long as the corresponding measured data exists.

Although the literature was selected meticulously for characterization in this study, this data does not belong to the actual buildings. In the upscaling process, possible errors of single building simulations would aggregate to more significant amounts. Therefore, model calibration was considered necessary to increase the reliability of the results.

According to the revised definitions of Fabrizio and Monetti (2015), four calibration methods can be performed with analytical and mathematical approaches;

i. Manual calibration methods based on an iterative approach,
ii. Graphical-based calibration methods,
iii. Calibration based on special tests and analysis procedures,
iv. Automated techniques,
    - Bayesian Calibration
    - Meta-Modeling According
    - Optimization-Based Methods

Nowadays, automated methods are popular because of their detailed control potential on the model for accuracy improvement. That is true for complex dynamic models with large datasets of measured data. However, they need a long simulation period due to many parameters and simulations. In reverse situations, calibration can be done simply by manual calibration with a trial-error approach (Fabrizio and Monetti 2015).

Manual calibration is based on the user experience and judgment and is the most common calibration method in simulations. The trial-and-error approach refers to a manual iterative input parameter adjustment. Input parameters are modified according to experience and knowledge in the simulation model until the results fit (Fabrizio and Monetti 2015).

In addition, statistical indices to measure the goodness of fit is generally necessary from an international reference for this process to be considered calibration (Fabrizio and Monetti 2015).

In this study, a manual calibration, trial-and-error approach with the limit values of the International Performance Measurement and Verification Protocol (IPMVP 2002) in

Table 8 was applied. Normally, according to various international organizations, the calculation of two indices is mandatory to fulfill this procedure. However, considering the interval, only the MBE index calculation is sufficient in IPMVP's definitions.

Table 8 Threshold limits of statistical criteria for calibration (IPMVP) (source: IPMVP 2002)

Statistical Indices	**Monthly Calibration**	**Hourly Calibration**
MBE [%]	±20	±5
Cv(RMSE) [%]	-	20

MBE stands for Mean Bias Error and is a calibration index that measures how closely simulation results match the monitored data. Equation 2 shows the calculation in which the sum value of the difference between monitored (M) and simulated (S) values at calculation intervals (hour, month, year) of the total period is divided by the sum of the monitored values (US Department of Energy 2015).

$$MBE\ (\%) = \frac{\sum_{period}(S-M)_{interval}}{\sum_{period} M_{interval}}\ x\ 100\% \qquad (2)$$

Unfortunately, there is no available data on the measurement side. For the basic calibration calculation, neither measured data such as meter readings, utility bills nor audited data such as energy certificates are not accessible. Furthermore, due to the current energy efficiency regulations and lack of recent retrofit information, the energy consumption ranges in the previous literature are not a good match for this study.

Therefore, using the previous energy simulation results of these very same samples from Ghiassi's (2017) dissertation were considered the most appropriate for calibration in this situation. For this reason, this literature data is assumed as measured data in MBE calculations for calibration

Consequently, for each sample building, an energy simulation was performed to calculate the ideal loads. Then the simulated energy consumption measure of "Heating Demand per Total Building Area" data was calibrated with the literature data. The calibrations were performed by changing the "insulation thickness" parameter within the defined range of the pertaining building component in the WKO handbook.

Typically, smaller timesteps mean better results; however, only one value (one interval) for an annual period exists on the monitored data side. Therefore, the monthly interval limits of IPMVP were assumedly applied for the MBE limit check as an annual limit.

Multiple simulations were performed continuously by changing the calibration parameter manually within its range until the MBE drops within ±20%. Table 9 illustrates the calibrated "Heating Demand per Total Building Area" values of the sample buildings and the MBE values of these calibrations.

Table 9 Energy consumption calibration results of the sample buildings

Heating Demand per Total Building	**Sample 1** (Cluster 1)	**Sample 2** (Cluster 2)	**Sample 3** (Cluster 3)	**Sample 4** (Cluster 5)	**Sample 5** (Cluster 7)
Literature kWh/m²a	99,37	88,38	85,20	96,33	43,46
Simulated kWh/m²a	87,43	94,20	80,43	99,84	50,75
MBE [%]	**-12,02%**	**6,59%**	**-5,60%**	**3,64%**	**16,77%**

2.2.8 Simulation of the calibrated models

Energy simulations were performed in the Grasshopper toolkit by EnegyPlus v9.5 (EnergyPlus 2021), an open-source building energy modeling engine that can simulate energy consumption and water use. In the first step, the calibrated sample buildings were simulated with respect to their heating systems which were determined in chapter 1.3.4 Suitable heating systems for Vienna. Initially, the first sample building was simulated with district heating and the rest with boilers. Afterward, the models were simulated several times by shifting their heating systems with the predefined alternative systems, ASHP, GSHP, and also additionally with district heating. At the end of each simulation, the end-use heating energy values for the different heating systems were noted for comparison.

The required weather file was downloaded from (EnergyPlus 2021), which is based on the data collected from Vienna Schwechat. Table 10 presents the critical settings used in the simulations.

For the simulations, the terrain type was set to "city." Further, to speed up the simulation while preserving accuracy, the simulation timestep per hour was set to "6." The solar distribution was set as "FullExterior" to avoid geometry-related shading calculation errors.

The other vital settings were heating system assignments. For these settings, instead of assigning COP values to ideal loads, the template systems from Honeybee-Energy's (an application of Ladybug Tools 1.2) "HB HVAC Heating Cooling Templates" component were embraced.

- "Baseboard Gas Boiler" was selected for natural gas boilers

- “Baseboard district hot water” was selected for district heating
- “Baseboard central air source heat pump” was selected for ASHP
- “Water source heat pumps with ground source heat pump” was adopted for GSHP.

Description of these templates are:

“Baseboard Gas Boiler” template corresponds to a central boiler system with hot water baseboard heaters (radiator, fan coil, etc.) as the terminal units. The defined efficiency of this system is 78% which is in the defined range for a non-condensing NGB. Similarly, the “Baseboard central air source heat pump” system is the combination of ASHP as a central unit and baseboard heater as the terminal units. As mentioned in 1.3.5.3 Coefficient of performance section, the COP of heat pumps depends on the supply and source temperature (outside temperature for ASHP). Hence the COP can vary easily due to outside temperature. For this reason, the template COP values were controlled if they are in the calculated range. According to the ASHP template definition, the COP curve results in a range between 2.3-3.65. Nevertheless, for 10°C (assumedly average outside temperature for heating according to the climate data), the COP is 3.4, which is also in the defined range.

The “Water source heat pumps with ground source” option in the templates can be described as a coupled system in which GSHP serves as a central unit, and water source heat pumps operate on the zones. The defined COP value for this system is 4.2 for heating and perfectly lays within the COP range determined in the 1.3.5.3 Coefficient of performance section.

Table 10 Critical simulation settings

Simulation Parameter	**Setting / Value**
Terrain	City
Solar Distribution	Full Exterior
Shading Calculation Method	Polygon Clipping
Timesteps per hour	6
Boiler Efficiency	78%
GSHP COP	4.2
ASHP COP	2.3-3.65

2.2.9 Emission conversion and upscaling

The simulated consumption values of heating systems defined for each sample building were then converted into CO_2 emissions equivalent. The equivalent CO_2 emission conversion factors (fCO_2eq) for the relevant fuels, as shown in Table 11, were adopted from the OIB-6 (ÖIB 2019b) directives published by the Austrian

Institute of Construction Engineering. Consumption values of boilers were converted with 247 g/ kWh “natural gas, “ and district heating with a value of 192,5 g/kWh, which is an average factor value of “District heating from the heating plant (non-renewable) and “District heating from CHP.“ It is because, as mentioned in 1.3.2 Most common space heating systems used in Vienna, district heat power capacity in Vienna is installed with a rate of approximately 45% in combined heat and power plants and 45% in heating plants. Moreover, the assumption is, employing DH proportionally with its full capacity to supply the loads continuously. Hence, in calculations, instead of past heat generation rates, the installed capacity rates are used (capacity expansion will be similar to the existing generation). This assumption also led to the presumption that no renewable resources are used in heat generation. As a result, it is considered that in heat production for DH, no CO_2 emission fluctuation occurs during the year related to primary energy source changes.

Table 11 CO_2 emission conversion factors for the relevant fuels (source:ÖIB)

Energy Source	**Conversion Factor (fCO_2eq) [g/kWh]**
Natural Gas	247
District heating from HP (renewable)	59
District heating from HP (non-renewable)	310
District heating from CHP	75
Electricity (mixed energy-sources)	227

These conversion factors represent the conventional fossil fuels well since the burning emissions of a unit of fossil fuel do not change over a period. However, electricity emission changes over a year because it is generated from different primary energy sources, including renewable energies, of which the contribution varies depending on seasons. For instance, in the winter season, where the heating consumption is high, the electricity-related emissions are higher due to lower renewable energy availability. Therefore, the monthly emission conversion factors for electricity were adopted from a recent report of the Federal Ministry for Climate Action, Environment, Energy, Mobility, Innovation and Technology (Mair am Tinkhof et al. 2017). These values can be seen in Table 12. Last, with the help of these factors, all consumption values were converted from kWh to gram (or GWh to tonne) monthly.

Table 12 Average monthly values of the CO_2eq factors of the Austrian consumer electricity mix (source: Federal Ministry for Climate Action, Environment, Energy, Mobility, Innovation, and Technology)

Factor	**Unit**	**Jan**	**Feb**	**Mar**	**Apr**	**May**	**Jun**	**Jul**	**Aug**	**Sep**	**Oct**	**Nov**	**Dec**
fCO_2eq	g/kWh	290	323	261	178	103	96	116	117	172	259	291	314

In the final step, the converted results were scaled up in how Swan and Ugursal (2009) identify the way for the physics-based method (please see 2.2.3 Representative building selection). The results were simply augmented by multiplying them with the number of buildings represented by corresponding samples (as appropriate weighting). Table 13 shows the numbers of the sampled buildings (cluster's size) in the study area for the upscaling.

Table 13 Number of sampled buildings (source: Ghiassi 2017; Oberwalder 2021)

	Sample 1 (Cluster 1)	**Sample 2** (Cluster 2)	**Sample 3** (Cluster 3)	**Sample 4** (Cluster 5)	**Sample 5** (Cluster 7)
Count	125	94	201	109	6
Total			535		

Finally, the upscaled CO_2 emission values were examined in three different scenarios to measure the decarbonization potential of alternative heating systems in Vienna.

2.3 Hypothesis

In an ambitious decarbonization scenario including a rapid transition of space heating systems due to fossil fuel phase-out regulations in Vienna by 2030, district heating or electrification of space heating systems can reduce at least 40% of the related emissions even compared to the current levels without further decarbonization in electricity generation and district heating production.

3 RESULTS

3.1 Overview

The results are presented in two scales. First, the individual building scale shows the effects of the different space heating systems on energy consumption and CO_2 emissions.

Second, three different heating system scenarios were created. These scenarios were applied to samples. Afterward, the consumption and emission results of these scenarios and the existing state were scaled up to see the heating systems' overall potential at the district scale.

These scenarios in Table 14 were formed by implementing natural gas boiler “NGB,” district heating “DH,” air-source heat pump “ASHP,” and ground-source heat pump “GSHP” in different combinations.

Table 14 Created scenarios for measuring decarbonization potential of mass implementation of alternative heating systems

Scenario	**Sample 1** (Cluster 1)	**Sample 2** (Cluster 2)	**Sample 3** (Cluster 3)	**Sample 4** (Cluster 5)	**Sample 5** (Cluster 7)
Current state	DH	NGB	NGB	NGB	NGB
Scenario 1	DH	DH	DH	DH	DH
Scenario 2	GSHP	GSHP	ASHP	ASHP	GSHP
Scenario 3	ASHP	ASHP	ASHP	ASHP	ASHP

These scenarios are:

- Current state: Existing systems
- Scenario 1: Space heating with district heating
- Scenario 2: Space heating with most efficient heat pump where available
- Scenario 3: Space heating with air source heat pumps

Therefore, in the “current state,” the existing heating systems are analyzed. “Scenario 1” depicts a situation in which all systems converted to DH while in “Scenario 3” to ASHP. “Scenario 2” is constructed upon the situation that the highest COP heat pumps are installed where possible.

3.2 Building Scale

This section shows different heating systems' energy consumption and CO_2 emission impacts on the sample building scale. Therefore, the results are more likely to demonstrate the heating systems' monthly effects.

Figures 13, 16, 19, 22, and 25 show the simulated monthly heating energy consumption values [kWh] of different heating systems on each sample. According to the monthly results, from May to October, there is no significant heating energy demand. The maximum consumption in all heating systems occurs in January, and it is slightly higher than the consumption in December. During January, the highest consumption occurred in sample 1. DH requires 145 MWh for heating, while for the same period, GSHP requires 46 MWh. Again, in January, the lowest consumption occurred in Sample 2. NGB requires 30 MWh for heating while 8 MWh is enough for GSHP. In all months and samples, the site energy consumption values of heat pumps are less than half of DH. Nevertheless, the consumption difference varies between the two heat pump types. The consumptions of these systems in April and October (Spring and Autumn) are not noteworthy since they are nearly the same. However, the consumption gap increases against ASHP because of the falling COP as the temperatures decrease in Winter. Additionally, according to the Figures, there is a general heating demand in the summer period due to the nighttime temperatures and the constant heating setpoint in the simulations.

In the same way, Figures 14, 17, 20, 23, and 26 present the simulated annual total heating energy values [kWh] of different heating systems and the change in the heating energy use intensity per total building area values [kWh/m^2.a] of the systems. As expected in annual results, the NGB consumes the highest site energy, and the DH follows it. Likewise, in the monthly figures, the annual consumption values of heat pumps are less than half of district heating values in all samples. The annual consumption values between GSHP and ASHP seem negligible. Sample 1 consumes the highest site energy for heating annually. According to Figure 14, to keep that building at the setpoint temperature throughout the year, 743 MWh is required with district heating, while only 239 MWh is required with GSHP. Sample 2 consumes the least site energy in each system. NGB can provide necessary heating for sample 2 with 160 MWh energy, while GSHP can provide it with only 39 MWh energy. The heat pumps change the heating energy use intensity per total building area values in all samples significantly. All samples' heating EUI values drop under 50 kWh/m^{2}a with any type of heat pump. In sample 5, the EUI drops even under 10 kWh/m^{2}a.

Figures 15, 18, 21, 24, and 27 show the calculated monthly and annual CO_2 equivalent emissions [tonne] of the related heating systems in the sample buildings. The bar graphs depict the monthly emissions of different heating systems in the first y-axis on the right, while the line chart depicts the monthly stacked values. According to the emission figures, the highest CO_2 equivalent emissions for NGB and DH occur in January. The emissions are nearly the same for these two systems in December. When the heat pumps are examined in detail, it is observed that GSHP (except sample 5) causes the highest emission in February while ASHP causes it in December. In Figures 18 and 27, where all heating system emissions are shown monthly, the emission difference among the systems and change in the emission gap between GSHP and ASHP can be seen clearly in Winter. The emission of NGB is near twice the size bigger than the DH. The emission difference between heat pumps and other systems increases as the average temperatures increases during the year. The emission difference is apparent between the two heat pumps in January and December, whereas it is neglectable in Spring and Summer as the temperatures increase. This situation can also be observed in the stacked line graph that shows the annual total emissions. Nevertheless, the annual total emissions of ASHP and GSHP seem very close, even overlapped in Figures 15, 18, and 27. The highest emission is seen in Figure 15 of Sample 1 with 28 CO_2 equivalent tonnes by DH. However, the same heating can be provided with a GSHP and causes only 14 tonnes of CO_2.

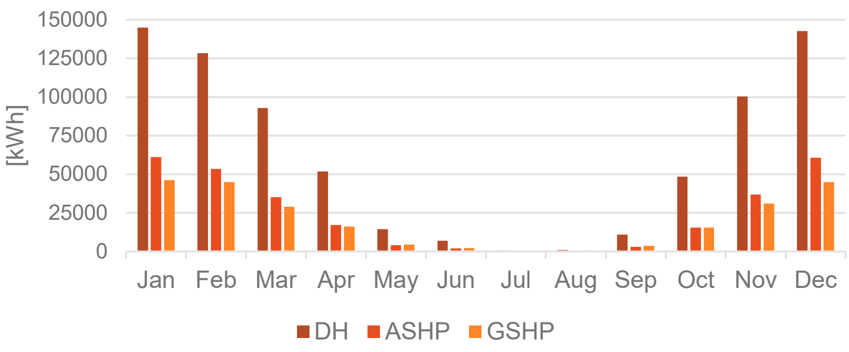

Figure 13 Monthly energy consumption values of sample 1

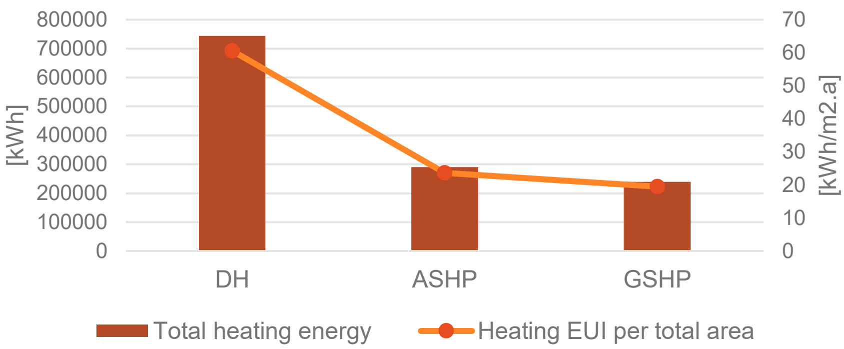

Figure 14 Annual energy consumption values of sample 1

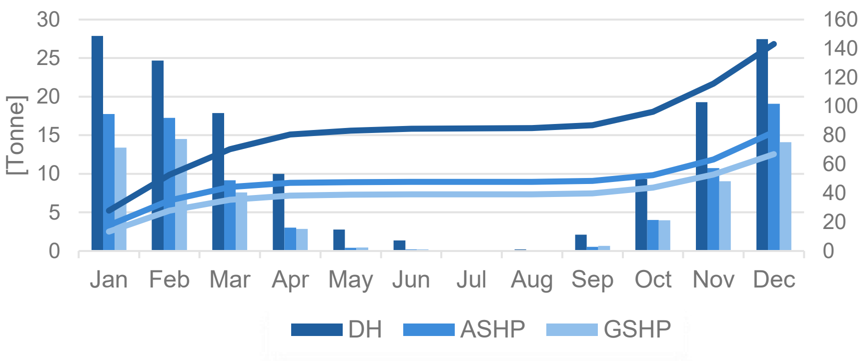

Figure 15 Monthly and annual CO_2eq emissions of sample 1

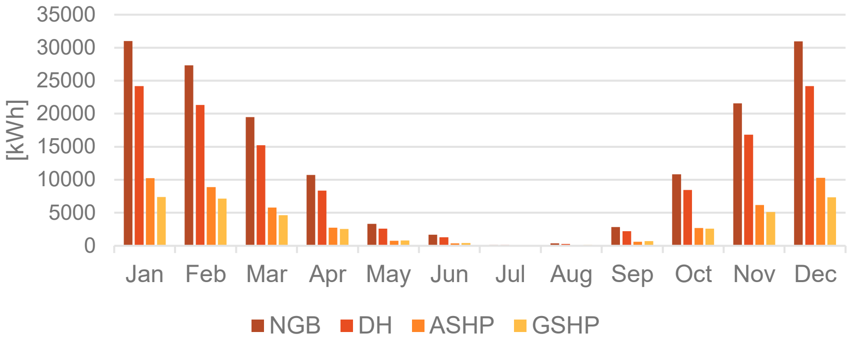

Figure 16 Monthly energy consumption values of sample 2

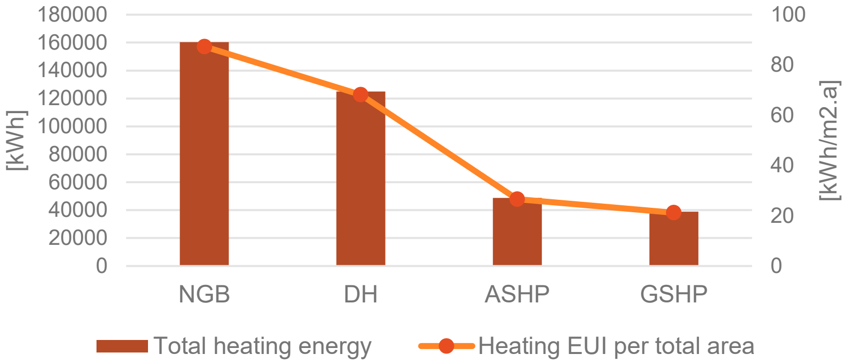

Figure 17 Annual energy consumption values of sample 2

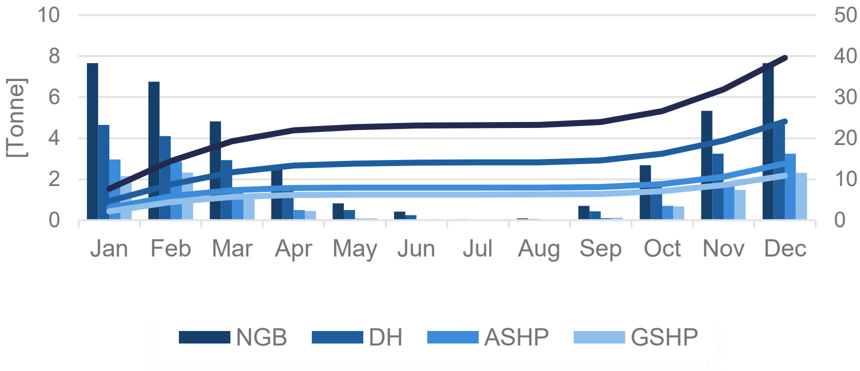

Figure 18 Monthly and annual CO_2eq emissions of sample 2

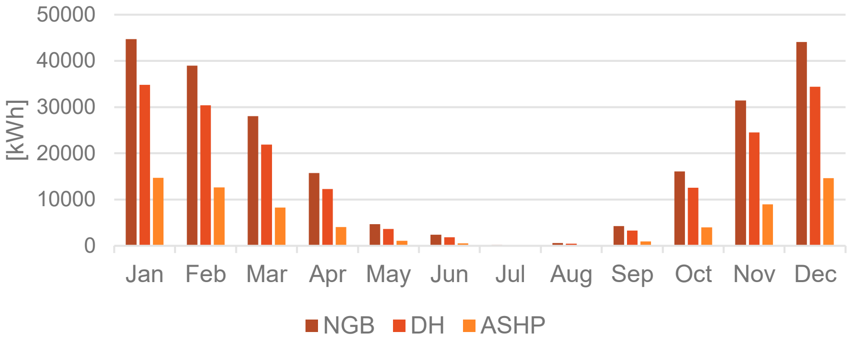

Figure 19 Monthly energy consumption values of sample 3

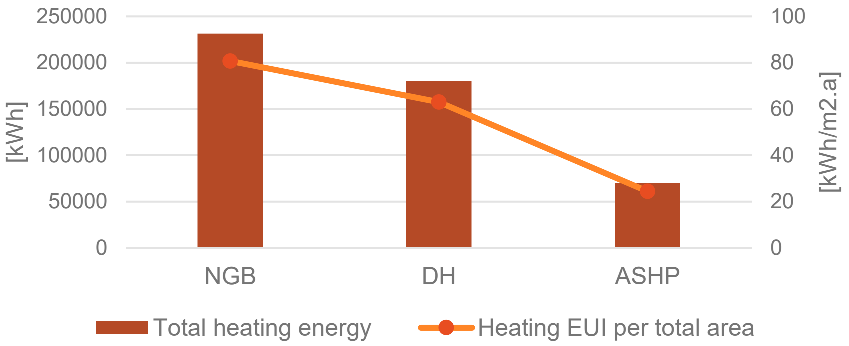

Figure 20 Annual energy consumption values of sample 3

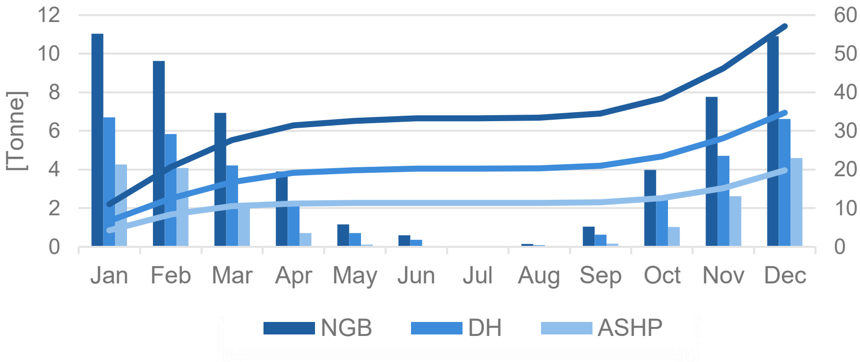

Figure 21 Monthly and annual CO_2eq emissions of sample 3

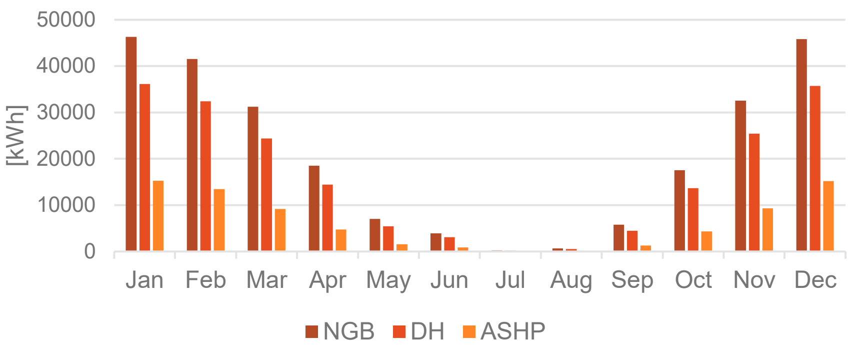

Figure 22 Monthly energy consumption values of sample 4

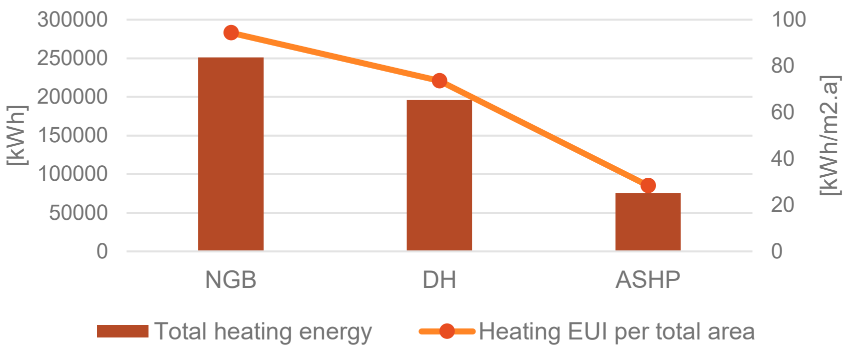

Figure 23 Annual energy consumption values of sample 4

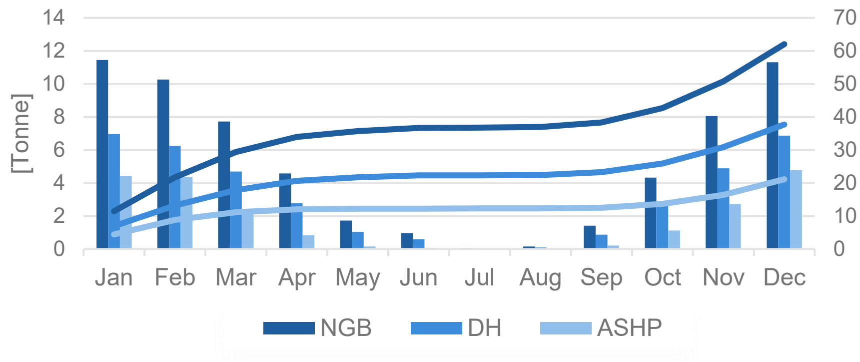

Figure 24 Monthly and annual CO_2eq emissions of sample 4

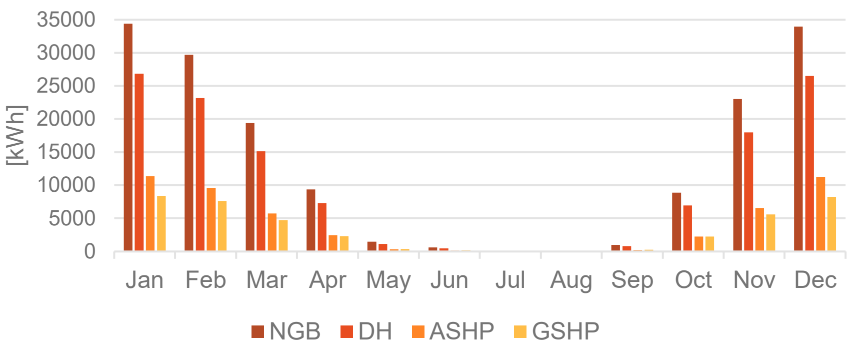

Figure 25 Monthly energy consumption values of sample 5

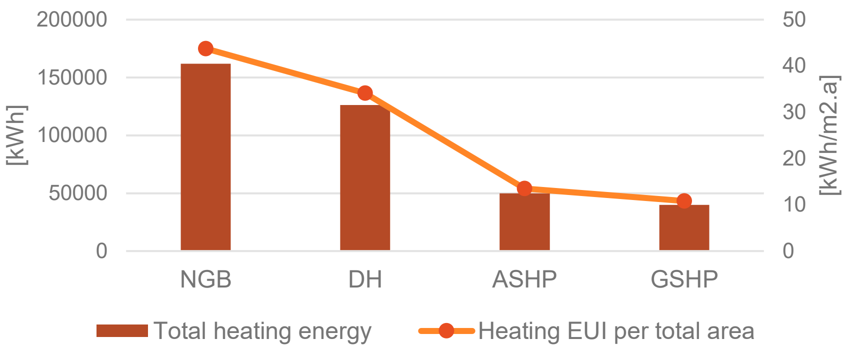

Figure 26 Annual energy consumption values of sample 5

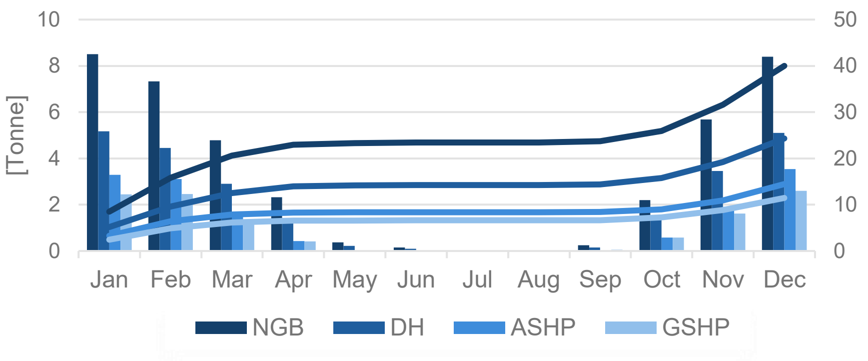

Figure 27 Monthly and annual CO_2eq emissions of sample 5

3.3 District Scale

The results in this chapter reveal the impacts of the scenarios on the stock level.

Figure 28 visualizes the effects of the implemented scenarios on annual heating energy consumption on the sample scale. The simulated consumptions of each five samples are clustered in four different scenarios in the x-axis. The first y-axis shows the annual individual sample consumptions. In contrast, the second y-axis on the right side shows the change in the sum of all energy consumption in different scenarios.

Additionally, Table 15 presents the simulated annual heating energy consumption values in [MWh] of the samples for each scenario. Their sums can be found on the right side of the table for comparison.

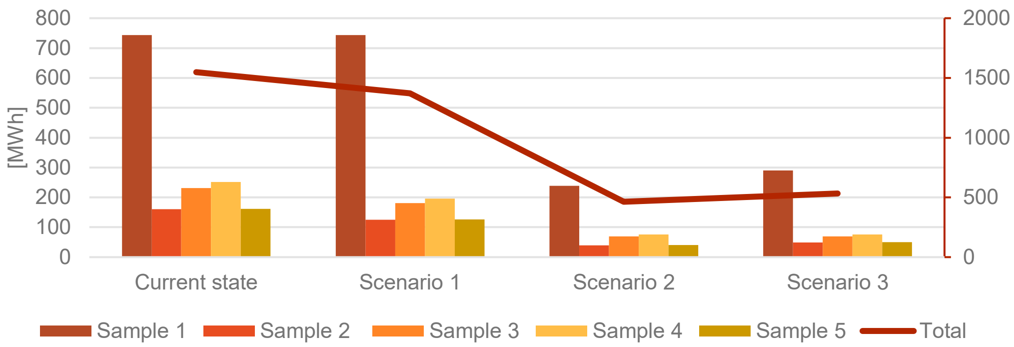

Figure 28 Annual energy consumption of the samples in different scenarios

Table 15 Annual energy consumption values of the samples in different scenarios

Building Scale	**Sample**						**Unit**
Scenario	**1**	**2**	**3**	**4**	**5**	**Total**	
Current state	743	160	231	251	162	1547	MWh
Scenario 1	743	125	180	196	126	1370	
Scenario 2	239	39	70	75	40	463	
Scenario 3	290	49	70	75	50	534	

According to Figure 28 and Table 15, the share of sample 1 is exceptionally high through others in all scenarios. From that figure, scenario 1 seems ineffective in decreasing consumption values in building scale. Meanwhile, scenario 2 shows the best performance about energy saving in building scale. Scenario 3 also shows good performance as scenario 2 when the annual values are inspected in the line chart. In scenarios 2 and 3, the samples consume 2/3 proportion less energy than the current state. Although scenarios 2 and 3 consume significantly less energy than the current situation, their difference is about 10% in favor of scenario 2.

Similarly, Figure 29 shows the effects of the implemented scenarios on annual heating energy consumption on the district scale. The simulated consumptions of each five samples are scaled up with the number of buildings they represent in the district, and results are clustered in four different scenarios on the x-axis. The first y-axis shows the annual total consumption of the buildings represented by pertaining samples. On the other hand, the second y-axis on the right side shows the annual total heating energy consumptions in the district and its change according to the different scenarios in [GWh] units. Table 16 presents the values numerically depicted in that figure. Each sample's simulated annual heating energy consumption values were multiplied by the number of buildings they represent in stock to obtain the district scale. The number of buildings represented by the samples is placed in the last row of the table. Regarding scenarios, the change in consumption values of the district can be seen on the right side of the table for comparison.

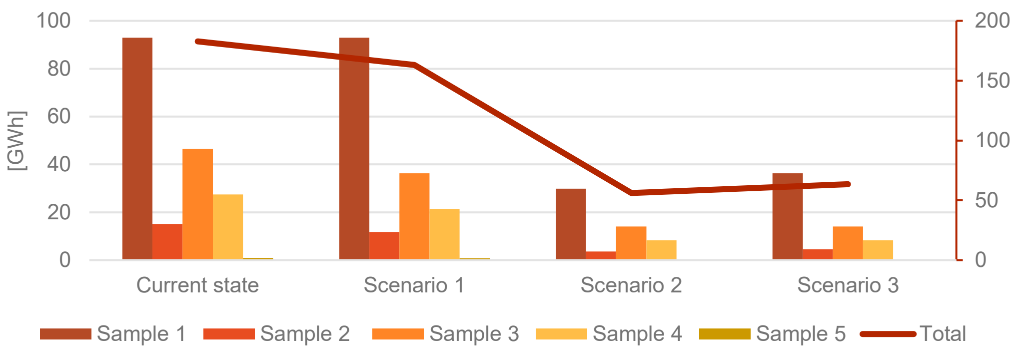

Figure 29 Annual energy consumption of the district in different scenarios

Table 16 Annual energy consumption values of the district in different scenarios

Urban Scale	**Sample**					**Total**	**Unit**
Scenario	**1**	**2**	**3**	**4**	**5**		
Current state	93	15	46	27	1	182	GWh
Scenario 1	93	12	36	21	0,8	163	
Scenario 2	30	3,7	14	8,2	0,2	56	
Scenario 3	36	4,6	14	8,2	0,3	63	
Count	125	94	201	109	6		

The upscaled results in Figure 29 reveal that half of the total heating energy in the district-scale is consumed by the only sample 1 type buildings. Meanwhile, sample 5 has clearly no effect on the total consumption values at the district level. The general scenario inferences which were deduced in the building scale are also valid for the district scale. Scenarios 2 and 3 show the best performance. The District's annual total heating energy consumption with the existing systems is 182 GWh. In scenario 2, it drops to 56 GWH, and in scenario 3 to 63 GWh. Their annual total district-scale consumption values seem very close to each other. However, the absolute difference between these two scenarios on the district scale is still 7 GWh annual.

Consequently, the calculated CO_2 equivalent emission values are shown in Figure 30. In the x-axis, the annual emissions of each five samples are clustered regarding the scenarios. In the first y-axis, the annual individual sample emissions are shown in [Tonne]. In the second y-axis on the right side, the change in the sum of all CO_2eq emissions in different scenarios can be observed. Table 17 presents the calculated annual CO_2 equivalent emissions in the unit [Tonne] of the samples for each scenario. Their sums can be found on the right side of the table for comparison.

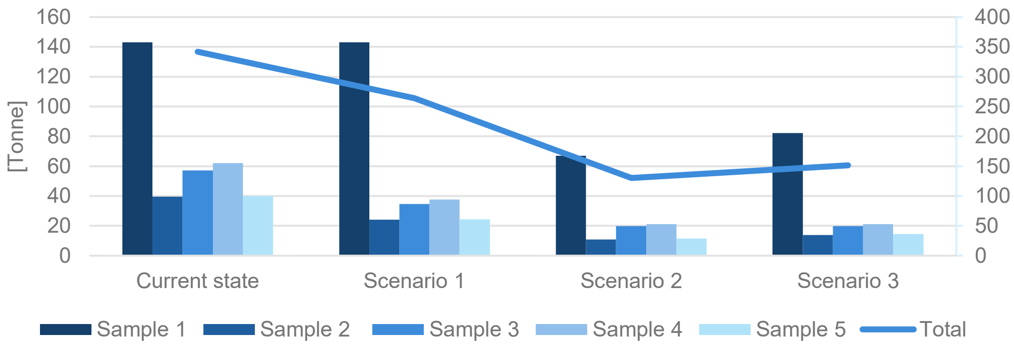

Figure 30 Annual CO_2eq emissions of the samples in different scenarios

Table 17 Annual CO_2eq emission values of the samples in different scenarios

Building Scale	**Sample**						**Unit**
Scenario	**1**	**2**	**3**	**4**	**5**	**Total**	
Current state	143	39	57	62	40	341	
Scenario 1	143	24	35	38	24	264	CO_2eq Tonne
Scenario 2	66	11	20	21	11	129	
Scenario 3	82	14	20	21	14	151	

According to the results, scenario 2 performs the best decarbonization scenario in building scale compared to the current state. Existing heating systems in the samples release 341 CO_2 equivalent tonnes emissions. Thanks to scenario 2, this value decreases to 129. In addition, the decarbonization potential of scenario 1 remain limited and cannot compete with scenario 2 and 3 in sample scale.

In the sample scale, the emission share of the first sample is the highest, the half of all emissions in the sample scale solely created by sample 1. Samples 2 and 5 shares the same emission rates and create the least emissions, among others. However, these results are deceiving since their total building area is not identical.

Finally, on the district scale, the calculated total CO_2 equivalent emission rates and changes due to the different scenarios are shown in Figure 31. The calculated annual emissions of each five samples are scaled up with the number of buildings they represent in the district. The results are clustered in four different scenarios on the x-axis. The first y-axis shows the annual total emissions of the buildings represented by pertaining samples. The second y-axis on the right side shows the district's annual total CO_2 equivalent emissions and their change according to the different scenarios in the unit [Kilotonne]. Table 18 gives the calculated annual total CO_2 equivalent emission values depicted in the figure. Calculated annual emission values of each sample in different scenarios were multiplied by the number of buildings they represent in stock to obtain the total emission reduction rate on the district scale. The number of buildings represented by the samples is placed in the last row of the table. Regarding scenarios, the change in emission values of the district can be seen on the right side of the table for comparison.

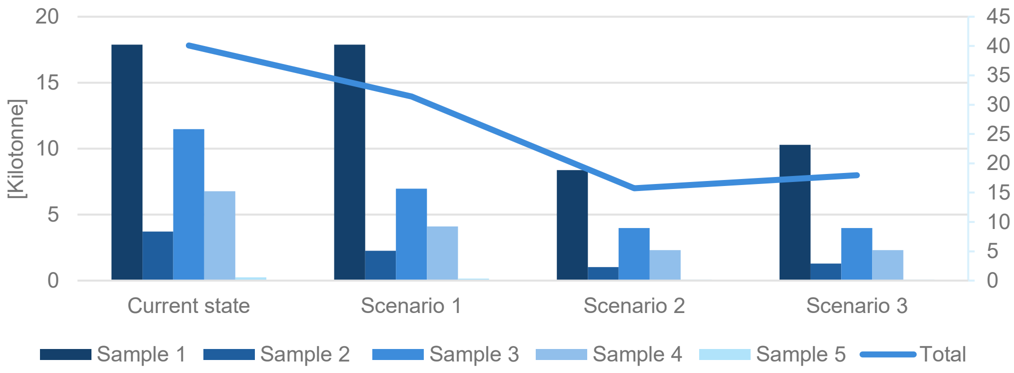

Figure 31 Annual CO_2eq emissions of the district in different scenarios

Table 18 Annual CO_2eq emissions values of the district in different scenarios

Urban Scale	Sample					Total	Unit
Scenario	**1**	**2**	**3**	**4**	**5**		
Current state	18	3,7	11	7	0,2	40	CO_2eq Kilotonne
Scenario 1	18	2	7	4	0,1	31	
Scenario 2	8,4	1	4	2,3	0,1	16	
Scenario 3	10	1,3	4	2,3	0,1	18	
Count	125	94	201	109	6		

The most significant results are shown in Figure 31 and Table 18. In the current state with the existing heating systems, 40 kt CO_2 equivalent emissions are annually released by the district. The most environmentally friendly scenario is scenario 2, with 16 kt CO_2eq emission. After that, scenario 3 comes with an 18 kt CO_2eq emission. The emission difference between the two best scenarios is 2 kt CO_2eq emission which corresponds to nearly 5% of all current emissions. Scenario 1 shows the worst performance with 31 kt CO2eq-emissions and separated from others negatively. According to Figure 31, sample 1 type buildings dominate the CO_2eq emissions. They cause half of all heating-related emissions released in the district. Then sample 3 type buildings come, their share is approximately 25% in all emissions. Sample 5 type buildings do not affect the total emissions regarding their output and frequency.

4 DISCUSSION

It can be easily seen that the heat pumps show a tremendous economic and environmental performance. They consume less than half of the site energy of district heating. Heat pump implementation scenarios show that they can pull energy use intensity per total area values below 50 [kWh/m^{2}a] in all sample buildings. That means a heating system transition theoretically can certificate those buildings at least to Class B energy level.

The trend in emission rates is similar to consumption. The heat pump application causes a sharp drop in emissions. They cause notably less CO_2 equivalent emissions than the other two systems. When the results are inspected roughly on the systems level, it is evident that heat pumps are the most environmentally friendly systems. However, there is still an emission difference between the two types of heat pumps. According to the results, the air-source heat pump causes approximately 13% more emissions than the ground-source heat pumps.

At the district level, sample 1 type buildings dominate the annual energy demand and CO_2 equivalent emissions. They are responsible for nearly half of the total emission in every scenario at the district scale, while their frequency in stock is only 20%. It is mainly because sample 1 and the represented buildings are large and old buildings with poor envelopes. Therefore a case-specific solution can be sought for the sample 1 type buildings to decrease the total emissions. For extra reductions, specific, fast, and affordable solutions such as windows retrofit, infiltration control can be applied to achieve the emission targets with less efficient and affordable systems.

On the contrary to sample 1, sample 5 has almost no effect on the total and individual emission and consumption rates. It is connected to the low frequency of sample 5 type buildings in the stock and sample 5's outstanding thermal quality. These new buildings are rare in the central districts of Vienna and can be excluded from urban level emission evaluations until the decarbonization efforts move to the next stage. Moreover, based on this sample type, a model can be developed that considers emissions besides consumptions. Thereby, in the future, the buildings will be designed and built based on these decarbonized models.

Table 19 shows the heating energy reduction potential of the district. A system transition to scenario 2 from the existing situation can cause a 126 GWh annual site energy saving. This rate is only 19 GWh annual in scenario 1. Therefore, the site energy consumption potential of district heating remains limited by 11%. However, this value is considered incomparable with heat pumps efficiency since district heating uses waste heat as site energy. The critical value is the efficiency difference between the two heat pump systems. Between scenarios 2 and 3, the combination causes 4% less electricity consumption on the district scale in favor of scenario 2, in which the ground-source heat pumps are implemented wherever possible. This 4% corresponds to 7 GWha electricity consumption in number. That value equals approximately 0,14% of the annual production of a 1300 MW NG-fueled power plant(Verbund 2008), while the total generation is 65.000 GWha in Austria (IEA 2020a).

Table 19 Energy consumption reduction potential in the district scale

Scenario	Current state	Scenario 1	Scenario 2	Scenario 3
Consumption [kWh]	182.825.258	163.047.560	56.084.658	63.395.506
Potential	100%	89%	31%	35%

Table 20 shows the related decarbonization potential of the implemented scenarios on the district scale. This study revealed that district heating could only achieve a 22% decarbonization on the district scale. Meanwhile, the air-source heat pumps can achieve 55%. The other important finding is about the decarbonization potential between scenarios 2 and 3. Due to the aforementioned 13% additional emission difference between two heat pumps systems, 6% more emissions occur at the district scale in scenario 3. The ground-source heat pump implemented (where possible) scenario can provide a 61% decarbonization.

Table 20 Decarbonization potential in the district scale

Scenario	Current state	Scenario 1	Scenario 2	Scenario 3
Emission [gr]	40.093.358.101	31.386.665.300	15.744.937.118	17.956.354.066
Potential	100%	78%	39%	45%

As mentioned earlier in chapter 1.1 Overview, two milestones are set to achieve the Paris Agreement goals by 2050. A 40% of the total carbonization is required to meet the first milestone by 2030 and 60% for the second by 2040. According to the results in a scenario that meets the conditions a) the residential space heating shares the same emission reduction goals with these global milestones and b) the electricity and district heat generation stays as it is now, the electrification of the space heating with the ASHP and GSHP (where possible) combination can achieve both milestones with a 61% overall reduction.

Additionally, the first milestone can be achieved if all existing heating systems are converted to ASHP systems by 2030. It can be assumed that, if these heat pump systems are implemented, the progress in the decarbonization of electricity generation will help decrease ASHP related emissions lower than the second milestone by 2040. That can also lead to total decarbonization for both heat pump systems in 2050. Therefore, due to GSHP's high investment costs and complicated installations, the ASHP can be preferred initially. However, as mentioned above, the HP mix still consumes 4% less site energy and releases 6% fewer CO_2eq emissions than the complete ASHP scenario in the current situation. Therefore, the decision should be made by policymakers according to the changing needs.

On the contrary to the recommendations, district heating seems to be far from meeting the decarbonization goals. It fails to achieve a 40% reduction with its current generation mix. The main reason is that almost half of the heat is generated by non-renewable sources in Vienna. If the percentage of the renewables or CHP sourced heat is increased, district heating might also achieve that target.

5 CONCLUSION

This study was conducted to explore the alternative systems' decarbonization potential in case of extensive conversion of common residential heating systems due to the latest regulations enacted in Vienna. The decarbonization potential at the district level was investigated with several energy simulations of the predefined sample buildings according to three different scenarios and the adopted UBEM method. These scenarios were determined regarding the reports published by the City of Vienna and the findings within this study.

According to the outcomes of this study, the decarbonization potential in the long term highly depends on the generation source mix of electricity and district heating. Currently, the heat pumps have performed exceptionally well in the simulations. But, unfortunately, the situation is not the same for district heating. In the short term, where every condition is assumed to be stable until 2030, the proposed conversion to district heating seems to fail to meet the decarbonization target. On the other hand, the amount of consumption and emission differences between the heat pump types is relative due to the total production. Considering the carbon emissions, the policymakers can decide between less efficient but inexpensive ASHP systems or highly efficient but expensive and complicated GSGP for implementation or promotion.

Additional measures can also increase the decarbonization potential. Energy performance-based design before new constructions and retrofitting the existing buildings envelope are other methods for residential decarbonization besides heating system regulations. With the help of this study, the critical buildings groups can be identified according to their resulting emissions, and retrofit priority can be established to speed up the decarbonization efforts via retrofitting and renovation.

The impact of residential heating system decarbonization on total decarbonization is undeniable. However, this study reveals that total decarbonization of heating systems is impossible with current technologies without decarbonization of electricity and district heating.

This study can be applied to analyze the decarbonization potential in districts and cities which share similar climate conditions with Vienna. For future studies, alternative system possibilities can be evaluated and diversified for all building sector in other regions. For policymaking, future energy capacity installations for electricity and heat generation can be calculated and planned regarding the desired CO_2 emission reduction targets in the buildings sector.

6 INDEX

6.1 List of Abbreviations

ASHP	Air source heat pump
ASHRAE	The American society of heating, refrigerating and air-conditioning engineers
BEM	Building energy modeling
CCS	Carbon capture and storage
CHP	Combined heat and power
COP	Coefficient of performance
DHW	Domestic hot water
EUI	Energy use intensity
GSHP	Ground source heat pump
HP	Heap pump
HVAC	Heating, ventilating, and air conditioning
IEA	International Energy Agency
P2G	Power to gas
PBBU	Physics-based bottom-up approach
PV	Photovoltaic
PVT	Photovoltaic thermal
SNG	Substitute natural gas
STH	Solar thermal heating
UBEM	Urban building energy modeling

6.2 List of Figures

6.3 List of Tables

6.4 List of Equations

7 LITERATURE

Ali, U., Shamsi, M.H., Hoare, C., Mangina, E., and O'Donnell, J., 2021. *Review of urban building energy modeling (UBEM) approaches, methods and tools using qualitative and quantitative analysis*. Energy and Buildings, 246, pp. 111073. The Author(s). DOI:10.1016/j.enbuild.2021.111073.

Ang, Y.Q., Berzolla, Z.M., and Reinhart, C.F., 2020. *From concept to application: A review of use cases in urban building energy modeling*. Applied Energy, 279, pp. 115738. Elsevier. DOI:10.1016/J.APENERGY.2020.115738.

Arnfield, A.J., 2020. *Koppen climate classification | Definition, System, & Map | Britannica*. Available from https://www.britannica.com/science/Koppen-climate-classification. [accessed 27 July 2021].

ASHRAE. , 2013. *2013 Standard 90.1-User's Manual*. ASHRAE, Atlanta.

ASHRAE., 2020. *2020 ASHRAE Handbook SI Edition*. *In* Ashrae Handbook, Fundamentals, 2020th edition. *Edited by* H.E. Kennedy. Mark S. Owen.

Austrian Federal Ministry for Sustainability and Tourism. , 2019. *Long-Term Strategy 2050 - Austria*.

Austrian Standards International (ÖNORM)., 2019. *ÖNORM B 8110-5:2019-03 ;Wärmeschutz im Hochbau: Klimamodell und Nutzungsprofile*. Austrian Standards International, Vienna.

Bertelsen, N., and Mathiesen, B.V., 2020. *EU-28 residential heat supply and consumption: Historical development and status*. Energies, 13(8). DOI:10.3390/en13081894.

Cerezo, C., Sokol, J., AlKhaled, S., Reinhart, C., Al-Mumin, A., and Hajiah, A., 2017. *Comparison of four building archetype characterization methods in urban building energy modeling (UBEM): A residential case study in Kuwait City*. Energy and Buildings, 154, pp. 321–334. Elsevier B.V. DOI:10.1016/j.enbuild.2017.08.029.

Cerezo Davila, C., Reinhart, C.F., and Bemis, J.L., 2016. *Modeling Boston: A workflow for the efficient generation and maintenance of urban building energy models from existing geospatial datasets*. Energy, 117, pp. 237–250. Elsevier Ltd. DOI:10.1016/j.energy.2016.10.057.

Chwieduk, D.A., 2016. *Active solar space heating*. Advances in Solar Heating and

Cooling, pp. 151–202. Woodhead Publishing. DOI:10.1016/B978-0-08-100301-5.00008-4.

Delbeke, J., Klaassen, G., and Vergote, S., 2015. *EU Climate Policy Explained*. *In* EU Climate Policy Explained, 2016th edition. *Edited by* J. Delbeke. European Union.

Dermentzis, G., Ochs, F., Thuer, A., and Streicher, W., 2021. *Supporting decision-making for heating and distribution systems in a new residential district - An Austrian case study*. Energy, 224, pp. 120141. Elsevier Ltd. DOI:10.1016/j.energy.2021.120141.

Dincer, I., and Rosen, M.A. , 2015. *Heat Pump Systems*. *In* Exergy Analysis of Heating, Refrigerating and Air Conditioning. Elsevier.

EIA., 2021. *U.S Energy Information Administration, Natural Gas Monthly*. Available from https://www.eia.gov/naturalgas/monthly/pdf/ngm_all.pdf. [accessed 8 July 2021].

Energy.gov. (n.d.). *Hydrogen Production: Natural Gas Reforming | Department of Energy*. Available from https://energy.gov/eere/fuelcells/hydrogen-production-natural-gas-reforming. [accessed 11 July 2021].

Energy Plus., 2021. *Weather Data by Location*. Available from https://www.energyplus.net/weather-location/europe_wmo_region_6/AUT//AUT_Vienna.Schwechat.110360_IWEC. [accessed 24 July 2021].

Erin Blanton, B.M., Melissa Lott, D.C., and Nicole Smith, K. , 2021. *Investing in the Us Natural Gas Pipeline System To Support Net-Zero Targets*. (April).

European Union. (n.d.). *Countries | European Union*. Available from https://europa.eu/european-union/about-eu/countries_en. [accessed 30 July 2021].

Fabrizio, E., and Monetti, V. , 2015. *Methodologies and advancements in the calibration of building energy models*. Energies, 8(4), pp. 2548–2574. DOI:10.3390/en8042548.

Federal Energy Management Program., 2015. *M&V guidelines: measurement and verification for performance-based contracts -Version 4.0*. U.S. Department of Energy, 3(November), pp. 1–108.

Ferrando, M., Causone, F., Hong, T., and Chen, Y. , 2020. *Urban building energy modeling (UBEM) tools: A state-of-the-art review of bottom-up physics-based* *approaches*. Sustainable Cities and Society, 62(June), pp. 102408. Elsevier. DOI:10.1016/j.scs.2020.102408.

Georges, L., Massart, C., Van Moeseke, G., and De Herde, A. , 2012. *Environmental and economic performance of heating systems for energy-efficient dwellings: Case of passive and low-energy single-family houses*. Energy Policy, 40(1), pp. 452–464. Elsevier. DOI:10.1016/j.enpol.2011.10.037.

Gheji, S.., Kamble, K.S., Gavde, A.A., and Mane, S.P. , 2016. *Basic Classification of HVAC Systems for Selection Guide*. International Journal of Innovative Research in Science, Engineering and Technology (An ISO Certified Organization), 5(4), pp. 6077–6086. DOI:10.15680/IJIRSET.2016.0504242.

Ghiassi, N., 2017. *An Hourglass Approach to Urban Energy Computing*. Ph.D. dissertation: Vienna University of Technology.

Ghosh, P., Shah, G., Sahota, S., Singh, L., and Vijay, V.K., 2020. *Biogas production from waste: technical overview, progress, and challenges*. *In* Bioreactors. Elsevier. pp. 89–104.

Hailu, G., 2021. *Energy systems in buildings*. *In* Energy Services Fundamentals and Financing. Academic Press. pp. 181–209.

Hudon, K., 2013. *Solar Energy - Water Heating*. *In* Future Energy: Improved, Sustainable and Clean Options for our Planet. Elsevier. pp. 433–451.

Hundy, G.F., Trott, A.R., and Welch, T.C. , 2016. *Heat Pumps and Integrated Systems*. *In* Refrigeration, Air Conditioning and Heat Pumps, 5th edition. Elsevier Ltd. pp. 393–408.

ICC., 2015. *IECC - International Energy Conservation Code*. International Code Council, Falls Chur, pp. Int. Code Counc.

IEA. , 2020a. *Austria 2020: Energy Policy Overview*.

IEA., 2020b. *Heat Pumps – Analysis - IEA*. Available from https://www.iea.org/reports/heat-pumps. [accessed 27 July 2021].

IPMVP., 2002. *International Performance Measurement & Verification Protocol*. *In* In Concepts and Options for Determining Energy and Water Savings.

IRENA, IEA, and REN21. , 2020. *Renewable Energy Policies in a Time of Transition: Heating and Cooling*.

Islam, M.M., Hasanuzzaman, M., Pandey, A.K., and Rahim, N.A. , 2019. *Modern* *energy conversion technologies*. *In* Energy for Sustainable Development: Demand, Supply, Conversion and Management. Academic Press. pp. 19–39.

Kavvadias, K., Jiménez-Navarro, J.P., and Thomassen, G., 2019. *Decarbonising the EU heating sector*. *In* EUR 29772 EN, Publications Office of the European Union. Luxembourg.

Kottek, M., Grieser, J., Beck, C., Rudolf, B., and Rubel, F. , 2006. *World map of the Köppen-Geiger climate classification updated*. Meteorologische Zeitschrift, 15(3), pp. 259–263. DOI:10.1127/0941-2948/2006/0130.

LT LCC, L.T.L., 2021. *Ladybug Tools*.

Lupu, A.G., Homutescu, V.M., Balanescu, D.T., and Popescu, A. , 2018. *Efficiency of solar collectors - A review*. IOP Conference Series: Materials Science and Engineering, 444(8). DOI:10.1088/1757-899X/444/8/082015.

Mair am Tinkhof, O., Strasser, H., Prinz, T., Herbert, S., Schuster, M., Tomschy, R., Figl, H., Fellner, M., Ploß, M., and Roßkopf, T. , 2017. *Richt- und Zielwerte für Siedlungen zur integralen Bewertung der Klimaver- träglichkeit von Gebäuden und Mobilitätsinfrastruktur in Neubausiedlungen*. *In* Nachhaltig Wirtschaften; Berichte aus Energie- und Umweltforschung 39/2017.

Martinopoulos, G., Papakostas, K.T., and Papadopoulos, A.M. , 2018. *A comparative review of heating systems in EU countries, based on efficiency and fuel cost*. Renewable and Sustainable Energy Reviews, 90(November 2016), pp. 687–699. Elsevier Ltd. DOI:10.1016/j.rser.2018.03.060.

Masea., 2014. *Masea Datenbank*. Available from https://www.masea-ensan.de/. [accessed 27 July 2021].

McDowall, R., 2007. *Fundamentals of HVAC Systems*. *In* Fundamentals of HVAC Systems. American Society of Heating, Refrigerating and Air-Conditioning Engineers eLearning. pp. 11–31.

McNeel, R., and others., 2020. *Rhinoceros 3D*.

Mohammadiziazi, R., Copeland, S., and Bilec, M.M. , 2021. *Urban building energy model: Database development, validation, and application for commercial building stock*. Energy and Buildings, 248, pp. 111175. Elsevier B.V. DOI:10.1016/j.enbuild.2021.111175.

Natural Resources Canada’s Office of Energy Efficiency. , 2004a. *Heating and cooling with a heat pump*. Available from https://www.nrcan.gc.ca/energy-efficiency/energy-star-canada/about/energy-star-announcements/publications/heating-and-cooling-heat-pump/6817#o2. [accessed 16 July 2021].

Natural Resources Canada’s Office of Energy Efficiency. , 2004b. *Heating and cooling with a heat pump*. Available from https://www.nrcan.gc.ca/energy-efficiency/energy-star-canada/about/energy-star-announcements/publications/heating-and-cooling-heat-pump/6817#o2. [accessed 16 July 2021].

NREL., 2021. *OpenStudio Software*. Alliance for Sustainable Energy LLC.

Oberwalder, V., 2021. *Impact of User Behaviour Assumptions on computed Urban Scale Building Energy Use*. Master's Thesis: Vienna University of Technology.

Österreichisches Institut für Bautechnik., 2019a. *Leitfaden OIB-RL 6 Energietechnisches Verhalten von Gebäuden*.

Österreichisches Institut für Bautechnik. , 2019b. *Richtlinie OIB-6 Energieeinsparung und Wärmeschutz*.

Potente Prieto, M., 2019. *Modelling, Simulation and Energy-Exergy Assessment of a Local District Heating Network in Vienna*. Ph.D. dissertation: Vienna University of Technology.

Reinhart, C.F., and Cerezo Davila, C. , 2016. *Urban building energy modeling - A review of a nascent field*. Building and Environment, 97, pp. 196–202. The Authors. DOI:10.1016/j.buildenv.2015.12.001.

The Republic of Austria. , 2020. *Government Programme 2020–2024 - Summary*.

Ritter, H., 2016. *Energy in Vienna, Stadt Wien MA 20 Workshop Output Report*.

Schöberl, H., Hofer, R., and Lang, C. , 2012. *Handbuch thermische Gebäudesanierung: Optimale Ausführungsvarianten*. WKO.

Seyam, S., 2018. *Types of HVAC Systems*. *In* HVAC System.

Sheikh, I.A., 2017. *Decarbonization of residential space and water heating in California*. Ph.D. dissertation: University of California.

Stadt Wien. (n.d.). *Biogas Wien - Biogas-Aufbereitungsanlage*. Available from https://www.wien.gv.at/umwelt/ma48/entsorgung/abfallbehandlungsanlagen/biogasanlage.html. [accessed 10 July 2021].

Stadt Wien., 2011. *Gebäude und Wohnungen Statistiken - Offizielle Statistik der Stadt*

Wien. Available from https://www.wien.gv.at/statistik/lebensraum/gebaeude/. [accessed 21 July 2021].

Stadt Wien., 2020. *Bauordnung für Wien § 118 7. Abschnitt Energieeinsparung und Wärmeschutz*. Austria.

Stadt Wien, Homeier, I., Pangerl, E., Tollmann, J., Daskalow, K., and Mückstein, G. , 2019. *Smart City Wien Framework Strategy 2019-2050: Vienna's Strategy for Sustainable Development*. Vienna.

Statistik Austria., 2020. *Energy balance, energy consumption of households*. Available from https://www.statistik.at/web_en/statistics/EnergyEnvironmentInnovationMobility/energy_environment/energy/energy_consumption_of_households/index.html. [accessed 18 June 2021].

Stern, J.P., 2019. *Narratives for Natural Gas in Decarbonising European Energy Markets*. Oxford.

Swan, L.G., and Ugursal, V.I. , 2009. *Modeling of end-use energy consumption in the residential sector: A review of modeling techniques*. Renewable and Sustainable Energy Reviews, 13(8), pp. 1819–1835. DOI:10.1016/j.rser.2008.09.033.

Treberspurg, M., and Stadt Wien. , 2019. *Zusammenfassung; Technisches Gutachten zur Novelle der BO f. Wien 2018 (§2b Energieraumpläne)-Wirtschaftlichkeitsvergleich unterschiedlicher Heizungs-und Warmwasserbereitungsanlagen*. Vienna.

Troi, A., 2011. *Historic buildings and city centres – the potential impact of conservation compatible energy refurbishment on climate protection and living conditions*. International Conference Energy Management in Cultural Heritage, (March), pp. 10.

U.S. Department of Energy. , 2020. *EnergyPlus | EnergyPlus*. Available from https://www.energyplus.net/. [accessed 24 July 2021].

UNEP, and IEA. , 2019. *Towards a zero-emissions, efficient and resilient buildings and construction sector. 2019 Global Status report*. *In* 2019 Global Status Report for Buildings and Construction.

UNFCC. , 2015. *The Paris Agreement*. *In* The Paris agreement. United Nations, Paris. pp. 24–45.

Vaillant., 2020. *Brine/water heat pumps - Vaillant*. Available from https://www.vaillant.info/customers/advice-knowledge/how-different-technologies-work/heat-pumps/brine-water-heat-pumps/. [accessed 16 July 2021].

Verbund. (n.d.). *Verbund errichtet Dampfkraftwerk Mellach*. Available from https://www.verbund.com/de-at/ueber-verbund/news-presse/presse/2008/07/30/mellach. [accessed 5 August 2021].

Viessmann. (n.d.). *Can You Still Buy Non-Condensing Boilers? | Viessmann*. Available from https://www.viessmann.co.uk/heating-advice/can-you-still-buy-non-condensing-boilers. [accessed 22 June 2021].

Weather-Atlas. (n.d.). *Austria - Climate data and average monthly weather | Weather Atlas*. Available from https://www.weather-atlas.com/en/austria-climate#cities. [accessed 14 July 2021].

Weiss, W., 2004. *Solar heating systems-status and recent development*. Renewable Energy World, 7(4), pp. 214–225.

Wien Energie., 2021. *Fernwärme von Wien Energie » Alle Infos zum Produkt*. Available from https://www.wienenergie.at/privat/produkte/waerme/fernwaerme/. [accessed 25 July 2021].

Woods, P., and Overgaard, J., 2015. *Historical development of district heating and characteristics of a modern district heating system*. *In* Advanced District Heating and Cooling (DHC) Systems. Woodhead Publishing. pp. 3–15.

Worcester-Bosch. (n.d.). *Boilers Explained | Worcester Bosch*. Available from https://www.worcester-bosch.co.uk/products/boilers/explained. [accessed 21 June 2021].

Yu, M., Wang, K., and Vredenburg, H., 2021. *Insights into low-carbon hydrogen production methods: Green, blue and aqua hydrogen*. International Journal of Hydrogen Energy, 46(41), pp. 21261–21273. Elsevier Ltd. DOI:10.1016/j.ijhydene.2021.04.016.

8 APPENDIX

A. Illustrations

The selected Viennese urban area for the case study

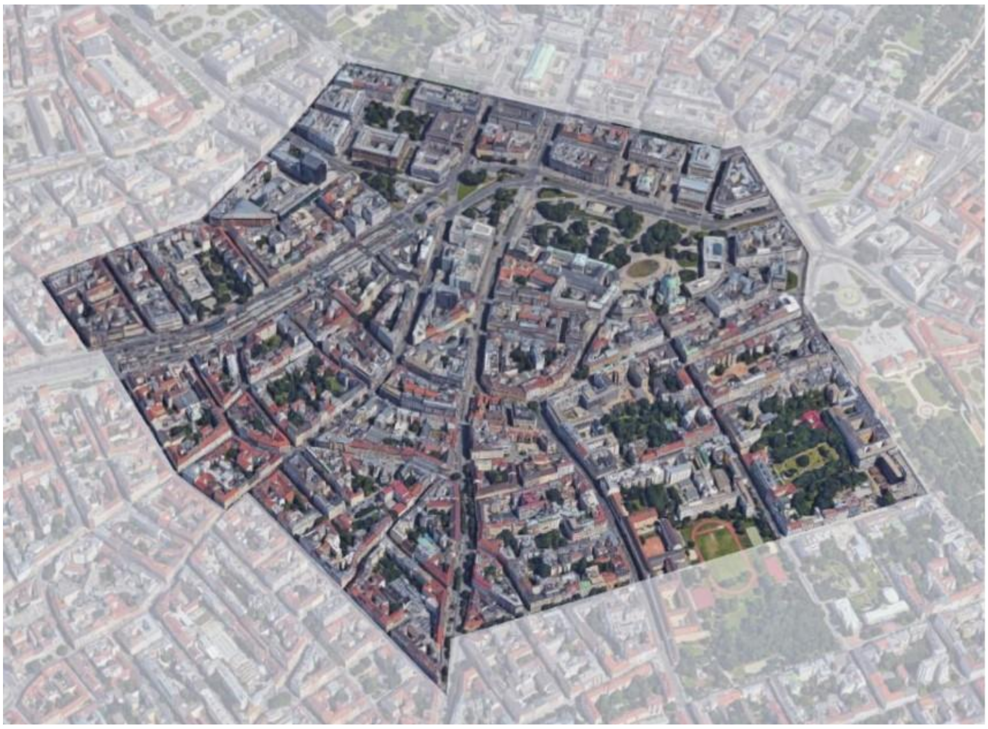

Figure 32 Selected neighborhood for the case study (source: Ghiassi 2017)

Sample building 1

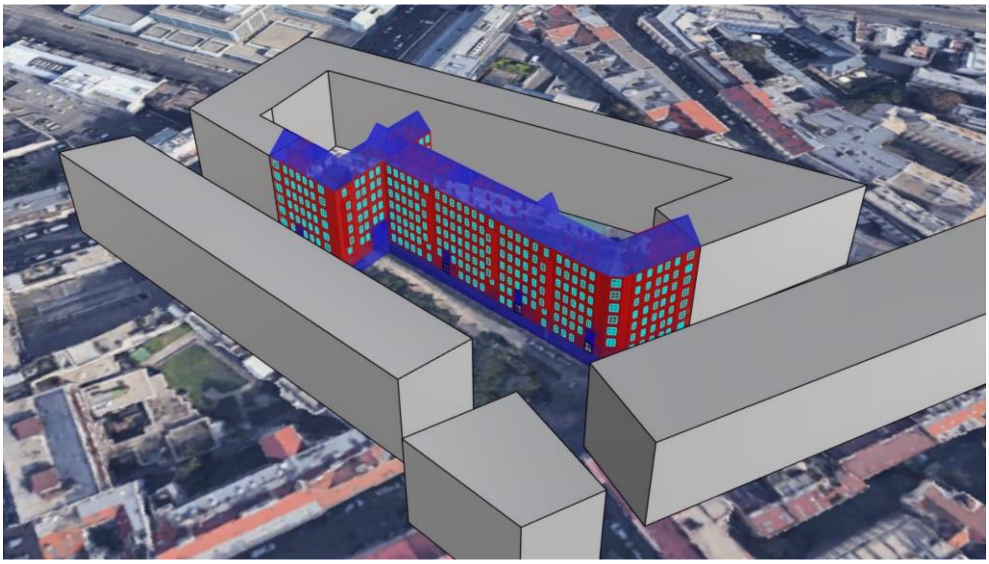

Figure 33 Urban context of sample building 1

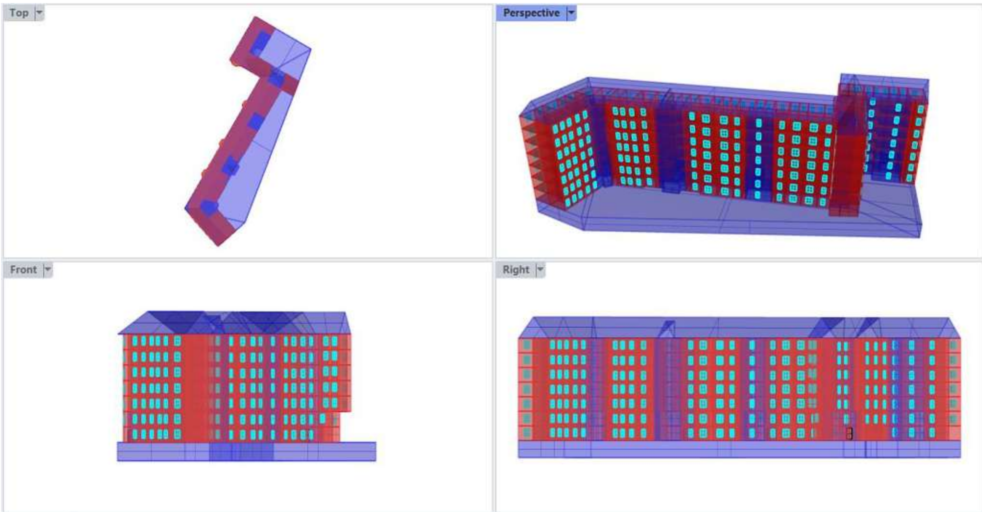

Figure 34 3-dimensional drawing views of sample building 1

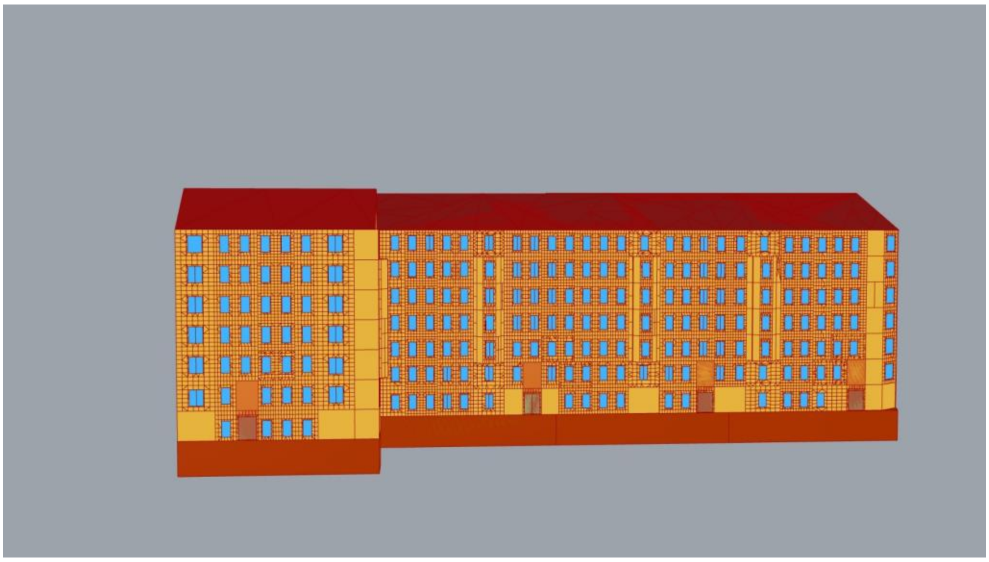

Figure 35 3-dimensional front perspective view after characterization of sample building 1

Sample building 2

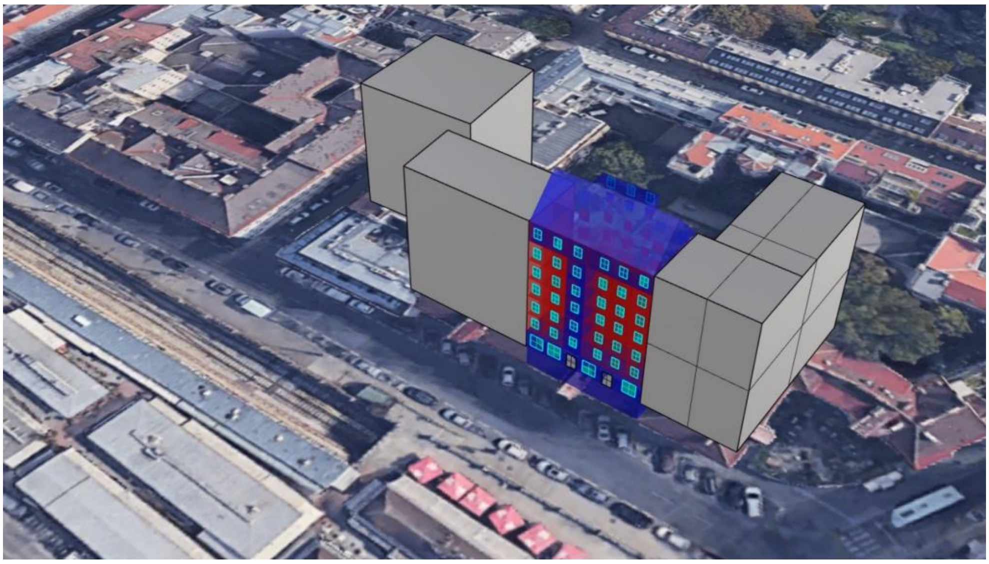

Figure 36 Urban context of sample building 2

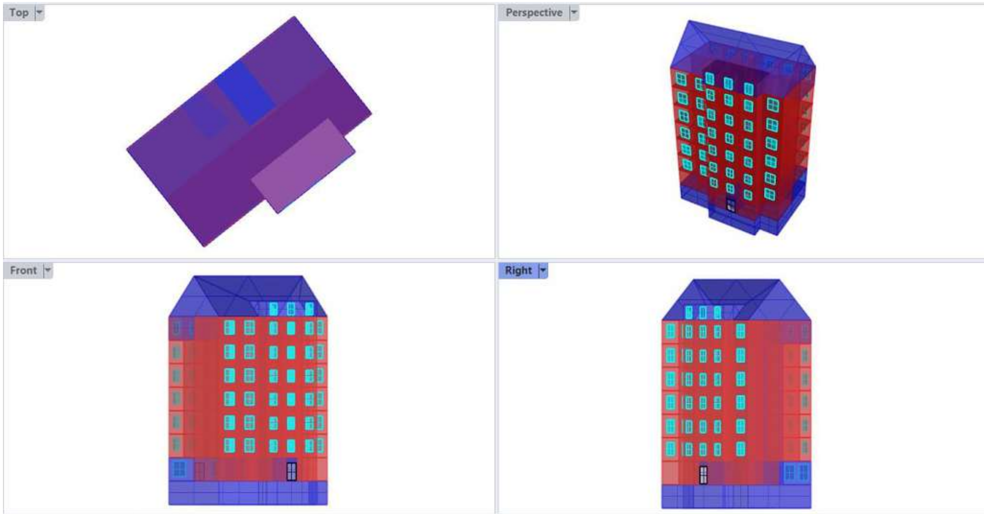

Figure 37 3-dimensional drawing views of sample building 2

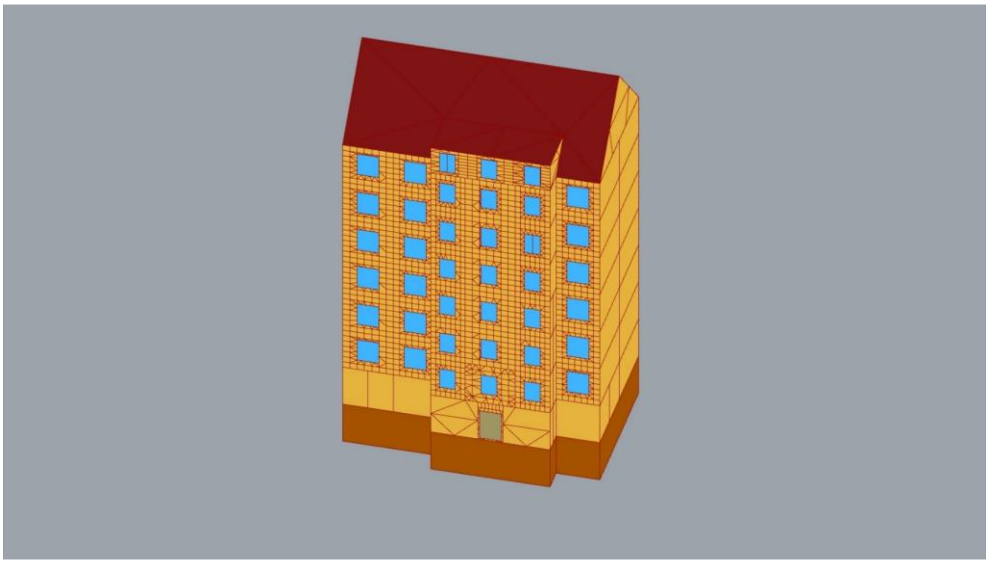

Figure 38 3-dimensional front perspective view after characterization of sample building 2

Sample building 3

Figure 39 Urban context of sample building 3

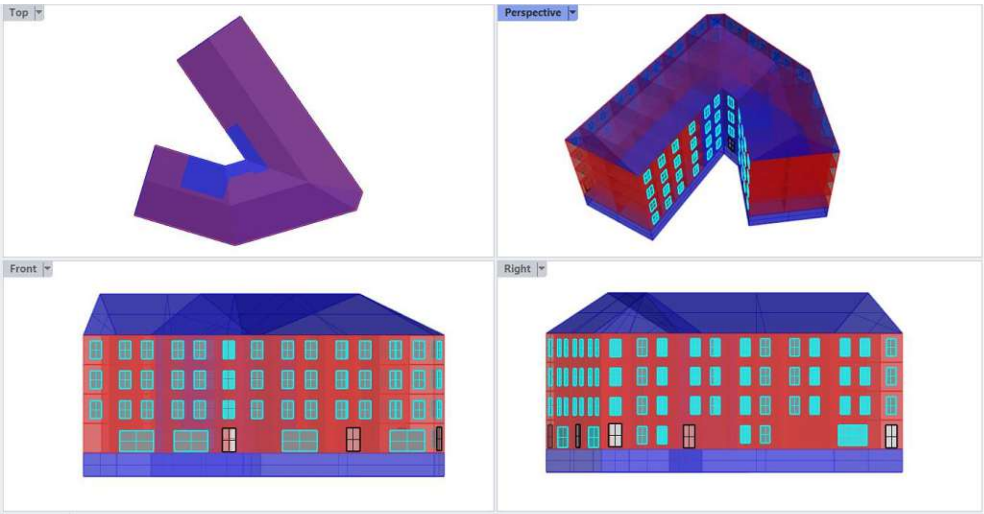

Figure 40 3-dimensional drawing views of sample building 3

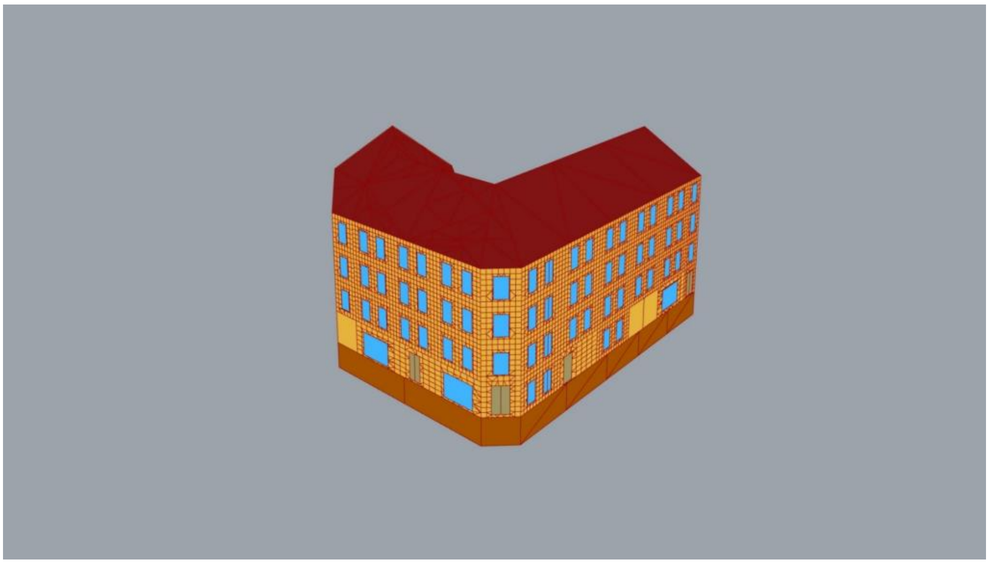

Figure 41 3-dimensional front perspective view after characterization of sample building 3

Sample building 4

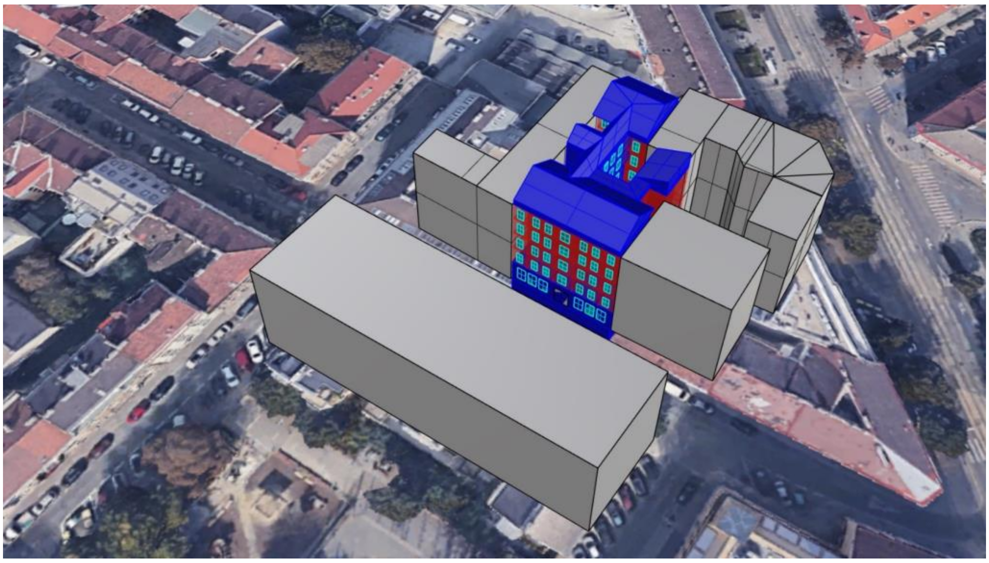

Figure 42 Urban context of sample building 4

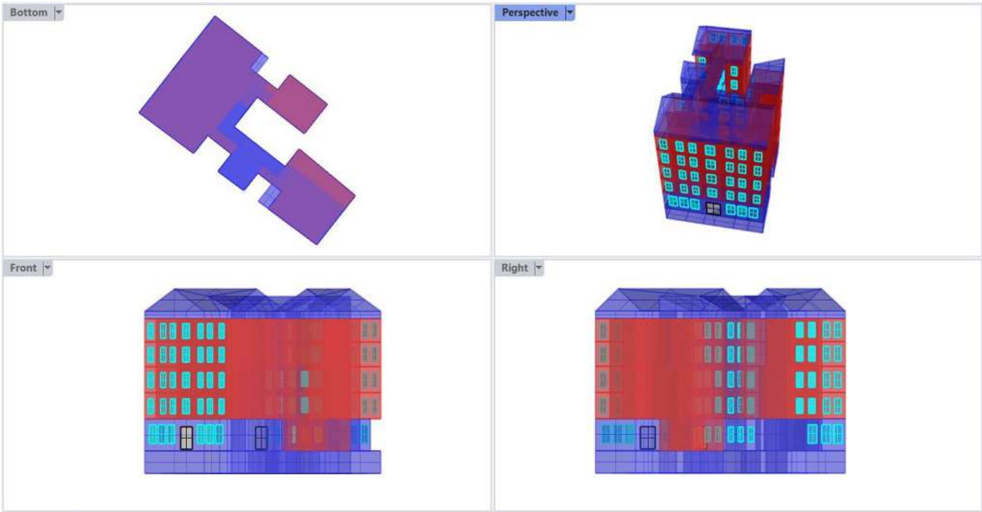

Figure 43 3-dimensional drawing views of sample building 4

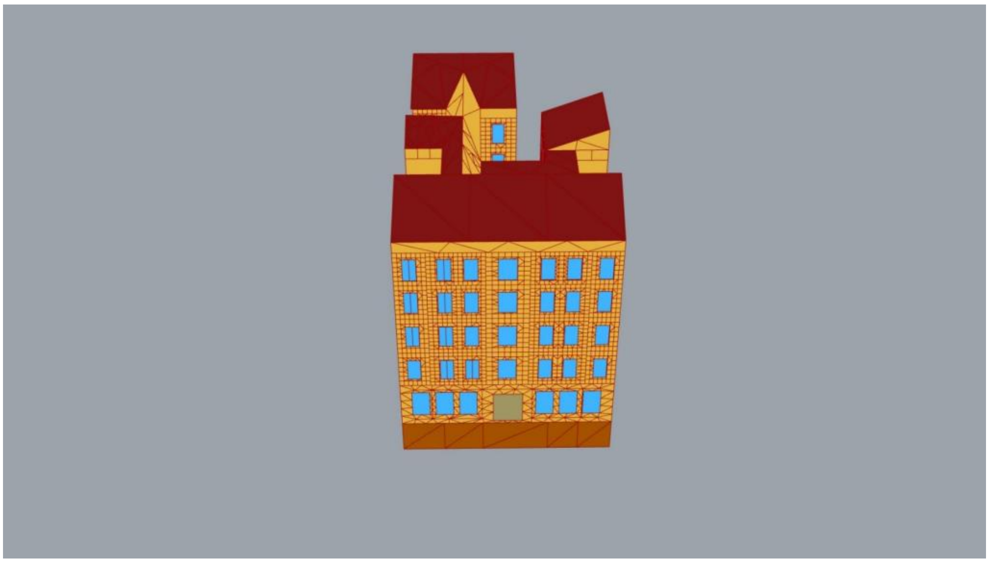

Figure 44 3-dimensional front perspective view after characterization of sample building 4

Sample building 5

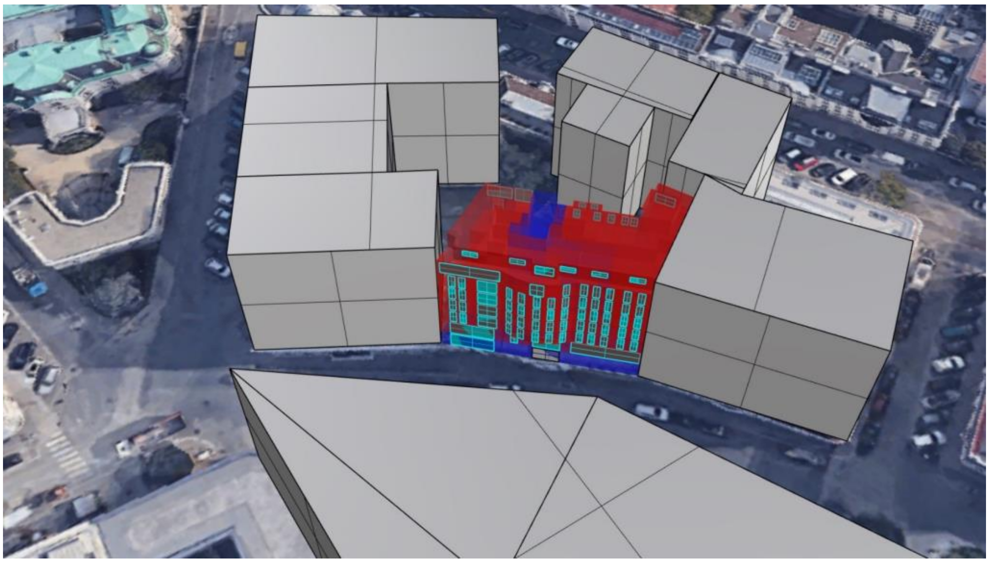

Figure 45 Urban context of sample building 5

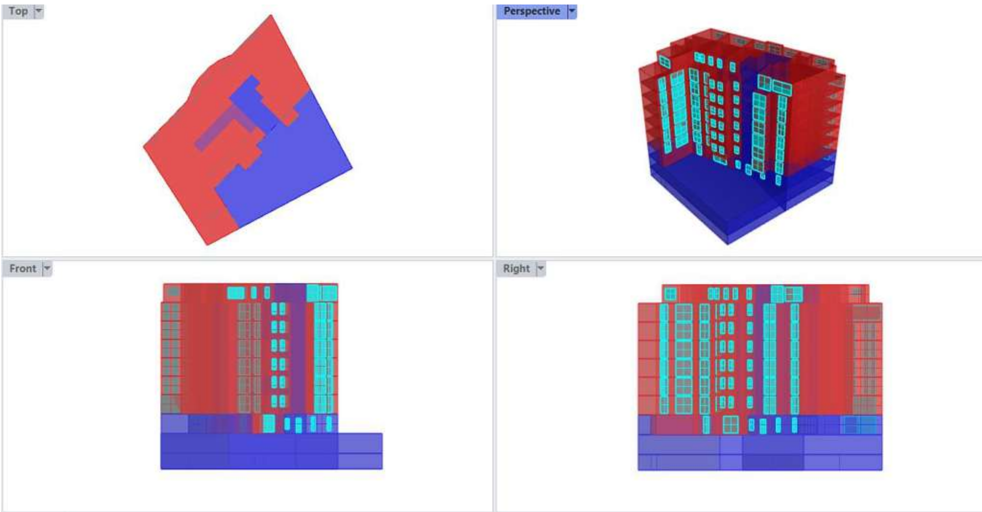

Figure 46 3-dimensional drawing views of sample building 5

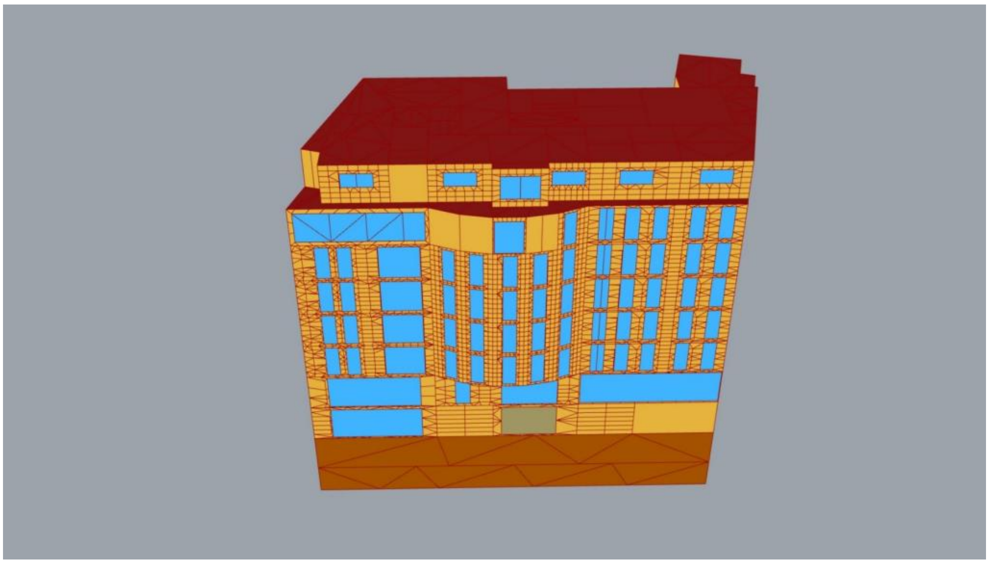

Figure 47 3-dimensional front perspective view after characterization of sample building 5

B. Results

Hourly energy consumption of

Sample building 1

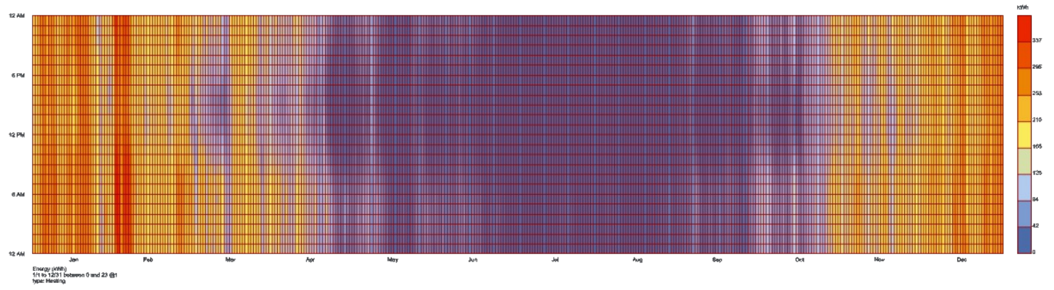

Figure 48 Hourly energy consumption of DH in sample building 1

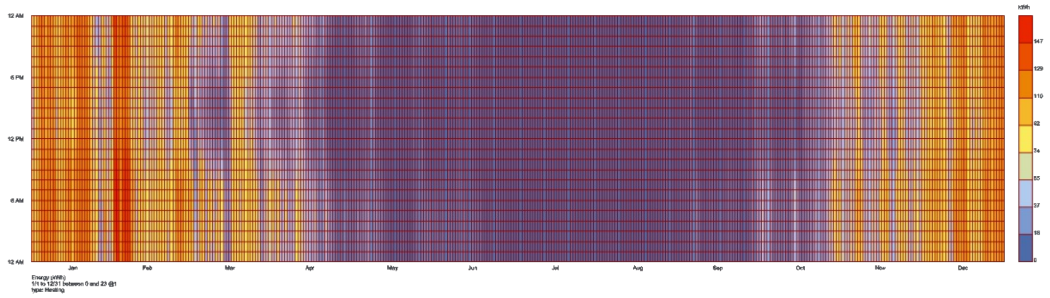

Figure 49 Hourly energy consumption of ASHP in sample building 1

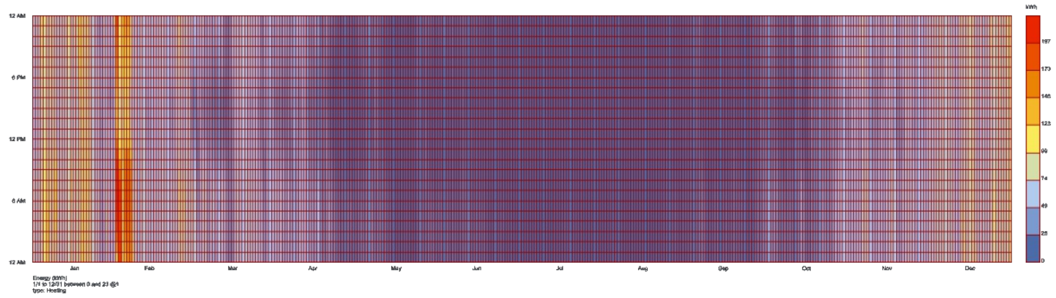

Figure 50 Hourly energy consumption of GSHP in sample building 1

Sample building 2

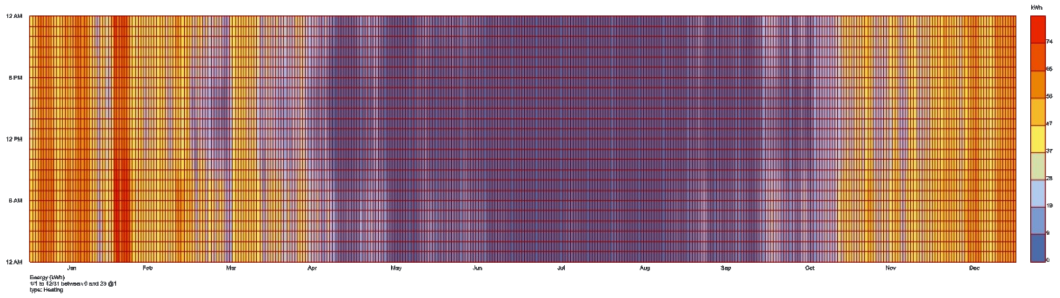

Figure 51 Hourly energy consumption of NGB in sample building 2

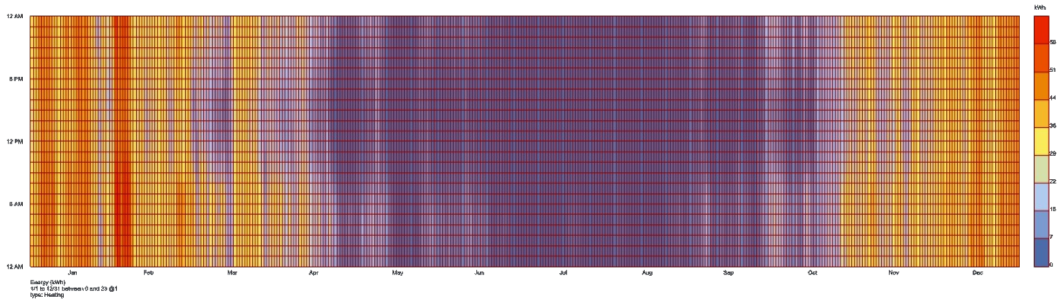

Figure 52 Hourly energy consumption of DH in sample building 2

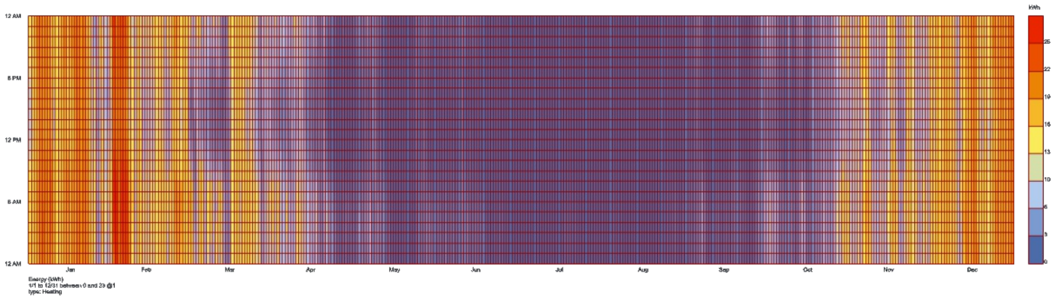

Figure 53 Hourly energy consumption of ASHP in sample building 2

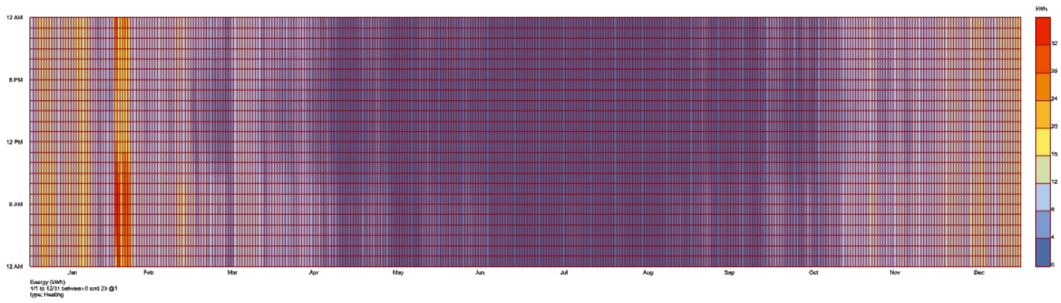

Figure 54 Hourly energy consumption of GSHP in sample building 2

Sample building 3

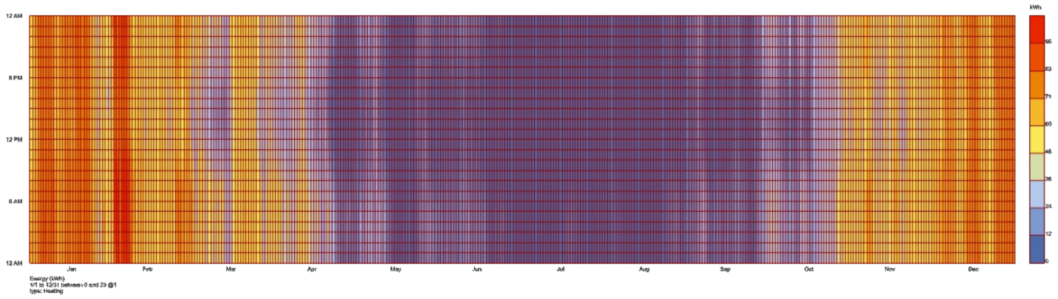

Figure 55 Hourly energy consumption of NGB in sample building 3

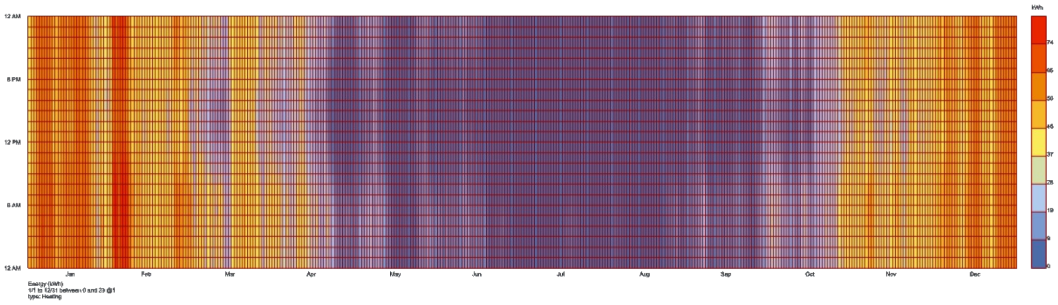

Figure 56 Hourly energy consumption of DH in sample building 3

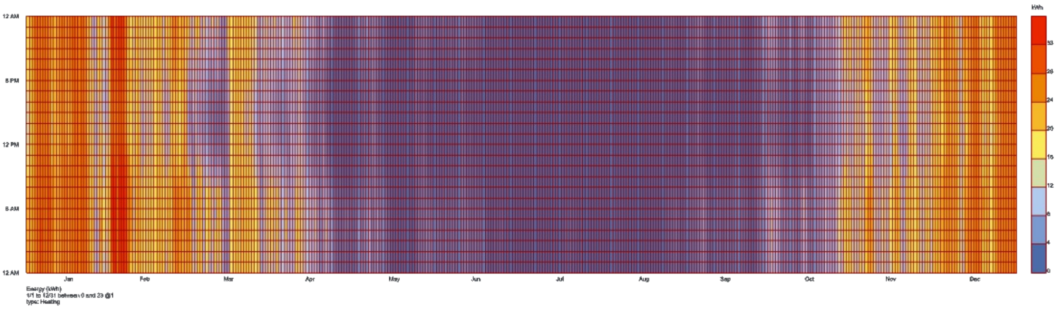

Figure 57 Hourly energy consumption of ASHP in sample building 3

Sample building 4

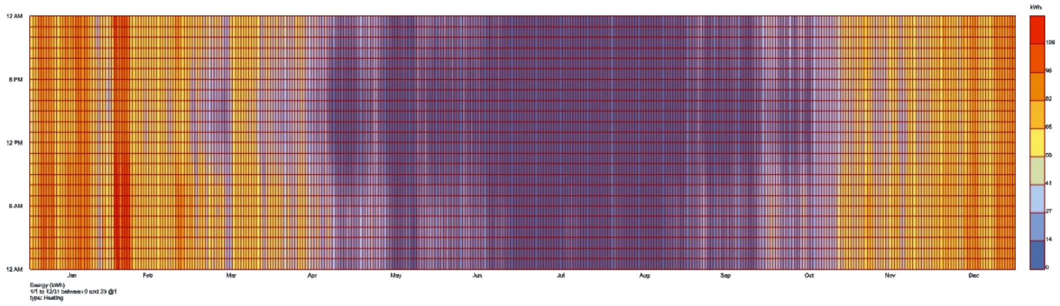

Figure 58 Hourly energy consumption of NGB in sample building 4

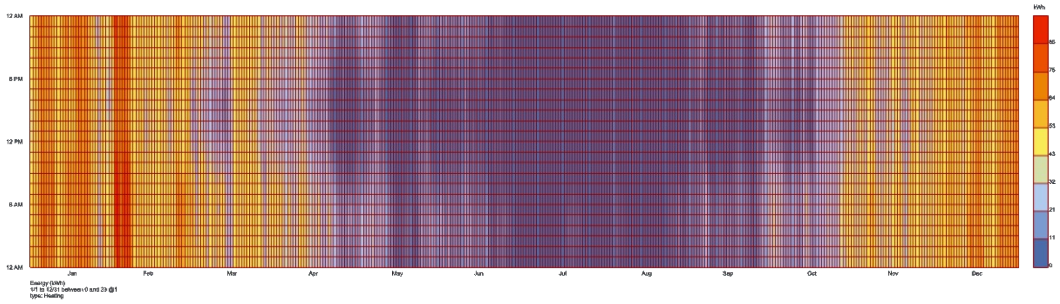

Figure 59 Hourly energy consumption of DH in sample building 4

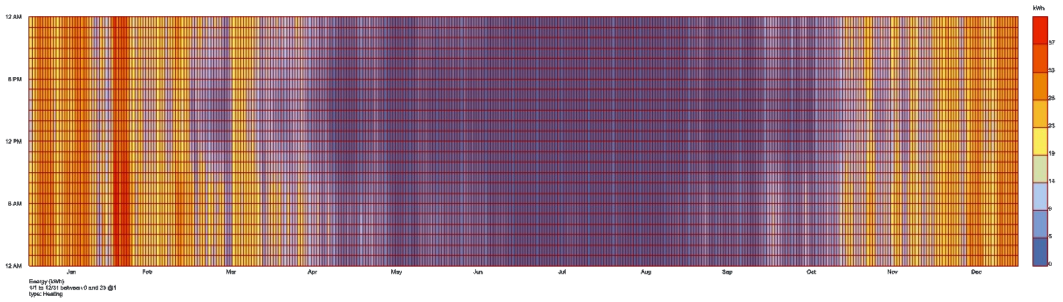

Figure 60 Hourly energy consumption of ASHP in sample building 4

Sample building 5

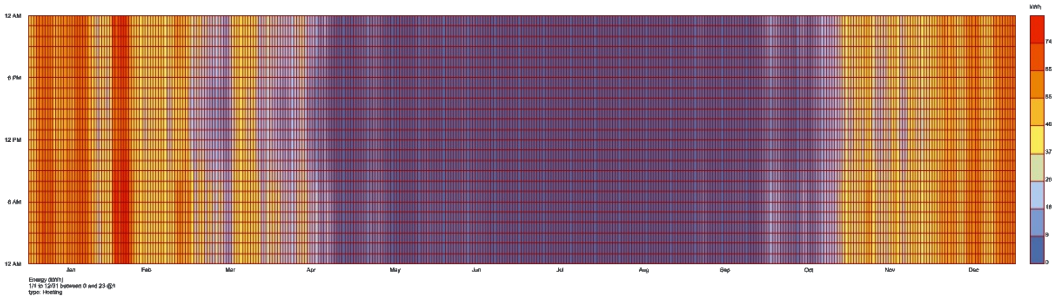

Figure 61 Hourly energy consumption of NGB in sample building 5

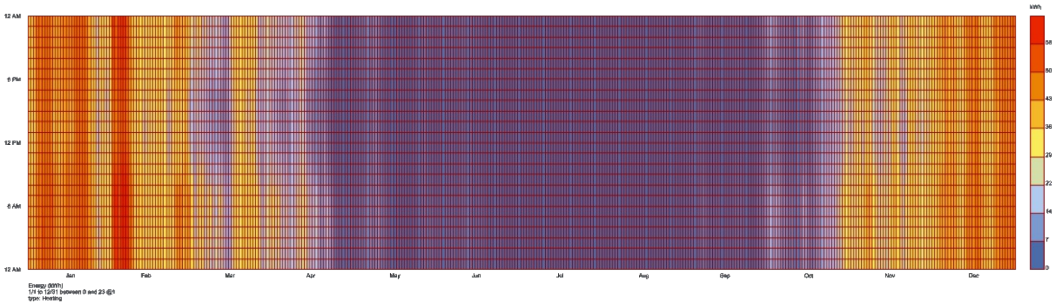

Figure 62 Hourly energy consumption of DH in sample building 5

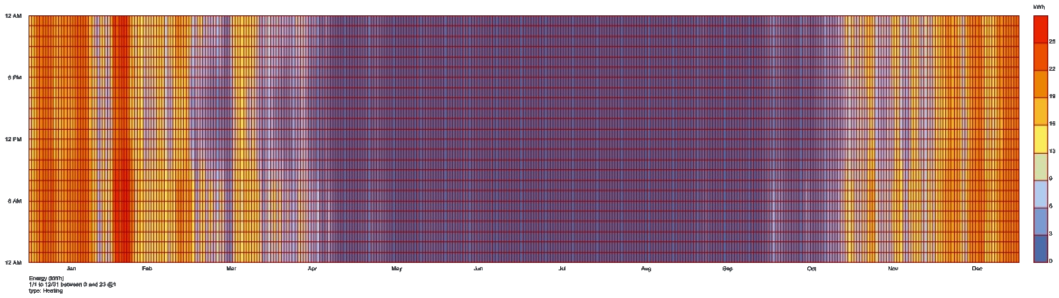

Figure 63 Hourly energy consumption of ASHP in sample building 5

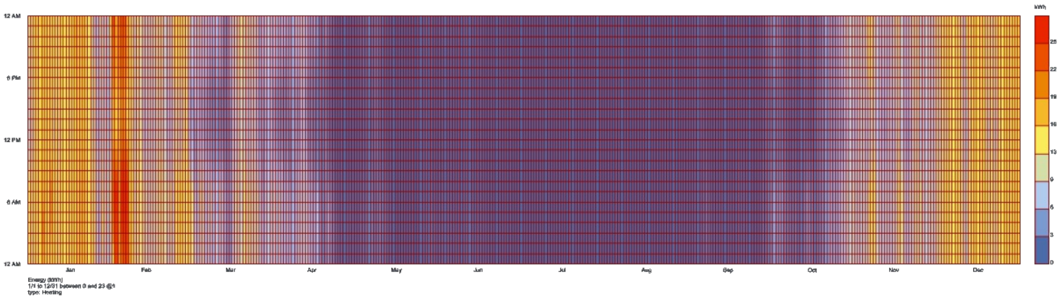

Figure 64 Hourly energy consumption of GSHP in sample building 5

Monthly energy consumption of

Sample building 1

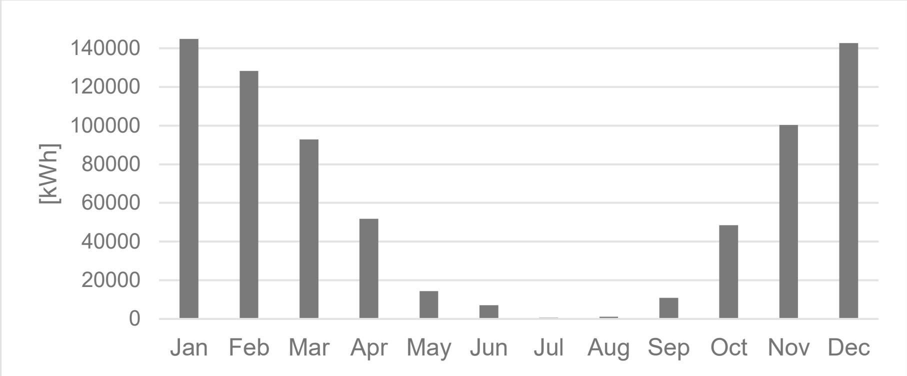

Figure 65 Monthly energy consumption of DH in sample building 1

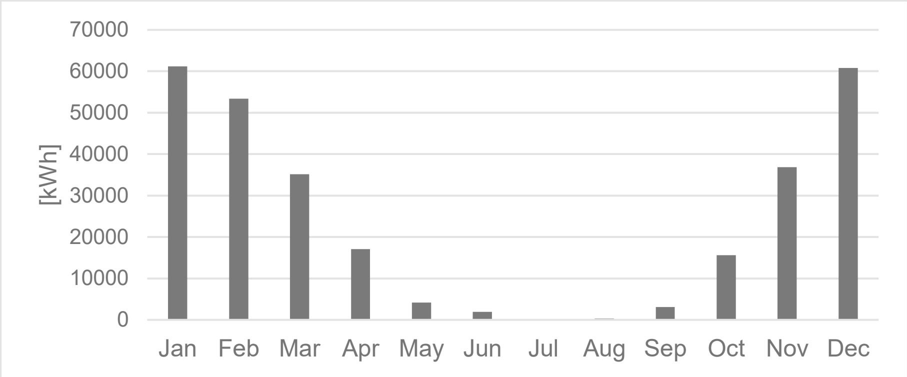

Figure 66 Monthly energy consumption of ASHP in sample building 1

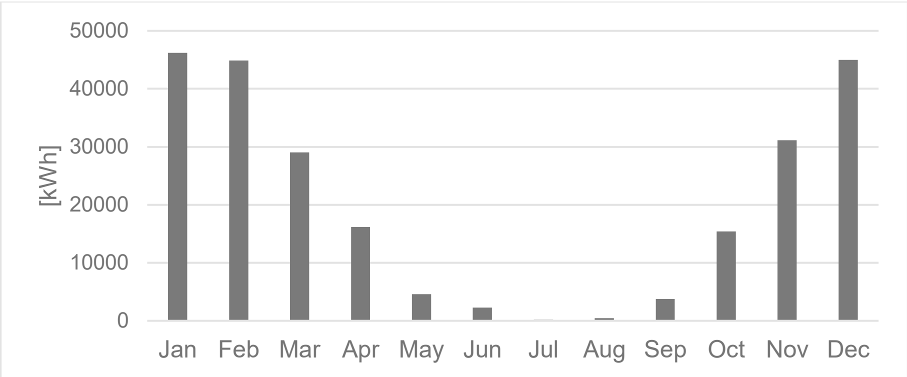

Figure 67 Monthly energy consumption of GSHP in sample building 1

Sample building 2

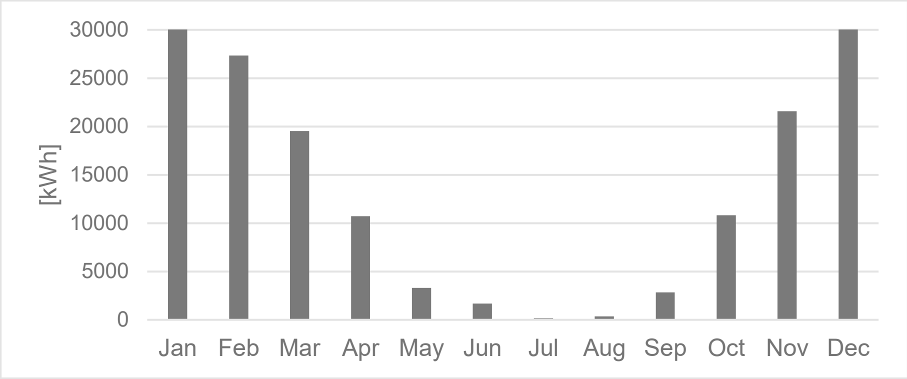

Figure 68 Monthly energy consumption of NGB in sample building 2

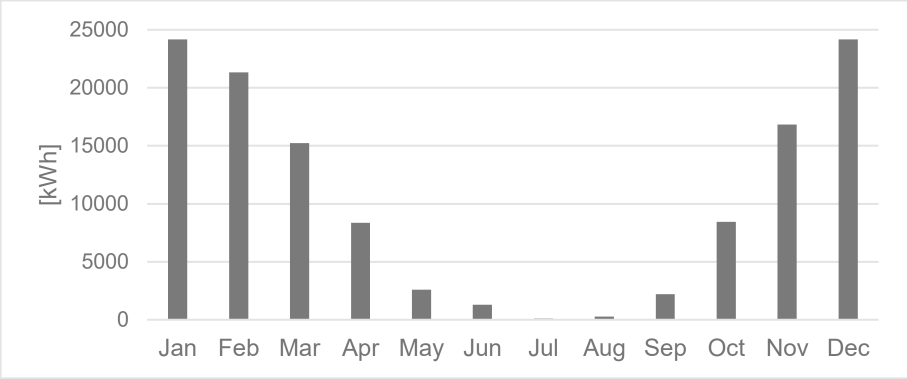

Figure 69 Monthly energy consumption of DH in sample building 2

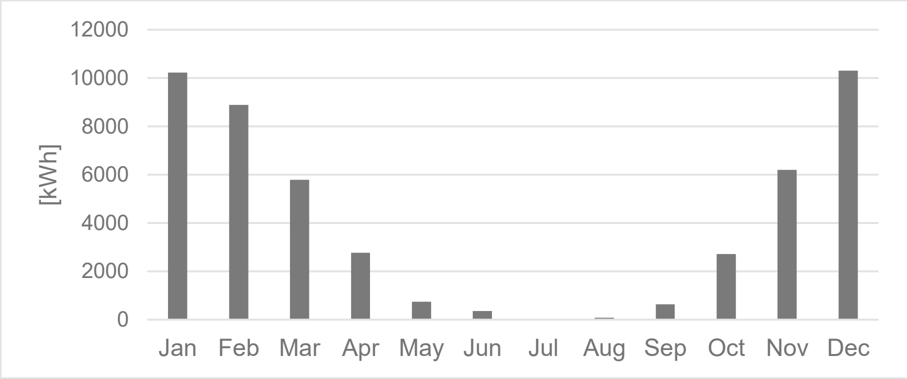

Figure 70 Monthly energy consumption of ASHP in sample building 2

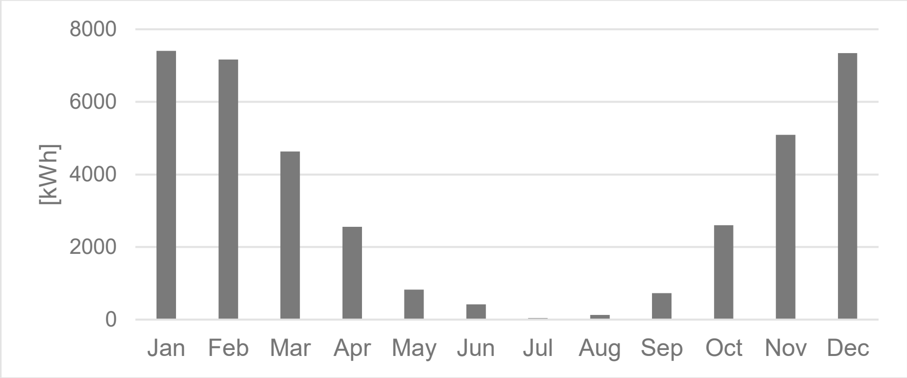

Figure 71 Monthly energy consumption of GSHP in sample building 2

Sample building 3

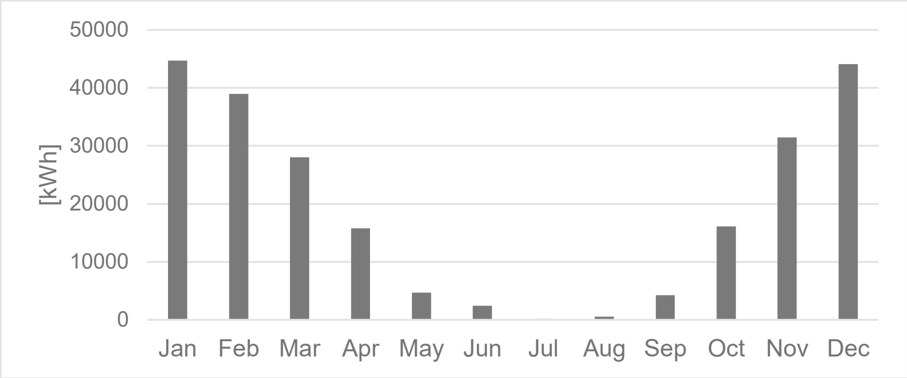

Figure 72 Monthly energy consumption of NGB in sample building 3

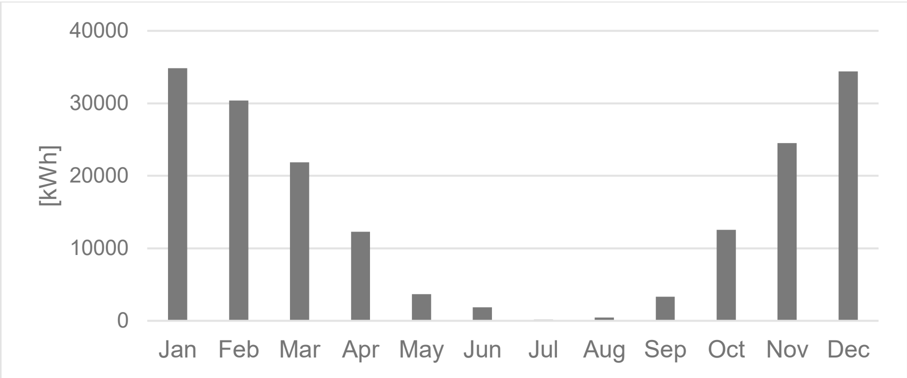

Figure 73 Monthly energy consumption of DH in sample building 3

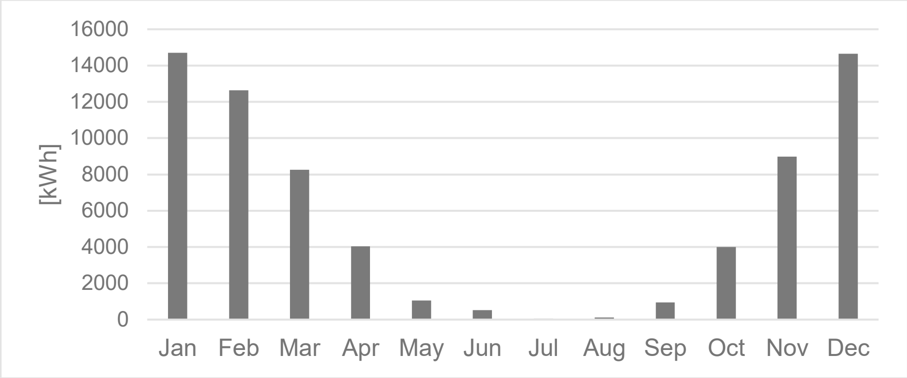

Figure 74 Monthly energy consumption of ASHP in sample building 3

Sample building 4

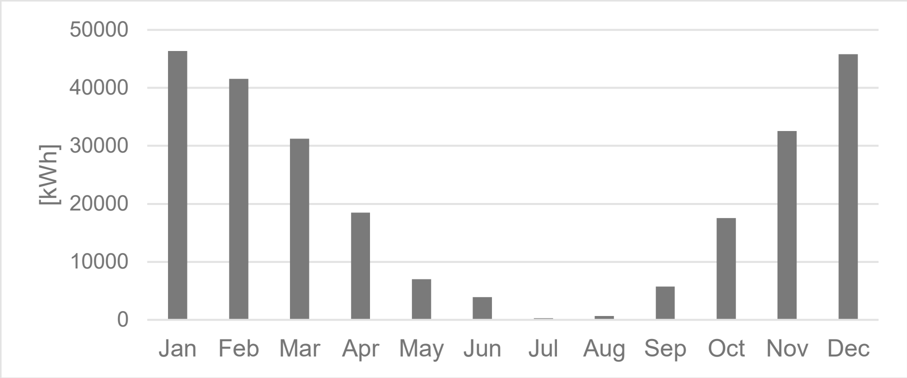

Figure 75 Monthly energy consumption of NGB in sample building 4

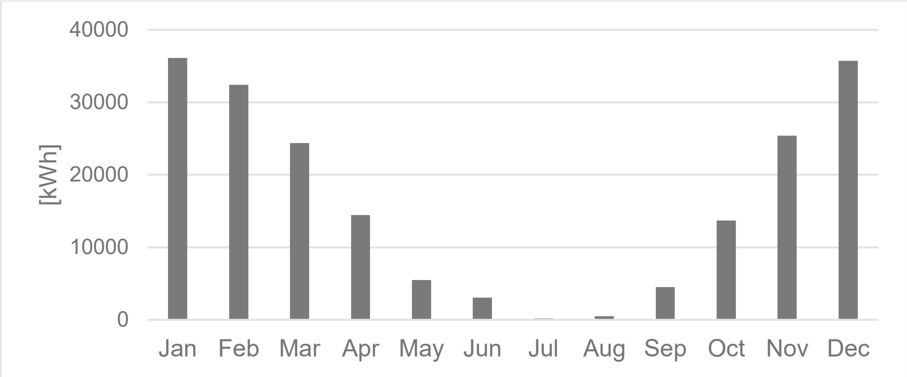

Figure 76 Monthly energy consumption of DH in sample building 4

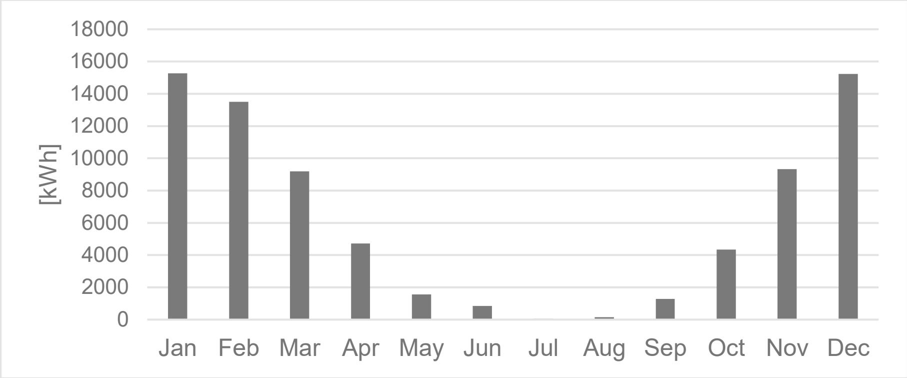

Figure 77 Monthly energy consumption of ASHP in sample building 4

Sample building 5

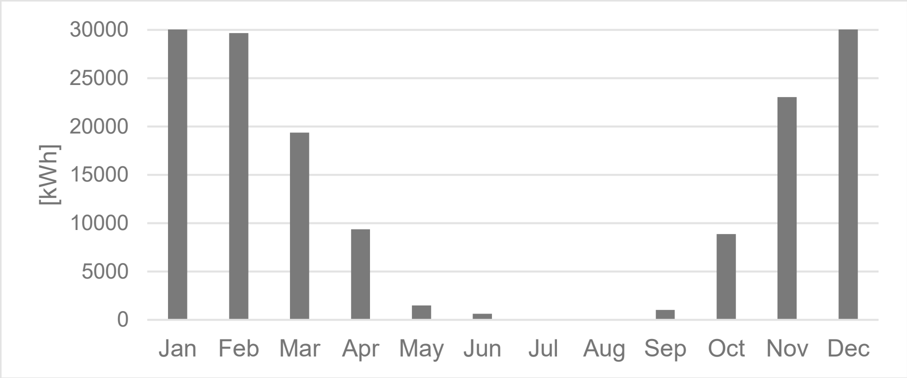

Figure 78 Monthly energy consumption of NGB in sample building 5

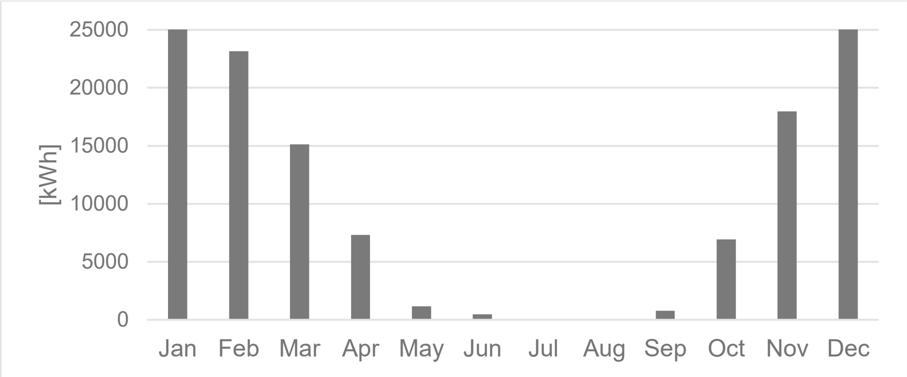

Figure 79 Monthly energy consumption of DH in sample building 5

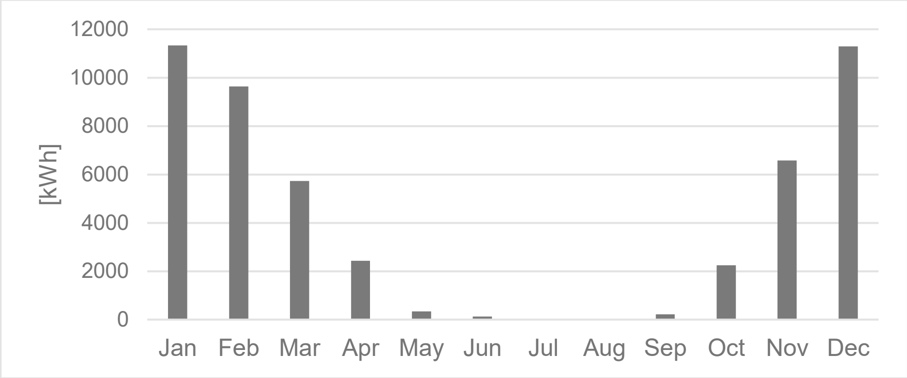

Figure 80 Monthly energy consumption of ASHP in sample building 5

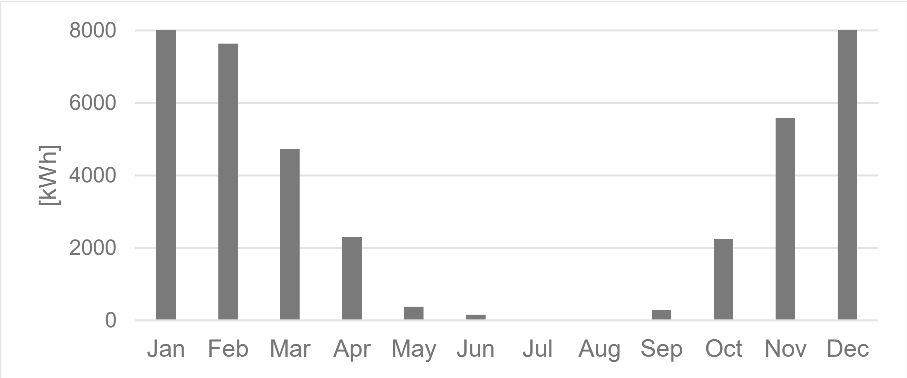

Figure 81 Monthly energy consumption of GSHP in sample building 5

Annual energy consumption of

Sample building 1

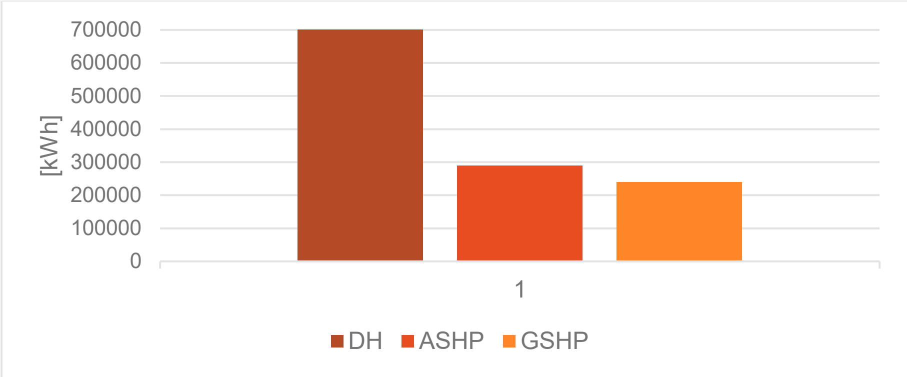

Figure 82 Annual energy consumption of different heating systems in sample building 1

Sample building 2

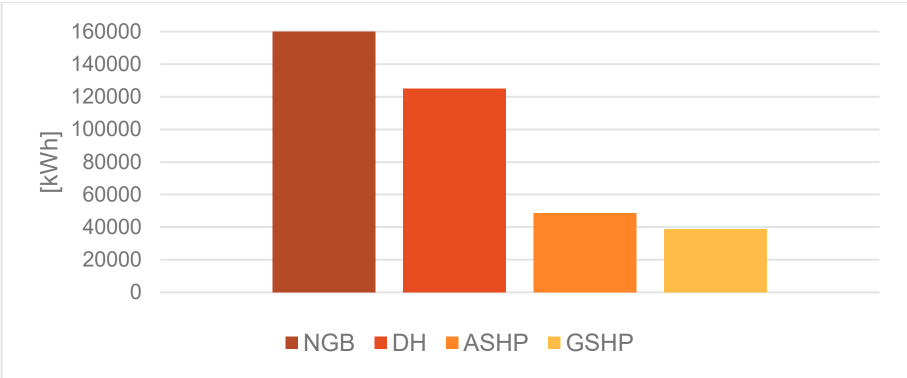

Figure 83 Annual energy consumption of different heating systems in sample building 2

Sample building 3

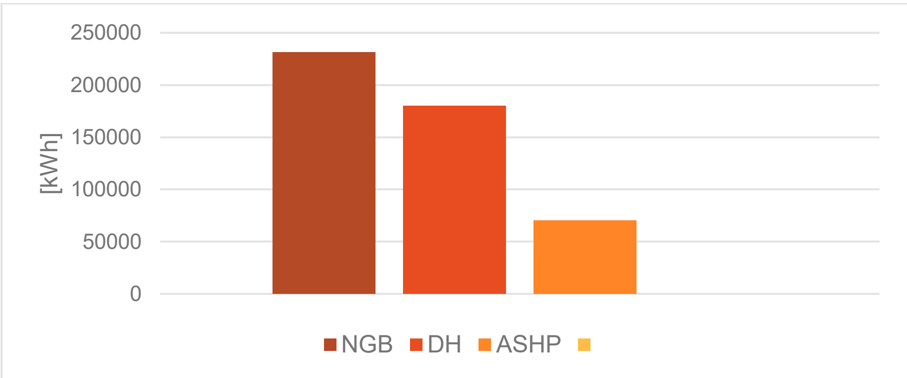

Figure 84 Annual energy consumption of different heating systems in sample building 3

Sample building 4

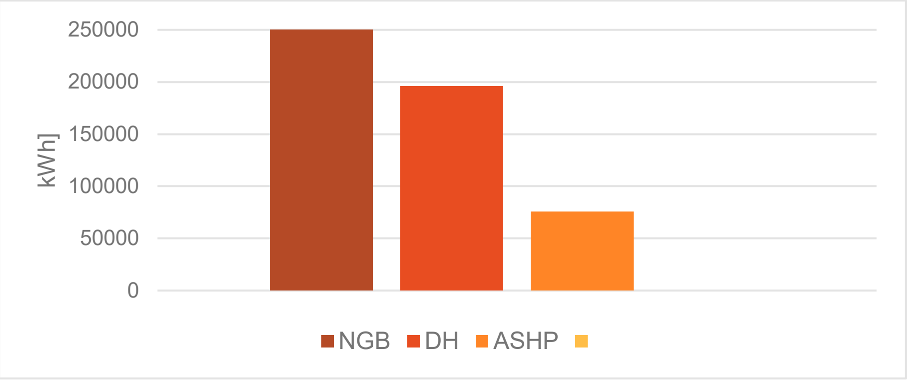

Figure 85 Annual energy consumption of different heating systems in sample building 4

Sample building 5

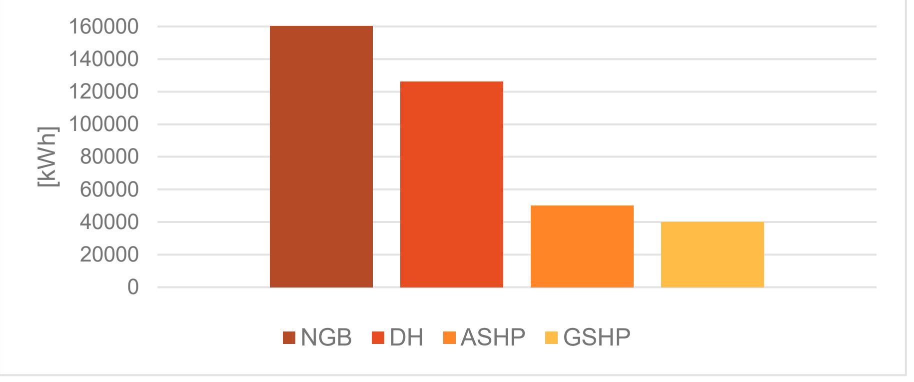

Figure 86 Annual energy consumption of different heating systems in sample building 5

Monthly CO_2eq GHG emissions of

Sample building 1

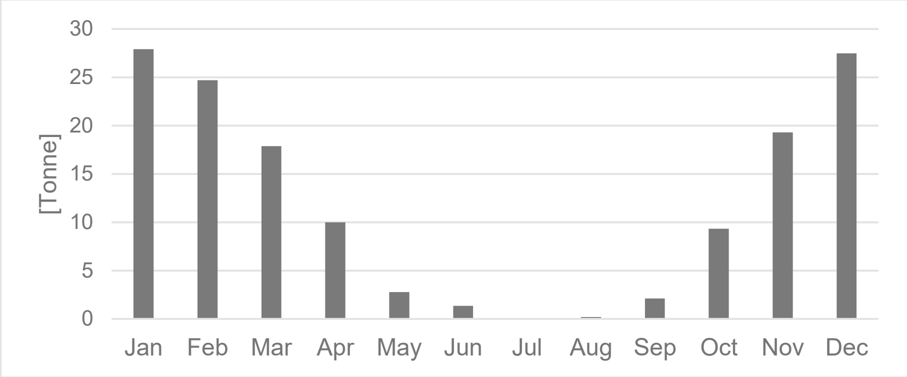

Figure 87 Monthly CO_2eq emission of DH in sample building 1

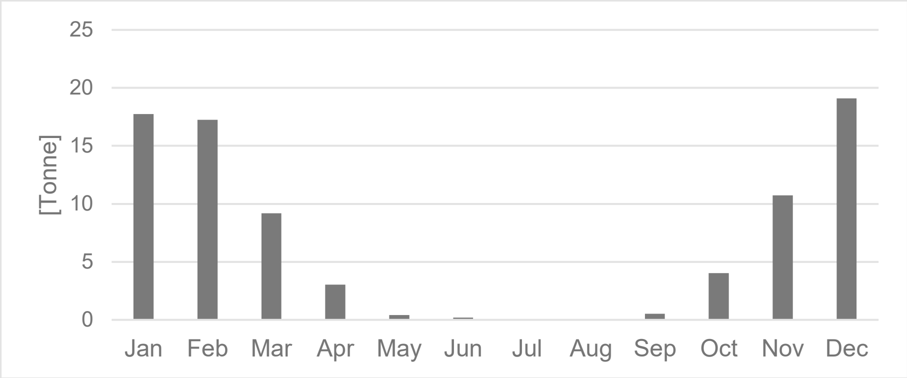

Figure 88 Monthly CO_2eq emission of ASGP in sample building 1

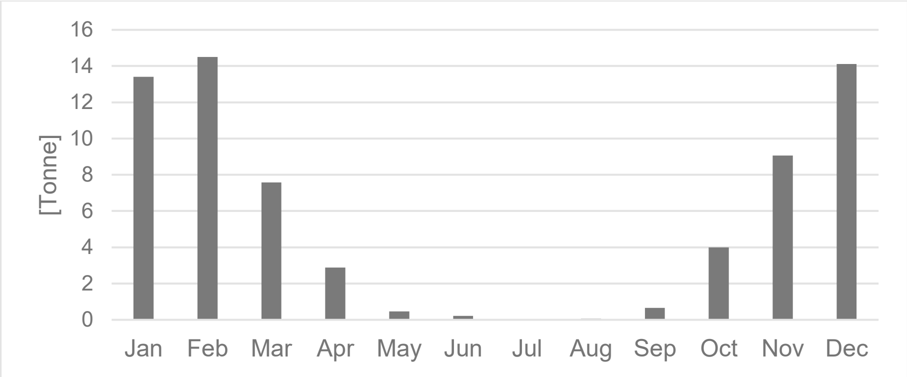

Figure 89 Monthly CO_2eq emission of GSHP in sample building 1

Sample building 2

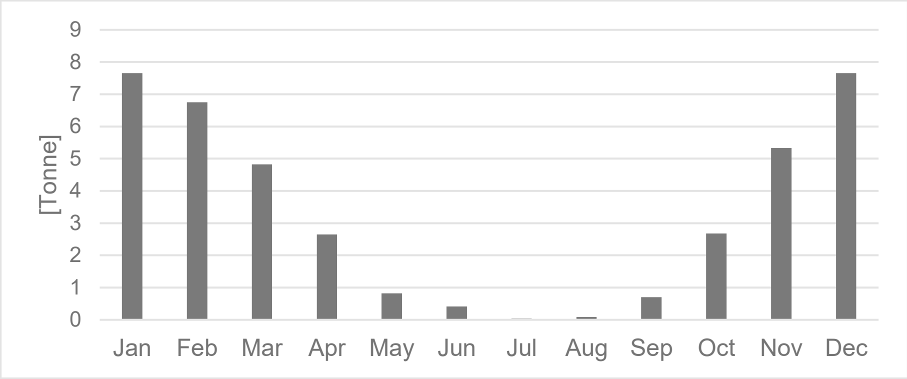

Figure 90 Monthly CO_2eq emission of NGB in sample building 2

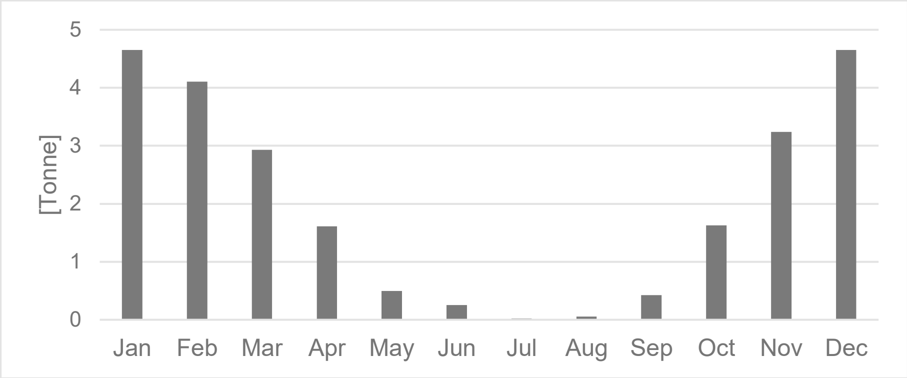

Figure 91 Monthly CO_2eq emission of DH in sample building 2

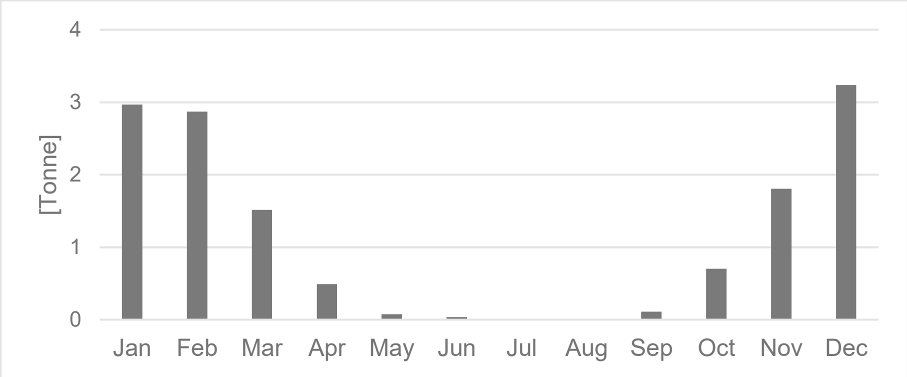

Figure 92 Monthly CO_2eq emission of ASHP in sample building 2

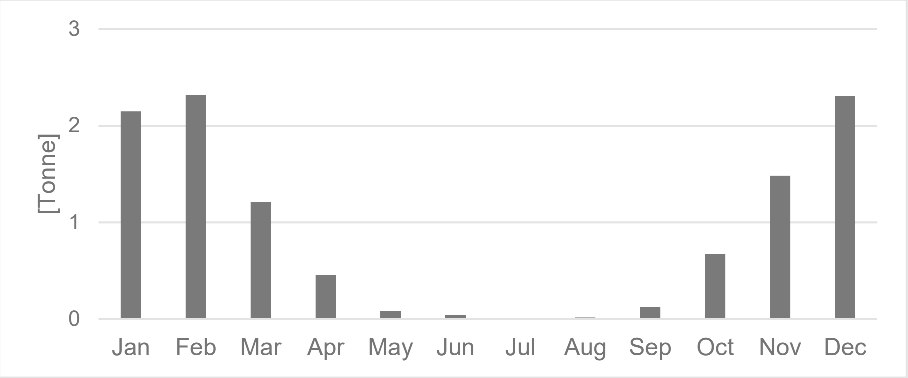

Figure 93 Monthly CO_2eq emission of GSHP in sample building 2

Sample building 3

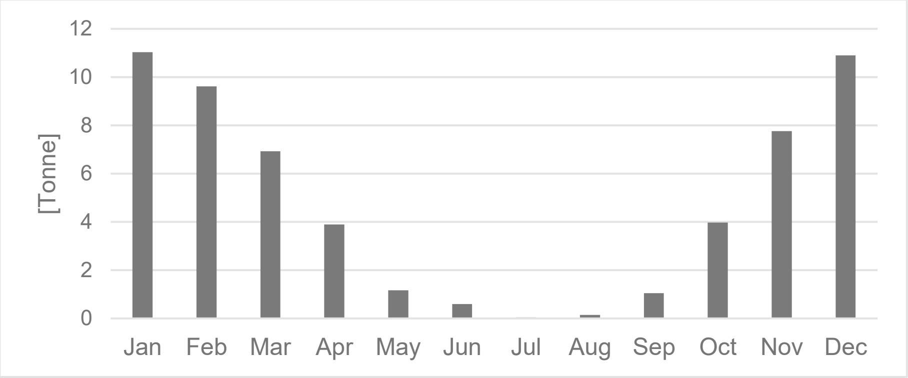

Figure 94 Monthly CO_2eq emission of NGB in sample building 3

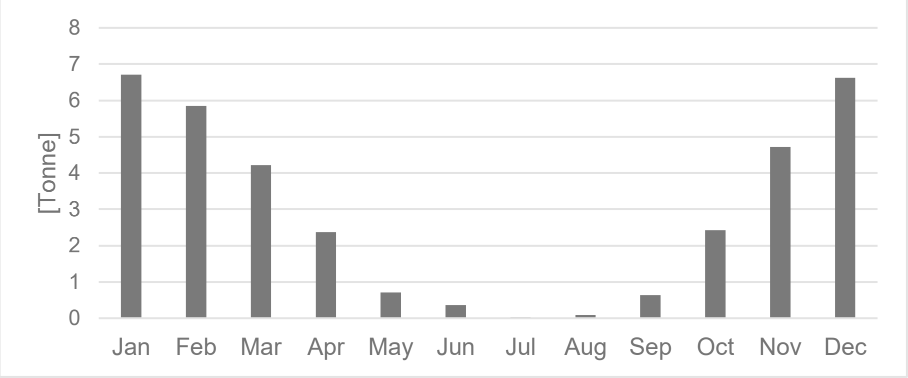

Figure 95 Monthly CO_2eq emission of DH in sample building 3

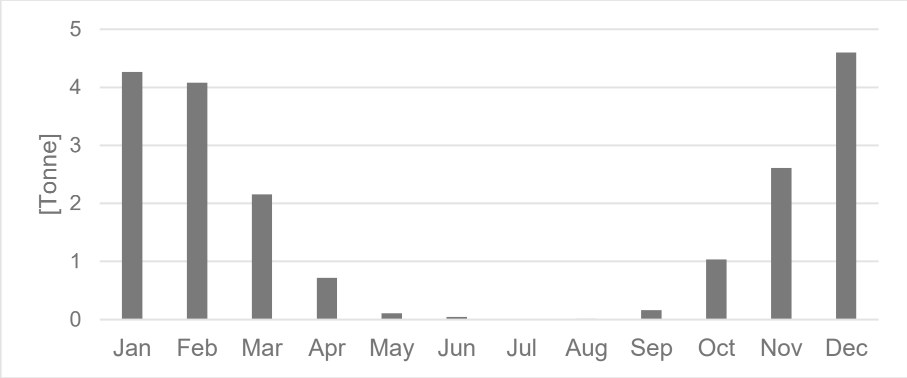

Figure 96 Monthly CO_2eq emission of ASHP in sample building 2

Sample building 4

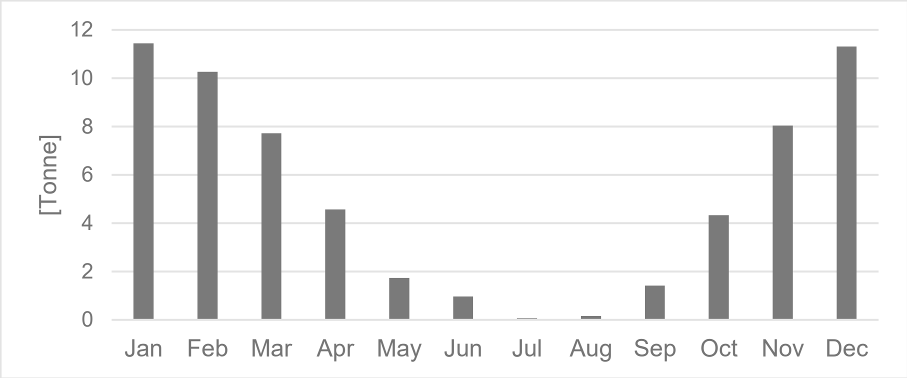

Figure 97 Monthly CO_2eq emission of NGB in sample building 4

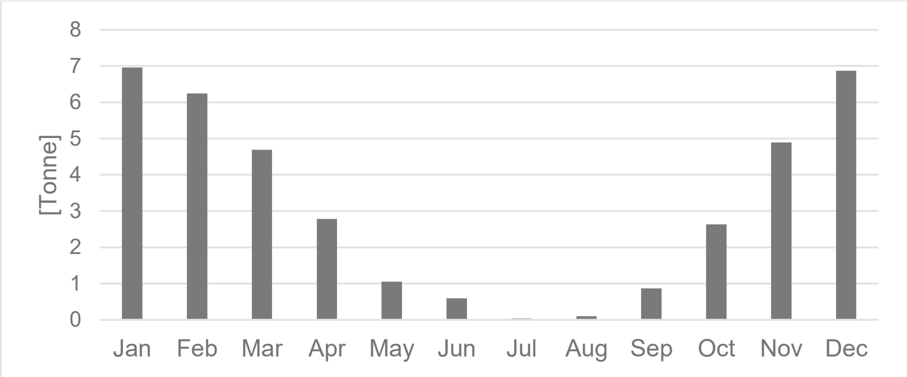

Figure 98 Monthly CO_2eq emission of DH in sample building 4

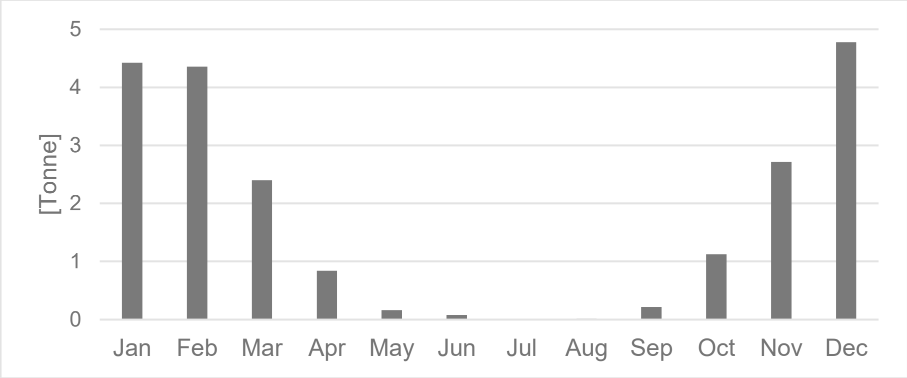

Figure 99 Monthly CO_2eq emission of ASHP in sample building 4

Sample building 5

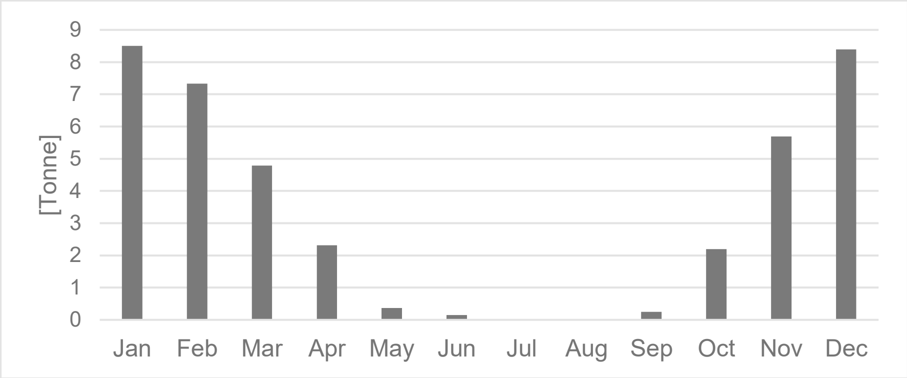

Figure 100 Monthly CO_2eq emission of NGB in sample building 5

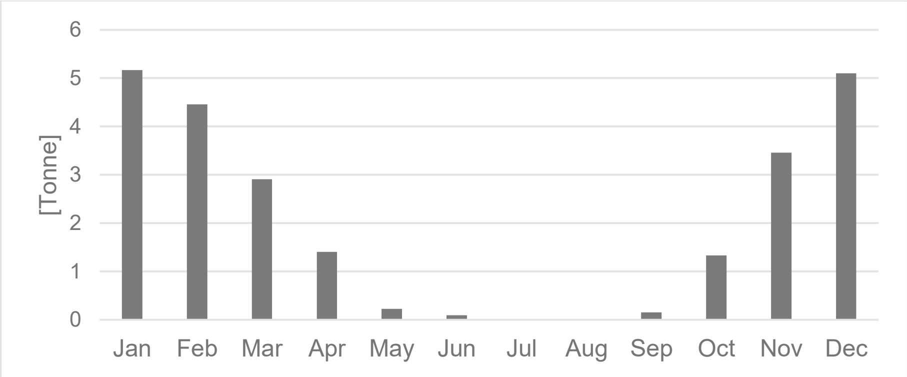

Figure 101 Monthly CO_2eq emission of DH in sample building 5

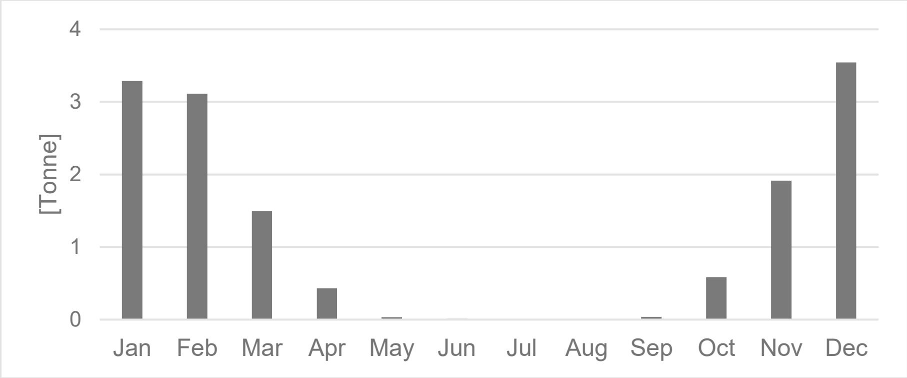

Figure 102 Monthly CO_2eq emission of ASHP in sample building 5

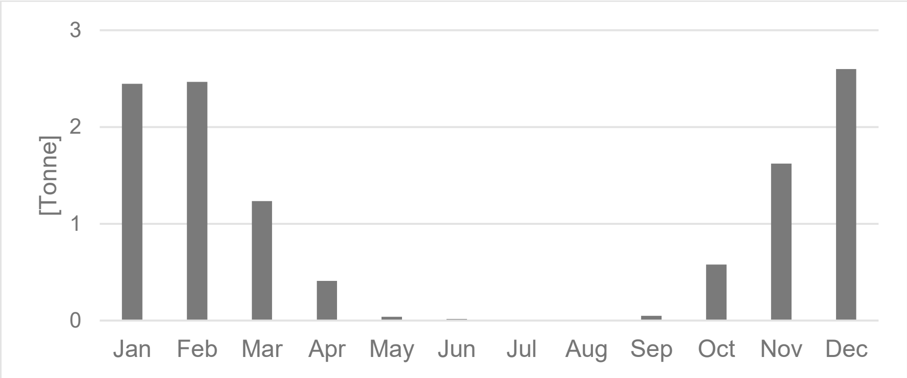

Figure 103 Monthly CO_2eq emission of GSHP in sample building 5

Annual CO_2eq GHG emissions of

Sample building 1

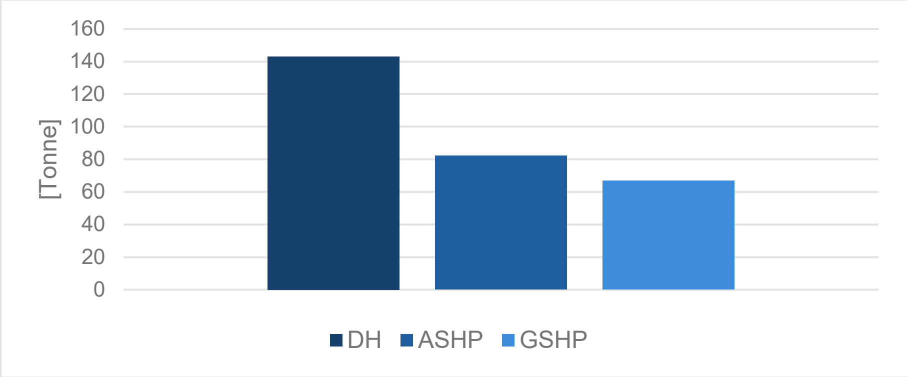

Figure 104 Annual CO_2eq emission of different heating systems in sample building 1

Sample building 2

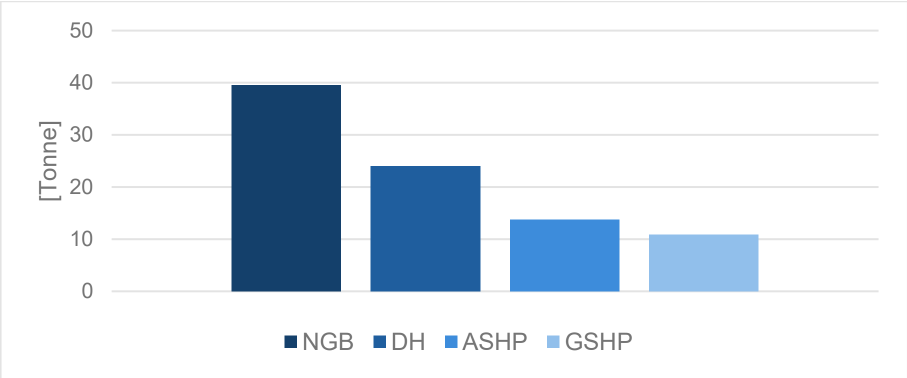

Figure 105 Annual CO_2eq emission of different heating systems in sample building 2

Sample building 3

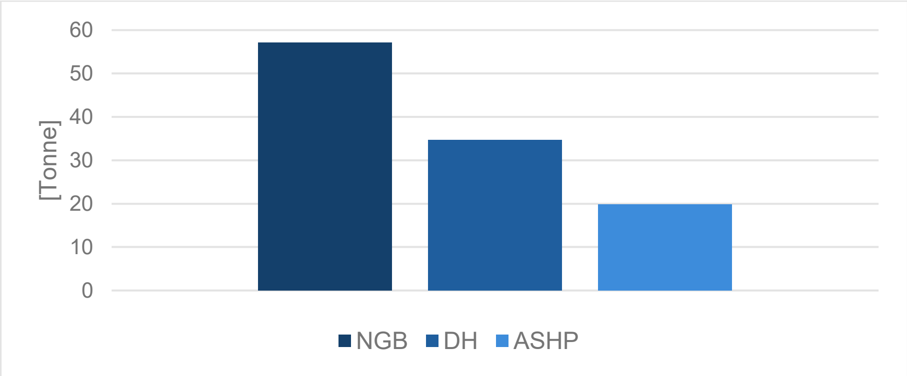

Figure 106 Annual CO_2eq emission of different heating systems in sample building 3

Sample building 4

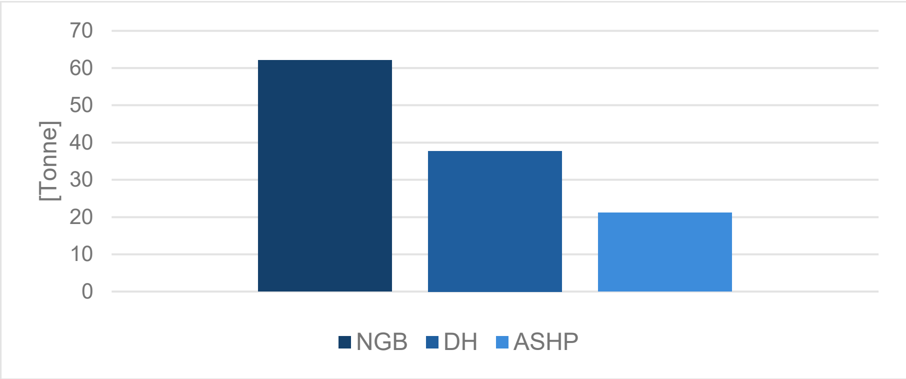

Figure 107 Annual CO_2eq emission of different heating systems in sample building 4

Sample building 5

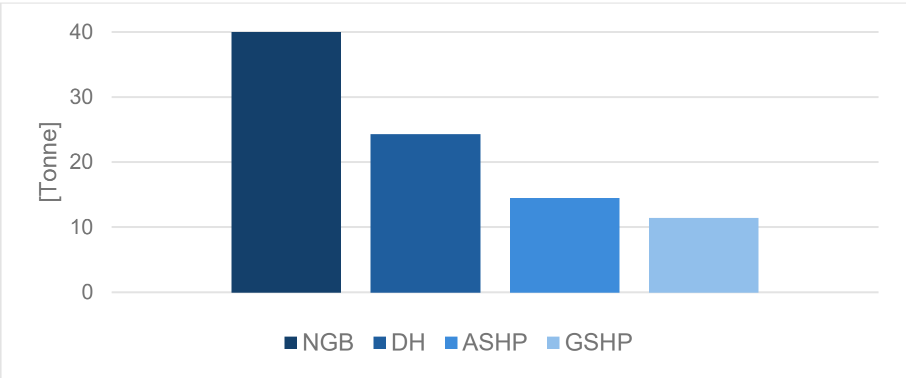

Figure 108 Annual CO_2eq emission of different heating systems in sample building 5